

REVIEW ARTICLE

Physics with coherent matter waves

Kai Bongs and Klaus Sengstock §

Institut für Laser-Physik, Universität Hamburg, Luruper Chaussee 149, 22761
Hamburg, Germany

Abstract. This review discusses progress in the new field of coherent matter waves, in particular with respect to Bose-Einstein condensates. We give a short introduction to Bose-Einstein condensation and the theoretical description of the condensate wavefunction. We concentrate on the coherence properties of this new type of matter wave as a basis for fundamental physics and applications. The main part of this review treats various measurements and concepts in the physics with coherent matter waves. In particular we present phase manipulation methods, atom lasers, nonlinear atom optics, optical elements, interferometry and physics in optical lattices. We give an overview of the state of the art in the respective fields and discuss achievements and challenges for the future.

§ To whom correspondence should be addressed (sengstock@physnet.uni-hamburg.de)

1. Introduction

Quantum mechanics as an important foundation of modern physics and its description in terms of probability densities naturally incorporates the fascinating wave nature of massive particles. These matter waves were postulated in 1925 by de Broglie [1] and demonstrated for electrons by Davisson and Germer [2]. Matter waves and their ability to interfere have been and still are the basis for many fundamental tests of the principles of quantum mechanics. In applications the interference of atomic matter waves nowadays sets the basis of time and allows the construction of some of the most sensitive sensors, e.g. for gravity, rotation, gravity gradients, atom polarisabilities, ... [3, 4, 5, 6, 7, 8, 9, 10, 11, 12].

The realisation of Bose-Einstein condensation in dilute atomic gases in 1995 [13, 14, 15] opened an exciting window to quantum mechanics and started a new era of matter wave research. The impact of this discovery was underlined by the Nobel prize 2001 awarded to the pioneering groups [16, 17]. Until this time all experiments were based on single particle interference with thermal ensembles of particles having a coherence length typically much below a μm . The phenomenon of Bose-Einstein condensation allows for the first time the creation of a macroscopically occupied matter wave with coherence length up to the mm scale. A Bose-Einstein condensate wavefunction compares to a thermal ensemble in an analog way as a laser in optics to a light bulb. The coherence and the macroscopic nature of this new type of matter wave have paved the way for a new field of physics and many fascinating experiments. As an example in analogy to laser physics, the interference of two individual Bose-Einstein condensate wavefunctions [18] clearly demonstrated multi-particle interference with matter waves, which could not be observed with thermal ensembles. In this article we will concentrate on the coherence aspects of the Bose-Einstein condensate wavefunction and discuss a selection of relevant experiments in the field.

The history of Bose-Einstein condensation goes back to the "golden time" of quantum mechanics, when in 1924 Bose developed a new, statistical approach to derive Planck's law for the radiation of a black body [19]. Due to publication problems Bose asked Einstein for advice, who recognised the importance of this work, supported the publication and already then added a note, that this new statistics could be extended from photons to massive particles. Einstein published the resulting statistics, later called "Bose-Einstein statistics" in 1925 [20], finding the solely statistically motivated condensation of particles into the ground state of the system without the involvement of interactions as an immediate consequence. It is interesting to note that Einsteins original proposal for the experimental realisation of this phase transition was based on electrons as at this time the distinction between "Bosons" and "Fermions" was not yet made. Einsteins prediction lead to many controverse discussions and at first was rejected by most physicists, in particular as there seemed to be no opportunity to observe this phenomenon in experiment.

For example, the BEC phase transition is usually masked by interparticle interactions, which for atomic gases lead to a gas to fluid or gas to solid transition, as it lies in a thermodynamically forbidden region of the phase diagram. The first experimental evidence of Bose-Einstein condensation was found by F. London in 1938 [21, 22], in analysing the superfluid state of liquid Helium. This connection was controversely discussed for a long time and hard to verify in experiment due to the interactions in He, which limit the Bose-Einstein condensate fraction to about

10%. Experimental attempts to observe Bose-Einstein condensation in a nearly ideal gas first concentrated on spinpolarized Hydrogen [23, 24, 25, 26, 27] and later also on alkali atoms. It took 70 years from Einsteins prediction until the combination of laser and evaporative cooling techniques finally lead to success in weakly interacting gases in 1995. The use of a dilute gas at extremely low temperatures was the key to these experiments as it allowed to work in a metastable regime from the point of view of classical phase transitions (needing 3-body collisions to form clusters) while having a thermalized gas phase (relying on two-body collisions).

The physics of BEC was already summarized in several review articles, e.g. [28, 29, 30, 31, 32, 33, 34, 35, 36, 37, 16, 38, 39] and textbooks, e.g. [40, 41, 42, 43, 44].

The intention of this article is to give an introduction to the coherent matter wave aspects intrinsically related to Bose-Einstein condensates. The remainder of this section will give an overview of the theory of Bose-Einstein condensation and condensates in ideal and in dilute gas systems.

1.1. Theoretical description of BEC

1.1.1. Statistics of the BEC phase transition As already mentioned the phenomenon of Bose-Einstein condensation directly follows from quantum statistics. It is thus based on very few fundamental principles of quantum physics, mainly on the indistinguishability of identical particles. Relying on the wave aspect in the quantum mechanical description of particles, one can also find an intuitive analogy to laser physics: We consider the temperature dependent thermal de Broglie wavelength

$$\Lambda_{\text{dB}}(T) = \sqrt{\frac{2\pi\hbar^2}{mk_B T}}, \quad (1)$$

with Planck's constant, \hbar , the particle mass, m , Boltzmann's constant, k_B , and the ensemble temperature, T . From this expression it becomes clear, that the particle wavelength, which could be thought of as being on the same order as the particle wave packet size, will grow with decreasing temperature. Decreasing the temperature or increasing the density, n , of an atomic ensemble will thus at some point lead to a wave packet overlap, when the so called phase space density

$$n\Lambda_{\text{dB}}^3(T) \quad (2)$$

becomes of order unity. Taking further into account Bose-enhancement of stimulated emission into occupied modes, scattering-based redistribution processes of the deBroglie waves will result in a non-classical equilibrium distribution. The ground mode of the system, typically having the largest occupation, will benefit most from this redistribution and the nonlinearity of Bose-enhancement results in a macroscopic occupation of this state. Fig. 1 gives a schematic view of this process. This intuitive picture is impressively reflected in the formation process of a Bose-Einstein condensate [45] as well as in matter wave amplification [46] discussed in section 5.4.

A quantitative derivation of the Bose-Einstein condensation phenomenon is obtained from the quantum statistical point of view. Treating an ideal gas system in the convenient framework of the grand canonical ensemble, the mean occupation number, N_i , of a state, i , with energy ϵ_i of the system is given by the Bose-distribution:

$$N_i = \frac{1}{e^{(\epsilon_i - \mu)/k_B T} - 1}. \quad (3)$$

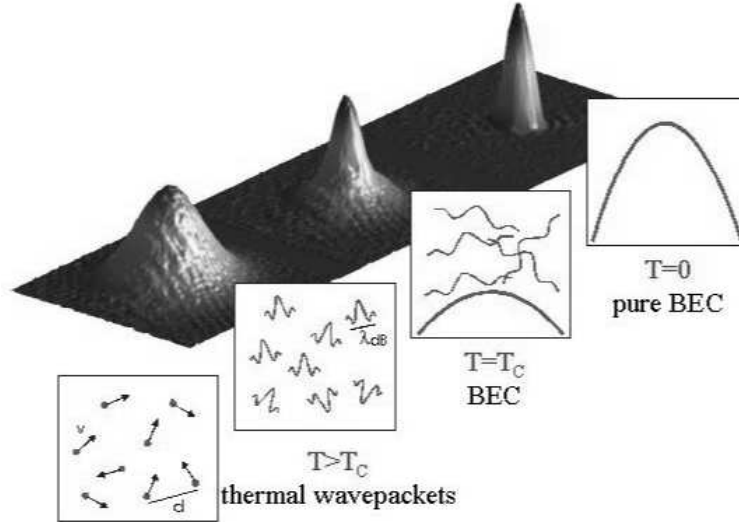


Figure 1. Simplified intuitive view of the Bose-Einstein phase transition in terms of a matter wave interpretation. The model system in the lower schematic images assumes constant particle number. The temperature decreases from the bottom left to the upper right, which leads to an increasing deBroglie wavelength of the particles. The phase transition occurs, when this wavelength becomes comparable to the mean particle distance. The upper images are experimental absorption images of an ensemble of ^{87}Rb atoms at corresponding temperatures. These pseudo 3d images show the density distribution of the ensemble after a time of flight period. They thus show the corresponding momentum distribution of the cloud. The images visualise the transition from a thermal cloud with a symmetric momentum distribution to a pure quantum mechanical wavefunction with an asymmetric momentum distribution, reflecting the asymmetry of the trap used in the experiment. Below but still close to the BEC phase transition the system shows a two-component distribution corresponding to the normal fraction and the condensate wavefunction.

In this description the parameters temperature, T , and chemical potential, μ fix the energy and particle number of the system via:

$$E = \sum_i \epsilon_i N_i = \sum_{i=0}^{\infty} \frac{\epsilon_i}{e^{(\epsilon_i - \mu)/k_B T} - 1} \quad (4)$$

$$N = \sum_i N_i = \sum_{i=0}^{\infty} \frac{1}{e^{(\epsilon_i - \mu)/k_B T} - 1}. \quad (5)$$

For a given temperature the chemical potential defines the occupation number of each energy level, which increases for increasing μ . Note that in order to avoid negative (and thus unphysical) occupation numbers the chemical potential always has to stay below the ground state energy, e.g. $\mu < \epsilon_0$. For a given temperature this effect leads to a maximum possible number of particles in excited states

$$N_{\text{ex}} = \sum_{i=1}^{\infty} \frac{1}{e^{(\epsilon_i - \mu)/k_B T} - 1} \quad (6)$$

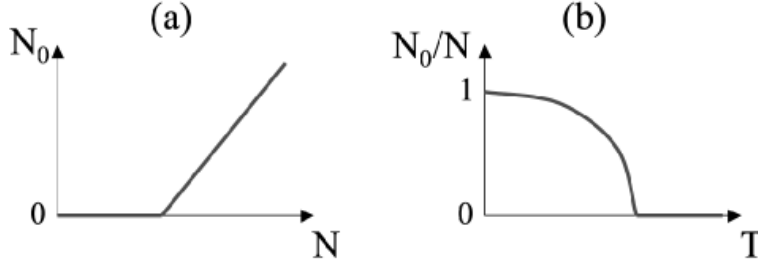


Figure 2. Schematic view of the dependence of ground state occupation number on the number of particles for a fixed temperature (a) as compared to the relative ground state occupation as a function of temperature for fixed particle number (b).

for $\mu = \epsilon_0$. This number, $N_{\text{ex}}(\mu = \epsilon_0)$ is finite for systems in which Bose-Einstein condensation occurs. It is nevertheless possible to host more particles in these systems as the ground state occupation diverges in the limit $\mu \rightarrow \epsilon_0$. Adding particles to such a system at fixed temperature first enlarges N_{ex} by increasing μ until its value becomes close to ϵ_0 . At this point the excited state population saturates and the ground state becomes macroscopically occupied (see Fig. 2 (a)), which is the essence of Bose-Einstein condensation.

A slightly different but equivalent common viewpoint closely related to the typical experimental realisation of Bose-Einstein condensation considers cooling of a system with fixed particle number. In this view the maximum possible excited state occupation decreases with decreasing temperature. Again at the point where $N_{\text{ex}}(\mu = \epsilon_0, T)$ becomes smaller than N , a macroscopic part of the particles starts to occupy the ground state (see Fig.2 (b)).

The critical temperature, T_c , and the corresponding critical particle number, N_c , for Bose-Einstein condensation can be found by considering the condition

$$N_{\text{ex}}(\mu = \epsilon_0, T_c) = N_c. \quad (7)$$

A more quantitative analysis for systems in a relatively general potential, $U(\vec{r})$, can be obtained approximating the sum in equation 4 for large particle numbers by the following integral [47, 48, 49]:

$$N = N_0 + \int_0^\infty \rho(\epsilon)N(\epsilon). \quad (8)$$

For this expression the ground state energy was set to be zero and the continuous Bose distribution

$$N(\epsilon) = \frac{1}{e^{(\epsilon-\mu^-)/k_B T} - 1} \quad (9)$$

as well as the energy density of states

$$\rho_\epsilon = \frac{1}{2\pi\hbar^3} \int \int d^3r d^3p \delta\left(\epsilon - \frac{p^2}{2m} - U(\vec{r})\right) \quad (10)$$

were introduced. Performing the momentum integration and comparing with $N = \int d^3r n(\vec{r})$ yields the particle density

$$n(\vec{r}) = \frac{g_{\frac{3}{2}}(e^{-(U(\vec{r})-\mu)/k_B T})}{\Lambda_{\text{dB}}^3(T)} \quad (11)$$

introducing the Bose-function $g_\alpha(x) = \sum_{l=1}^{\infty} \frac{x^l}{l^\alpha}$. The critical temperature immediately follows by considering $\mu \approx 0$ (assuming the minimum of the potential $U(\vec{r}_0)$ to be zero) from

$$n(r_0) \cdot \Lambda_{\text{dB}}^3(T_c) = g_{\frac{3}{2}}(1) \approx 2.612 \quad (12)$$

The product of density and the cube of the de Broglie wavelength occurring in this equation is called the phase space density

$$D(T, n) = n \cdot \Lambda_{\text{dB}}^3(T) \quad (13)$$

of the ensemble and represents a central parameter in the description of Bose-Einstein condensation. Above T_c its cubed root can be interpreted as the ratio of thermal de Broglie wavelength and mean interparticle spacing with the above condition corresponding to the intuitive picture given at the beginning of this section. Note, that the condition 12 is independent of the potential (as long as it has a minimum, with the box potential as limiting case).

For the experimentally relevant case of an anisotropic harmonic trap with frequencies ω_x , ω_y and ω_z one can extract a condition involving critical temperature and particle number

$$k_B T_c \approx 0.94 \hbar (N_c \omega_x \omega_y \omega_z)^{\frac{1}{3}}. \quad (14)$$

The above equations for the critical temperature are strictly valid only for noninteracting gases in the thermodynamic limit of particle numbers going to infinity. In the experimentally important case of weakly interacting dilute atomic gases with finite particle number (typically $N = 10^3 \dots 10^7$) corrections on the order of a few percent appear (see e.g. [50, 32]). These corrections are observable in experiment and an active area of research [51, 52, 53]. Furthermore in the regime of finite particle number differences between different thermodynamic treatments occur, in particular concerning fluctuations. Detailed descriptions via the most appropriate microcanonic ensemble and corrections to it are an active area of research [54, 55, 56, 57, 58, 59, 60, 61, 62, 63, 64, 65].

It is important to note, that the critical temperature is usually several orders of magnitude higher than the temperature corresponding to the energy level spacing between the ground and first excited state of the system. In this sense Bose-Einstein condensation has nothing to do with naturally freezing out the atomic motion but really is a high temperature phenomenon. This availability of a single macroscopically occupied wave function is one of the experimentally most intriguing aspects of Bose-Einstein condensation as it gives access to coherent matter waves with large coherence length. We will discuss role of finite temperature effects concerning the coherence properties later in this article.

1.1.2. Condensate wave function - Gross Pitaevskii equation The Bose-Einstein condensation phase transition discussed above is only weakly influenced by interactions. For temperatures above the critical temperature the interaction energy of the system is small compared to the kinetic energy of the system. The Bose-Einstein condensation phase transition itself is not significantly influenced by interactions. On the other hand for temperatures below the critical temperature, the condensate wavefunction, which is of main interest to this report, is significantly altered. Interparticle interactions significantly change the shape and size of the condensate wavefunction but also introduce collective excitations such as oscillations and sound

as well as nonlinear effects. For the condensate fraction the kinetic energy is usually much smaller than the interaction energy (so called "Thomas Fermi regime"). A good overview of the condensate wavefunction theory can be found in [32] on which the following introduction of main concepts and approximations is based. In the Heisenberg picture in second quantization, the time evolution of a dilute gas of bosonic atoms can be expressed as

$$i\hbar \frac{\partial}{\partial t} \hat{\Psi}^\dagger(\vec{r}, t) = \left[-\frac{\hbar^2 \nabla^2}{2m} + U_{\text{ext}}(\vec{r}) + \int d\vec{r}' \hat{\Psi}^\dagger(\vec{r}', t) U(\vec{r} - \vec{r}') \hat{\Psi}(\vec{r}', t) \right] \hat{\Psi}^\dagger(\vec{r}, t). \quad (15)$$

$\hat{\Psi}^\dagger(\vec{r})$ ($\hat{\Psi}(\vec{r})$) is the boson field operator creating (annihilating) a particle at position \vec{r} and $U(\vec{r} - \vec{r}')$ is the two particle interaction potential. Solving the corresponding many body problem is nontrivial and usually involves elaborate numerical simulations.

A very useful approximation for the case of low temperatures $T \approx 0$ is to replace the bosonic field operators in lowest order by their expectation value

$$\Phi(\vec{r}, t) \equiv \langle \hat{\Psi}(\vec{r}, t) \rangle, \quad (16)$$

introducing the condensate wave function, $\Phi(\vec{r}, t)$. The introduction of a well defined phase as associated with this condensate wave function is relevant to matter wave interference experiments discussed below. It corresponds to the assumption of a spontaneously broken symmetry in connection with the Bose-Einstein phase transition.

Using the above definition in equation 15 results in the Gross Pitaevskii equation

$$i\hbar \frac{\partial}{\partial t} \Phi(\vec{r}, t) = \left(-\frac{\hbar^2 \nabla^2}{2m} + U_{\text{ext}}(\vec{r}) + g|\Phi(\vec{r}, t)|^2 \right) \Phi(\vec{r}, t), \quad (17)$$

the time independent version of which is obtained using the ansatz $\Phi(\vec{r}, t) = \phi(\vec{r}) \exp(-i\mu t/\hbar)$:

$$\left(-\frac{\hbar^2 \nabla^2}{2m} + U_{\text{ext}}(\vec{r}) + g|\phi(\vec{r})|^2 \right) \phi(\vec{r}) = \mu \phi(\vec{r}). \quad (18)$$

In these equations, μ , is the chemical potential and

$$g = \frac{4\pi\hbar^2 a}{m} \quad (19)$$

is the coupling constant representing the interparticle interactions. The parameter a is the so called s-wave scattering length. The approximation that the interactions are described by s-wave scattering only is very well fulfilled for the low temperature regime in typical experiments. $\phi(\vec{r})$ can be chosen to be a real function with $N = N_0 = \int d\vec{r} \phi^2$ and thus related to the particle density as $\phi^2(\vec{r}) = n(\vec{r})$.

In the low temperature regime the Gross Pitaevskii equation [66, 67] is the main approximation for the condensate wave function. It has been shown in many experiments to be valid up to a high precision for the case of weakly interacting atomic gases discussed in this report. The Gross Pitaevskii equation not only very well describes the ground state wave function, but also many other effects such as collective excitations, the condensate expansion, interference properties, sound propagation, solitons and vortices.

It is intuitive to consider the energy contributions to a trapped atomic Bose-Einstein condensate in order to better understand the properties of the condensate wavefunction:

$$E[n] = \int d\vec{r} \left[\frac{\hbar^2}{2m} |\nabla \sqrt{n}|^2 + n U_{\text{ext}}(\vec{r}) + \frac{gn^2}{2} \right] = E_{\text{kin}} + E_{\text{ho}} + E_{\text{int}}. \quad (20)$$

E_{kin} is the kinetic energy and can be interpreted as a "quantum pressure", E_{ho} is the potential energy due to the trapping potential and E_{int} is the mean field interaction potential energy of the atoms.

The kinetic and interaction energy terms determine the scale over which density variations of the condensate wavefunction can occur. This scale is given by the so called healing length and stems from the fact that the condensate density can not grow from 0 to n on arbitrarily short distances as this would imply a divergence of the "quantum pressure" term, E_{kin} . The shortest possible distance, ξ for such a change in density is given by the balance of $E_{\text{kin}} \sim \hbar^2/(2m\xi^2)$ and interaction energy $E_{\text{int}} \sim 4\pi\hbar^2 an/m$ which defines the healing length

$$\xi = \frac{1}{\sqrt{8\pi na}}. \quad (21)$$

For ^{87}Rb and a density of $n = 10^{14}$ this length is $\xi \approx 0.3 \mu\text{m}$. A singularity as in the center of a vortex or a matter wave soliton thus have a dimension of at least the healing length.

The Gross Pitaevskii equation can be extended to include small amplitude collective excitations [67, 68] using the Bogoliubov approximation. This extension can be derived by writing the atom field operator from equation 15 as

$$\hat{\Psi}(\vec{r}, t) = \Phi(\vec{r}, t) + \hat{\Psi}'(\vec{r}, t). \quad (22)$$

$\Phi(\vec{r}, t)$ is the ground state wave function defined in equation 16 and

$$\hat{\Psi}'(\vec{r}, t) = \sum_j (u_j(\vec{r})\alpha_j(t) + v_j^*(\vec{r})\alpha_j^\dagger(t)) \quad (23)$$

represents excitations. In this equation $\alpha_j(t)$ and $\alpha_j^\dagger(t)$ are Bogoliubov quasiparticle annihilation and creation operators with the respective amplitude functions $u_j(\vec{r})$ and $v_j^*(\vec{r})$. In a uniform gas u and v can be represented as plane waves obeying the Bogoliubov dispersion law [69]

$$\hbar\omega = \sqrt{\frac{\hbar^2 q^2}{2m} \left(\frac{\hbar^2 q^2}{2m} + 2gn \right)}, \quad (24)$$

with the excitation wavevector, \vec{q} . In the case of large momenta the excitations behave as free particles with energies $\hbar^2 q^2/2m$. Low momenta yield a phonon dispersion law $\omega = cq$ with the sound velocity of the system

$$c = \sqrt{\frac{gn}{m}}. \quad (25)$$

For typical experimental parameters the sound velocity is on the order of a few $\frac{\text{mm}}{\text{s}}$.

1.1.3. Beyond the Gross Pitaevskii equation In principle the Gross Pitaevskii equation only describes the physics of weakly interacting systems for $T \rightarrow 0$, i.e. the pure condensate fraction. Nevertheless the Gross Pitaevskii equation has shown to give an excellent qualitative and quantitative description for nearly all experiments to date. Finite temperature effects are key to important experimental effects such as damping of excitations and especially decoherence phenomena like phase fluctuations. The theory can be very involved, and suitable approximations are an active area of research. Promising theoretical routes for temperatures close to and below T_c consist in extensions of the Gross Pitaevskii equation, modifying the well known pure condensate fraction with an additional reservoir [70, 71, 72, 73, 74, 75, 76, 77, 78, 79, 80].

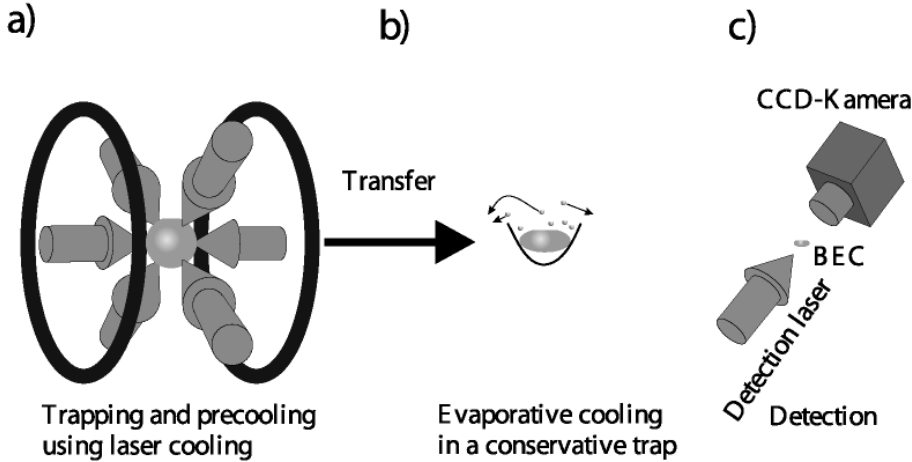


Figure 3. Typical setup for the creation of a Bose-Einstein condensate in dilute alkali gases. Note that the steps a)-c) are taking place sequentially in time but at the same position in space. First atoms are collected and precooled in a magneto-optic trap (MOT)(a). In order to avoid photon induced heating processes the ensemble is then transferred to a conservative potential trap (here: a magnetic trap). Further cooling and compression in the conservative trap is done by evaporative cooling, which removes hot atoms from the ensemble until the BEC phase transition is reached (b). At all stages of the experiment the ensemble can be observed by direct imaging onto a CCD chip with absorption or dispersive techniques (c).

For the case of sufficiently strong interactions, e.g. for Bose-Einstein condensates in strong periodic potentials, the system becomes strongly correlated. The physics of such a system goes fully beyond the Gross Pitaevskii equation and demands for different theoretical descriptions. In this regime effects like large phase uncertainty due to number squeezing [81] and the superfluid to Mott insulator transition can occur [82].

2. Experimental realisation of BEC

In this section we will give a short summary of the experimental realization of Bose-Einstein condensation in dilute atomic gases. Detailed descriptions can be found in several review articles, e.g. [31, 30]. The typical experimental approach consists in cooling a magnetically or optically trapped ensemble of atoms in an ultra high vacuum ($\approx 10^{-11}$ mbar) environment, which provides thermal isolation. For alkali atoms cooling is typically a two step process. First $10^8 - 10^{11}$ atoms are collected and precooled to $10 - 100 \mu\text{K}$ at densities around $10^{10} - 10^{11} \text{ cm}^{-3}$ using laser cooling techniques. This step increases the phase space density from around 10^{-12} to $D \approx 10^{-6}$. Then the ensemble is transferred into a conservative potential and further cooled and compressed with evaporative cooling until the Bose-Einstein phase transition ($D = 2.612\dots$) occurs. This point is typically reached with $10^4 - 10^7$ atoms at $100 \text{ nK} - 1 \mu\text{K}$ and densities around 10^{14} cm^{-3} . The whole experimental cycle typically takes between 10 and 100 s. These steps are summarised in Fig. 3.

It is interesting to note, that this typical experimental approach to reach Bose-

Einstein condensation via cooling is "orthogonal" to the original idea of Einstein [20]. Einstein suggested an isothermal compression of the system, which for trapped atomic ensembles would correspond to an isothermal increase of particle number (see Fig. 2 (a)). From this viewpoint the condensation is very intuitive, as the new particles first all add to the normal component (the so called "thermal cloud") until it reaches its saturated occupation for the given temperature after which practically all further particles exclusively add to the condensate wavefunction. The constant temperature approach was recently realised in an experiment [83] using spinor condensates.

3. Coherence properties of BEC

The occurrence of a macroscopically occupied ground state wavefunction, i.e. a "single mode" coherent matter wave, is one of the most intriguing aspects of Bose-Einstein condensation. The experimental observation of Bose-Einstein condensation in dilute alkali gases initiated many research activities concerning the "physics with coherent matter waves". The coherence was impressingly demonstrated in pioneering interference experiments [18, 84, 85] short after the first experimental realisation of Bose-Einstein condensation in dilute atomic gases. This research covers fundamental aspects of quantum coherence as well as promising applications in the field of high precision atom interferometry [10]. The most outstanding prospect connected to Bose-Einstein condensation as source for coherent matter waves lies in the analogy to the revolution of light optics with the introduction of laser sources.

A theoretical description of the coherence properties of dilute Bose gases based on the theory of optical coherence can e.g. be found in [86]. In the following we will discuss the coherence properties of a Bose-Einstein condensate in view of experimental possibilities and limitations.

3.1. First order coherence

In a simple picture first order coherence is intrinsically related to the visibility of interference fringes, when two waves overlap. Furthermore the coherence length defines the maximum relative position shift two interfering wavepackets can have while still displaying interferences. These aspects are of major importance for the implementation of interferometric schemes and lead to several fundamental investigations and fascinating experiments.

The coherence of the Bose-Einstein condensate wavefunction as a macroscopic matter wave and its capability to interfere were some of the most intriguing questions after the first realisation of Bose-Einstein condensation in dilute atomic gases. In order to understand the controversies over this subject, despite the theoretical prediction of an order parameter with well defined phase (see eq. (16)), one has to consider the experimental realisation. While the theoretical prediction is based on the thermodynamic limit, i.e. infinite particle number, the experiments were performed with dilute atomic gases, reaching Bose-Einstein condensation with typically $10^3..10^7$ atoms. As indicated above, in this case the thermodynamic ensembles for the statistical treatment are not equivalent. The most appropriate description of the experiment seems to be via the microcanonical ensemble, dealing with a given finite particle number with given energy in a trap. Fixing the particle number directly in the microcanonical ensemble in comparison to ensuring a statistically most probable particle number via the chemical potential in the grand canonical ensemble would

suggest a description of the condensate wavefunction as a Fock state rather than a coherent state. Due to the number phase uncertainty relation a Fock state with well defined particle number has maximum phase uncertainty. The fundamental controversy of major importance concerning the matter wave coherence was if two separately created condensates would be able to form a visible interference pattern and if this would be consistent with a Fock state description. This controversy was resolved by the experiment described below and the theoretical prediction, that two Fock states can indeed form an interference pattern, when overlapped [87, 88, 89, 90, 91, 92, 93].

It is important to note, that this effect relies on the availability of a macroscopically occupied wavefunction. Due to macroscopic occupation a random relative phase between the two interfering Fock states can be detected in a single shot experiment. For the average over many single particle experiments the randomness of the relative phase washes out any interference visibility. In this case there is a fundamental difference between a single experiment with many particles and many experiments with single particles!

A very intuitive approach to explain the relative phase in Fock state interference experiments was developed in [92]. The relative phase is built up by Bose enhancement effects during the detection process. If some out of many bosons occupying the same wavefunction are detected (localised on some screen position) Bose enhancement leads to a modification of the detection probability of further bosons. Due to the position resolved detection the Fock state is projected onto a state with well defined phase. This phase is expected to be random for different experiments but fixed for each single experiment. Note that there is also no contradiction between well defined particle number and phase at the same time, as the detection introduces a local number uncertainty for each screen position.

3.2. Interference experiments

The groundbreaking experiment establishing Bose-Einstein condensates in dilute atomic gases as coherent matter waves was performed by the group of W. Ketterle at MIT [18]. This experiment established the interference capability of Bose-Einstein condensates in a twofold way. It demonstrated self interference (similar to the interference in typical light interference schemes performed with one laser) as well as the interference of two distinct condensate wavefunctions (similar to "beat signal interferences" between two distinct lasers).

This experiment made use of a trap for the atomic ensemble, which could be divided into two separate traps with an adjustable repulsive potential well created with a light sheet. Switching off the trapping potential with a Bose-Einstein condensate in each trap causes the condensate wavefunctions to spread during time of flight. When these wavefunctions spread into each other they show interference fringes according to their coherence properties in the overlap region (see Fig. 4).

With this setup a self interference experiment was performed by first creating a Bose-Einstein condensate in the undivided trap before slowly splitting the trap and thus also the condensate in two parts. In this case (and neglecting decoherence effects) there should be no distinct condensate wavefunctions, but only one with a double peak distribution. Each atom should be in a superposition state of both trap wavefunctions. There should thus be an interference pattern after the time of flight expansion due to interference of "each atom with itself" with a fixed phase only depending on the splitting process.

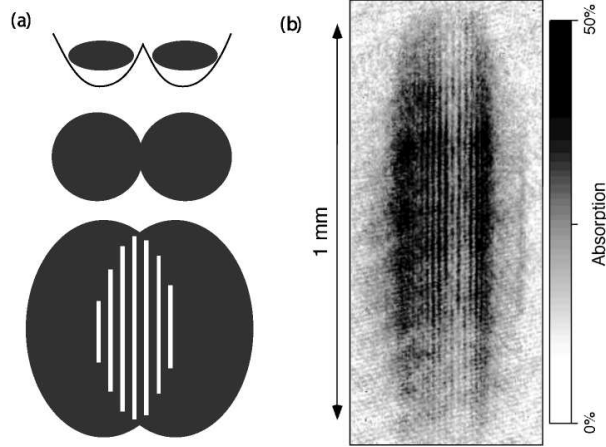


Figure 4. (a) Schematic view of the interference of two separately produced Bose-Einstein condensates. After switching off the double well trapping potentials the condensate wavefunctions fall in gravity and expand. When they start to overlap interference fringes appear in the overlapping region. (b) Absorption images on BEC interference obtained in the group of W. Ketterle at MIT. Experimental image with courtesy of W. Ketterle, MIT.

The second experiment performed with this setup started with a split trap and the creation of two distinct Bose-Einstein condensates from a thermal cloud in each trap. In this case an interference pattern would result from two individual matter waves and the experiment should correspond to the controversy discussed above. Note that now the relative phase of subsequent experiments is expected to have a random distribution, shifting the position of the interference pattern with each experimental run.

In both cases the experiments showed a clearly visible interference pattern, confirming the first order coherence of the Bose-Einstein condensate wavefunction for dilute atomic gas experiments. Due to the technical difficulty of these experiments, a distinction between a fixed and arbitrarily moving interference pattern for the two preparation cases could not yet be observed.

The coherence of the condensate wavefunction in connection with its macroscopic size open a new window to quantum mechanics. It becomes possible to directly observe textbook examples for interferometry [18, 84, 85, 94, 95, 96, 97, 98] and for the propagation of wavefunctions in experiment and use them to investigate atom optical elements. An easy realisation is already the reflection of a matter wave by a potential, e.g. an atom mirror [95]. In this case self interference effects occur, similar to the case of numerically propagating a Schrödinger wavepacket towards a potential step.

3.3. BEC as minimum uncertainty state

One important issue concerning the coherence of a Bose-Einstein condensate wavefunction is whether its coherence length is equal to its size or shorter. From another viewpoint this corresponds to the question, if the wavefunction of a trapped Bose-Einstein condensate represents a minimum uncertainty state with respect to the Heisenberg position momentum uncertainty relation.

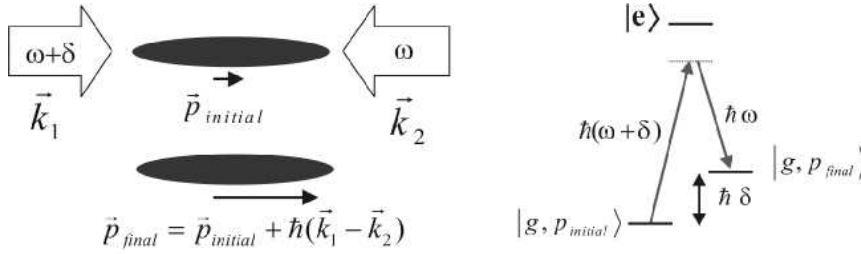


Figure 5. Scheme for Bragg diffraction as a Raman process.

The spatial distribution of the condensate wavefunction can be deduced from experiment by the standard technique of absorption imaging in a straightforward way. The momentum distribution of the trapped sample is however more difficult to obtain, as ordinary time of flight measurements (converting the momentum distribution into spatial distribution) are strongly influenced by the release of mean field energy, the nonlinear term in the Gross Pitaevskii equation 18. The first measurements of the condensate momentum spread implemented Bragg spectroscopy as a new tool [94, 99] in BEC experiments. Bragg spectroscopy is a special case of Bragg scattering [100], which has become a versatile instrument for the manipulation and investigation of the condensate wavefunction.

In principle Bragg diffraction simply corresponds to the scattering of a matter wave off a light intensity grating, similar to the scattering of light waves off crystal planes in crystallography. From an atomic physics viewpoint Bragg scattering can be interpreted as a Raman process, giving intuitive insights into the relevant parameters [94]. In the corresponding picture two momentum states $|g, \vec{p}_{\text{initial}}\rangle$ and $|g, \vec{p}_{\text{final}} = \vec{p}_{\text{initial}} + \hbar(\vec{k}_1 - \vec{k}_2)\rangle$ connected with an atomic ground state are coupled by a two-photon transition. The coupling is typically induced by a pulse from two laser beams having wave vectors \vec{k}_1 and \vec{k}_2 . For the following discussion we will specialise on the case of counterpropagating laser beams as depicted in Fig. 5.

Fig. 5

Imposing energy conservation for the above example of Bragg diffraction with counterpropagating laser beams leads to the relation

$$\hbar\delta = E_{\text{final}} - E_{\text{initial}} = \frac{2}{m}(\hbar k p_{\text{initial}} + \hbar^2 k^2). \quad (26)$$

For this Bragg condition the approximation $k_1 = k_2 = k$, the laser frequency detuning, $\frac{\delta}{2\pi}$ and the particle mass, m were used. Energy conservation (26) introduces a velocity dependence of Bragg scattering, enabling momentum spectroscopy with this technique.

It is important to visualise, that the velocity selectivity corresponds to the frequency width of the Fourier transform of the temporal Bragg pulse envelope. As an example for ^{87}Rb and counterpropagating laser beams the velocity dependence of the resonance condition is given by $\frac{\Delta v}{\delta/2\pi} \approx 0.39 \frac{\text{mm/s}}{\text{kHz}}$. In this sense there are two regimes for Bragg diffraction employed on Bose-Einstein condensates: 1. Bragg spectroscopy, with long pulses corresponding to a higher velocity selectivity than the condensate velocity spread [94, 99, 39] and 2. Bragg condensate optics, relying on short intense pulses, coupling an entire condensate (with all its velocity classes) to a different mean momentum state, e.g. to realise beamsplitters or mirrors [94, 101, 102, 96].

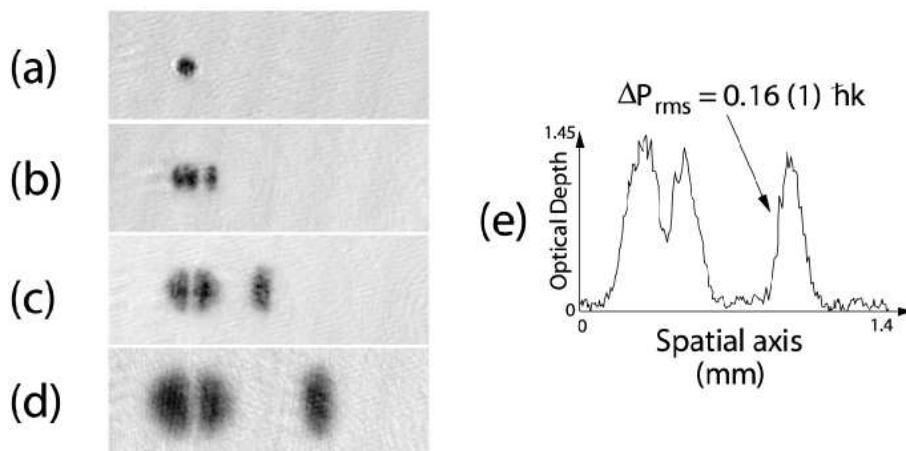


Figure 6. Bragg spectroscopy of a Bose-Einstein condensate. (a)-(d) show absorption images of the ensemble with an increasing time of flight after its interaction with the Bragg laser pulse. These images show the growth of the ensemble due to its momentum spread and the separation of the Bragg scattered momentum component (moving to the right). (e) shows the density distribution of the ensemble along the Bragg laser axis after separation of the scattered component from the remaining part of the condensate. Note that only a narrow momentum component, corresponding to a width of 0.16 photon recoil momenta $\hbar k$, is scattered by the Bragg pulse. This graph clearly demonstrates the velocity selectivity of Bragg scattering in the long pulse regime. Images and graph with courtesy of the National Institute of Standards and Technology, USA.

Bragg scattering is very useful for Bose-Einstein condensate physics, as the associated momentum transfer is typically larger than the momentum spread of the condensate. It consequently leads to a time of flight separation of the atoms which have been scattered from the remaining atoms by $\Delta x = \frac{2\hbar k t_{\text{tof}}}{m}$, where t_{tof} is the time of flight after the Bragg pulse. Fig. 6 demonstrates this splitting with an experimental example of high momentum resolution Bragg spectroscopy.

Using the long pulse regime of Bragg spectroscopy results in the transfer of a certain momentum component to a momentum state which separates from the condensate ensemble during time of flight. With this process it is possible to extract the condensate wavefunction momentum spread. A comparison with the expected value, based on the spatial wavefunction spread and the minimum uncertainty given by the Heisenberg uncertainty relation resulted in a good agreement [99].

3.4. Phase measurements of BEC

The predictability of the spatially varying phase of a Bose-Einstein condensate is intrinsically related to its coherence properties. For applications it is useful to know how the phase of the condensate wavefunction evolves in different experimental situations, e.g. during free expansion or inside a matter waveguide. Phase measurements have to be relative measurements with respect to a suitable reference object, as absolute phase is not accessible in experiment. The phase evolution of the condensate wavefunction can be studied in a well defined and controlled way by the

means of interferometric methods.

Here we discuss a method using a Bragg interferometer scheme (see section 8.1), in which the condensate phase evolution was measured during expansion in free fall [103] as well as in a matter waveguide [104]. The experiments were based on open interferometers, i.e. asymmetric interferometers in which the wavefunction was split in a coherent superposition of two momentum states, but then was subjected to a variable spatial overlap in the output ports. The autocorrelation function of the condensate wavefunction can be extracted by systematic variation of the spatial displacement of the two interfering wavepackets in addition to spatially resolved detection of the interference pattern (see also Fig. 20).

In the measurements of [103] an equidistant fringe pattern was found with a spatial fringe frequency varying with the spatial overlap of the wavepackets. This can be explained within the Thomas-Fermi approximation for the condensate wavefunction. In this limit the ensemble is dominated by mean-field energy and the phase of the trapped condensate wavefunction is constant. After release from the trap the mean-field energy is converted to kinetic energy, which for an initial harmonic trapping potential leads to a quadratic phase profile for each wavepacket [105, 106]. In addition mean field energy leads to a repulsion of the wavepackets during the Bragg beamsplitting process, which adds a relative velocity and thus a linear phase term to the wave function. The phase of the wave function $f e^{i\phi}$ in the direction of the splitting can thus be assumed as [103]

$$\phi = \frac{\alpha}{2}x^2 + \beta x, \quad (27)$$

with the spatial coordinate x and α and β as parameters. The interference pattern originates from the two overlapping wavepackets at the last beamsplitter $f(x - \delta x)e^{i\phi(x - \delta x)}$ and $f(x)e^{i\phi(x)}$, with the spatial distance of the wavepacket centers, δx . The resulting fringes are predicted to be equidistant with a spatial frequency [103],

$$\kappa = \alpha\delta x + 2\beta. \quad (28)$$

The above experiments clearly showed the coherence of the Bose-Einstein condensate wavefunction in important experimental situations with a coherence length comparable to its extends. Furthermore the finding of an equidistant fringe spacing confirmed the Thomas-Fermi mean field approximation theory to provide an accurate description of the coherent matter wave dynamics.

3.5. Phase fluctuations

The conclusion that a trapped Bose-Einstein condensate has a coherence length corresponding to its extends is not true in general. It is only valid for the case of nearly spherical condensates and very low temperatures $T \ll T_c$. For the case of very elongated trapping geometries and temperatures comparable to T_c important discrepancies occur.

In this case the excitations connected to finite temperature cause phase fluctuations. Also concerning the dynamics of the formation process of a condensate wavefunction the condensation process can be assumed to occur in two steps, first establishing the density equilibrium distribution and only later full phase coherence. The ensemble thus shows temporal phase fluctuations [107, 108, 109, 110] during the phase transition.

The character of Bose-Einstein condensation strongly depends on the dimension of the system. In 1D even no Bose-Einstein phase transition occurs but regimes like the Tonks gas appear. Thus one can understand that deforming a spherical condensate geometry towards 1D will already change the physics.

Here we focus on the equilibrium state of a low-dimensional (1D and 2D) quantum gas [110, 111, 112, 113, 114, 115, 116, 117] which is expected to show persistent phase fluctuations and similar effects in finite temperature condensates in very elongated 3D trapping geometries [118]. These fluctuations are connected to thermal excitations with energies below the lowest radial excitation energies but high enough to cause axial excitations. In a handwaving picture one could argue, that information on fluctuations on one end of an elongated condensate wavefunction (e.g. due to interaction with atoms from the normal component) cannot travel to the other end on a timescale smaller than the fluctuation to occur. In corresponding investigations it was indeed found that the phase coherence length in this case can be much smaller than the axial size of the sample [119, 120, 121, 122, 123, 124, 125, 126, 127, 128]

Theoretical predictions result in a temperature dependent phase coherence length, l_ϕ [Petrov2001a, Kreutzmann2002a], with

$$R_z/l_\phi = 16 \left(\frac{am^{1/2}}{15^{3/2}\hbar^3} \right)^{2/5} \frac{k_B T}{N_0^{3/5}} \left(\frac{\lambda}{\omega_z} \right)^{4/5}. \quad (29)$$

In this equation $R_z = \sqrt{\frac{2\mu}{m\omega_z^2}}$ is the Thomas Fermi axial radius of the condensate wavefunction, $\lambda = \frac{\omega_\rho}{\omega_z}$ is the ratio of the radial and axial trap frequencies and N_0 represents the number of condensed atoms. The phase coherence length becomes smaller than the axial size of the condensate below the characteristic temperature [118]

$$T_\phi = \frac{15\hbar^2\omega_z^2 N}{32\mu}, \quad (30)$$

with the chemical potential μ .

One example for the experimental observation of phase fluctuations is given by release measurements from the elongated trapping potential as shown in Fig. 7. For phase fluctuating Bose-Einstein condensates random striations in time of flight measurements occur due to higher momentum components in the condensate wavefunction.

Phase fluctuations are of central importance for many applications of Bose-Einstein condensates. They pose severe limits on the realisation of matter waveguides and are thus particularly important for the rapidly evolving field of microscopic traps and atom chips [129, 130, 131].

3.6. Second and third order coherence measurements

Considering the comparison of light and atom optics, the question whether the matter wavefunction created in the Bose-Einstein phase transition also shows higher order coherence, is of particular importance to distinguish "atom laser" like behaviour from "just" monochromatic matter waves. The link between higher order loss processes and the according condensate correlations [84, 132] represented an important step towards the measurement of higher order correlations of the condensate wavefunction. Second and third order correlations of the condensate wavefunction were determined by a comparison of the measuring rate coefficients for two- and three-body loss processes

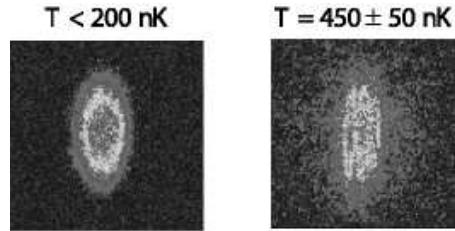


Figure 7. Absorption images of Bose-Einstein condensates produced in an elongated trap after 24.5 ms time of flight. For low temperature (left) the ensemble exhibits long range phase coherence, while for temperatures close to T_c (right) phase fluctuations occur (quasicondensate regime). The new momentum components due to phase fluctuations convert to density modulations after some time of flight, as visible in the right image. Images from the group of W. Ertmer, Hannover university.

for the case of a thermal (i.e. uncorrelated) gas and a Bose-Einstein condensate. The experiments indeed found a two-fold reduction of the two-body loss rate [132] as well as a six-fold reduction of the three body loss rate [84] for the condensed sample. These reduction factors clearly demonstrate second and third order coherence of the condensate wavefunction and are also expected from quantum statistics due to the indistinguishability of atoms occupying the condensate wavefunction. Note, that this type of measurements is restricted to small distance (on the order of particle scattering lengths) correlations, as the typical interatomic distance relevant to loss processes is much smaller than the dimension of the condensate wavefunction.

Although second and third order correlations have been investigated for the short distance regime higher order condensate correlations on distances comparable to the size of the condensate are relatively unexplored. There is however growing interest in corresponding measurements, as they promise significantly expand our knowledge on coherent matter waves. As one example higher order correlation measurement techniques have been used to gain detailed information on phase fluctuating Bose-Einstein condensates [126].

The field of large distance second and higher order correlations of coherent matter waves is at the beginning of an interesting development with still many open questions.

4. Phase manipulation of BEC

The large size of the Bose-Einstein condensate wavefunction opens unique possibilities for the study of quantum mechanics. While most experiments rely on the "direct" detection of this coherent matter wave by optical imaging, the process of its "direct" local manipulation with suitable potentials or interactions seems even more exciting. One possible realisation of this quantum engineering makes use of destructive interactions, e.g. by the controlled removal of atoms from the condensate with a resonant laser beam. As an example this method has been used to increase the average rotation in rapidly rotating condensates, by selective removal of atoms from the low angular momentum centre of the ensemble [133].

In this section we will introduce the concept of non-destructive quantum engineering by phase manipulation of the condensate wavefunction, in particular by phase imprinting.

4.1. Concept of phase imprinting

Phase imprinting relies on the (simplified) idea, that the local phase evolution of a quantum mechanical wave function is governed by its Hamiltonian evolution

$$\psi(\vec{r}, t) \propto e^{\frac{i}{\hbar} H(\vec{r}, t)t} \psi(\vec{r}, 0). \quad (31)$$

In case ψ is an Eigenfunction of the Hamiltonian and E is the corresponding Eigenenergy, this relation simplifies to a pure phase change

$$\psi(\vec{r}, t) \propto \psi(\vec{r}, 0) e^{\frac{i}{\hbar} E(\vec{r}, t)t}. \quad (32)$$

In experiment the Hamiltonian $H(\vec{r}, t) = H_0(\vec{r}, t) + V(\vec{r}, t)$ can be controlled by adding an external potential $V(\vec{r}, t)$ to the remaining energy terms contained in H_0 . The external potential can be produced in a convenient way with a pulsed, spatially modulated and far off resonant laser beam, leading to a light shift potential. The main idea is that the additive potential creates an additional phase distribution along the condensate wavefunction on a very short timescale, such that other phase influences during the exposure are nearly constant and negligible. The pure phase shifting action aimed at in experiment can be approximately realised in this way, if the following is fulfilled: the external potential is arranged to act on all occupied Eigenfunctions of the Hamiltonian in the same way and in addition it is much larger than the other energy terms, i.e $V \gg H_0$. In this way the phase of the quantum mechanical wavefunction can be significantly changed, by pulsing on a strong laser field for a time much shorter than its correlation time, τ_c . The correlation time, $\tau_c = \frac{\xi}{c}$ is given by the time a wave function disturbance moving with the condensate sound velocity, c , (see Eq. (25)) over a distance corresponding to the condensate healing length, ξ (see Eq. (21)).

The method of phase imprinting has been proposed with the main aim to create circular flow with vortices in a Bose-Einstein condensate [134]. It was however already pointed out, that this method is very general and that nearly arbitrary manipulations of the wave function can be performed with it. This is in particular true, if the method is extended by additional resonant laser fields, allowing amplitude manipulations also, so that amplitude and phase can be "designed". In principle full control of the condensate wavefunction could be attained if the optical resolution would be below the healing length scale.

Note that the method of phase imprinting is related to holographic laser beam manipulation techniques in optics and represents a similarly powerful tool for coherent matter wave optics.

4.2. Experiments on phase manipulation of BEC

The intriguing possibility to "engineer" the quantum mechanical wavefunction of a Bose-Einstein condensate using controlled phase manipulation enables fascinating experiments. Phase manipulation with the help of the earth gravitational potential or a similar acceleration pseudopotential was employed to modify the interference pattern in experiments with Bose-Einstein condensates in optical lattices [81, 135]. Furthermore the creation of a new hyperfine state condensate component with a circular 2π phase gradient by spatially phase modulated coupling with an ordinary condensate resulted in the first experimental creation of a Bose-Einstein condensate vortex state in dilute atomic gases [136].

Direct imprinting of a phase pattern with the help of suitably shaped laser fields as discussed above has the advantage of being very flexible. In principle all kinds



Figure 8. Experimental example of the possibilities of phase imprinting. The image is created from four different absorption images of condensates with different letters imprinted in the phase of the wavefunction. The images are taken in an interferometric setup which converts the phase information into density information (see [137]). Images with courtesy of the National Institute of Standards and Technology (NIST), USA.

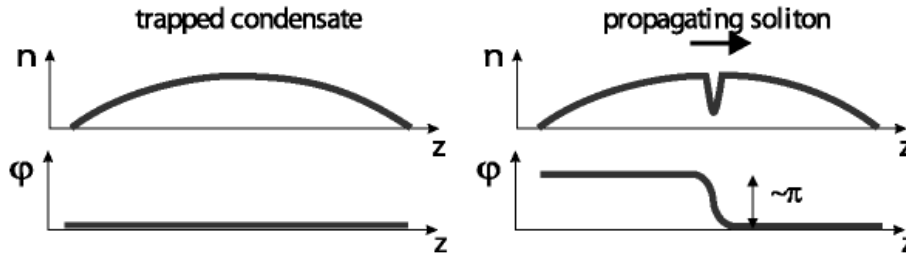


Figure 9. Schematic view of the density and phase distribution of a dark soliton in a Bose-Einstein condensate wavefunction (right) as compared to the condensate ground state (left).

phase distributions can be created within the condensate wavefunction, e.g. the letters "NIST" as shown in Fig. 8.

In this section we will concentrate on the creation of dark solitons as a first use of the method of phase imprinting [138, 137]. The physics of dark solitons themselves will be addressed in more detail in section 6.2. In order to understand their creation with the help of phase imprinting it is however important to visualise their density and phase distribution. The schematic view in Fig. 9 shows that the density distribution of a condensate with a dark soliton differs from the density distribution of an unperturbed Bose-Einstein condensate wavefunction only in a small spatial region, in which it displays a kinklike minimum. The dark soliton phase distribution however shows a two-valued distribution with a steep gradient transition at the kink position. A "black" soliton with a stationary zero density minimum would result for a π phase jump, i.e. an infinite phase gradient. Starting from the phase distribution difference it becomes clear, that a dark soliton excitation in a Bose-Einstein condensate can be produced, by imprinting a phase (typically close to π) on one half of the condensate. This was experimentally accomplished by shining a far detuned laser beam on one half of a trapped Bose-Einstein condensate. One important aspect in these experiments was the fact, that the optical resolution of a few μm was larger than the condensate healing length, which was below 500 nm. This resulted not only in a phase gradient as compared to a phase jump, but also in a momentum kick for this position. The momentum introduced into the condensate wavefunction removed density from the kink position in the form of density sound waves and thus helped to create the intended dark soliton excitation. The resulting dynamics is clearly displayed in the

experimental images shown in Sec. 6.2, Fig. 16. The experiment displays a density and a dark soliton wave moving in opposite directions and with different velocities, with the soliton significantly slower than the system sound velocity.

5. Physics of "atom lasers"

The availability of coherent matter waves with macroscopic occupation in analogy to the optical laser soon led to the idea of an "atom laser" associated to Bose-Einstein physics. In fact the phenomenon of Bose-Einstein condensation itself shows many analogies to laser physics [132, 139]. The modes of the harmonic trapping potential holding the atoms can be associated with the electromagnetic modes of the light field, with the trap ground mode being analogous to the laser mode. The atoms in the higher trap modes can be regarded as gain medium reservoir, from which they can be transferred to the ground state mode via stimulated elastic scattering processes in analogy to stimulated emission from excited atomic states in an optical laser. Furthermore the optical pumping process could be associated with the cooling of the sample, leading to an "oversaturated" population of excited trap states, similar to population inversion. These analogies find support in the experimental observation of condensate wavefunction growth after a sudden evaporation step in an ensemble with parameters close to the Bose-Einstein phase transition [45, 140]. These experiments clearly showed an initial exponential increase of the condensate wavefunction population, which is consistent with stimulated scattering processes into this ground state. Despite the large similarities between Bose-Einstein condensation and the optical laser, there are also significant differences. One important aspect is that a Bose-Einstein condensate is a state reached in thermodynamic equilibrium, while the optical laser requires working conditions far from this equilibrium. Furthermore a laser is typically associated with a beamlike output and one might also wish for a cw operation.

These aspects and according experiments will be discussed in more detail in the following sections.

5.1. Ideas and concepts of atom lasers

The ideas and concepts for atom lasers can be roughly split in two categories, addressing output coupling and continuous loading processes. One basic idea is to use a trapped Bose-Einstein condensate as reservoir and to couple part of this matter wave field out into untrapped states. This is conceptually similar to partial transmission of the photon field inside a laser resonator through the outcoupling mirror. Corresponding experiments will be discussed in the following section. There have been many theoretical investigations on the physics of the output mechanism and the resulting matter wave field outside the trap [141, 142, 143, 132, 144, 145, 146, 147, 148, 149, 150, 151, 152, 153, 154, 155, 156, 157, 158, 159, 160, 161, 162]. The internal degrees of freedom and their coherent manipulation with external fields opens more possibilities for this process than the optical analogue of tunneling through a potential barrier. The most commonly used mechanism starts from a magnetically trapped Bose-Einstein condensate, which is transferred to magnetically untrapped states. Other suggested schemes reach up to the controlled formation of molecules from an atomic Bose-Einstein condensate, resulting in a molecular matter wave laser beam (e.g. [160]).

Other important concepts aim at an increased matter wave flux by the realisation of a continuously loaded Bose-Einstein condensate. These ideas ideally complement the above output coupling schemes, which can only provide a pulsed beam, if starting from a finite condensate. Several approaches build on the well established techniques of laser cooling. They try to circumvent typical temperature and density limitations due to photon scattering and reabsorption processes [163, 164, 165, 166, 167, 154, 168, 169, 170]. In recent experiments phase space densities on the order of 1/10th were achieved using narrow linewidth transitions in strontium as well as by using advanced Raman cooling schemes in optical lattices [171, 172, 173, 174, 175].

An again different approach relies on continuous evaporative cooling in a continuously loaded long magnetic guiding structure [176]. First experiments on this scheme demonstrated the principal ability to reach dense cold atomic beams [177] and are very promising to achieve quantum degeneracy in a beam setup.

Conceptually similar attempts to realise continuous or quasi-continuous Bose-Einstein condensation are based on repetitive or even continuous loading of a conservative trap with thermal atoms and evaporation therein.

The first temporally maintained Bose-Einstein condensate was however realised by repetitively loading an optical dipole trap with conventionally produced Bose-Einstein condensates [178]. Bose-Einstein condensates were produced with well established standard techniques in a "production chamber" and then transferred to a spatially separated "experiment chamber" with an optical tweezer [179]. In the experiment chamber they were joined with a continuously stored Bose-Einstein condensate. This experiment demonstrated the feasibility of joining coherent matter waves for long term observation.

In summary the highly intriguing prospect of a continuous "atom laser" has triggered experimental efforts aiming at diverse schemes and aspects. Until today the goal of a high flux coherent matter wave source and the interest in deeper understanding of the properties of atom lasers motivate this work. It should be however noted, that the current state of the art technology for the production of Bose-Einstein condensates poses severe limitations on the practical realisation of orders of magnitude more flux by simple power arguments. Nowadays the production of coherent matter waves with a population of 10^7 atoms every 10 s requires typical laser powers of at least 100 mW for trapping and precooling a large enough number of atoms. Following a simple extrapolation even a modest coherent matter wave flux of 10^{10} atoms/s (compared to optical lasers with on the order of 10^{20} photons/s) would require kW laser power. Future sources will have to significantly increase efficiencies or realise new technological approaches to coherent matter waves, e.g. cryogenic techniques [180]. Once a suitable source is realised the success of the "atom laser" will be determined by our ability to manipulate and use its properties, which will be discussed in the following.

5.2. Experiments on atom lasers

The first "atom laser" was realised by pulsed output coupling from a magnetic trapping potential [181]. In this experiment a conventionally produced ^{23}Na Bose-Einstein condensate in a magnetic trap was subjected to rapid radiofrequency sweeps. The radiofrequency partially coupled the condensate wavefunction from the trapped $F = 1, m_F = -1$ state to the untrapped $F = 1, m_F = 0$ and antitrapped $F = 1, m_F = 1$ states, resulting in matter wave pulses (see Fig. 10).

The swept radiofrequency output coupling has the advantage of reproducible

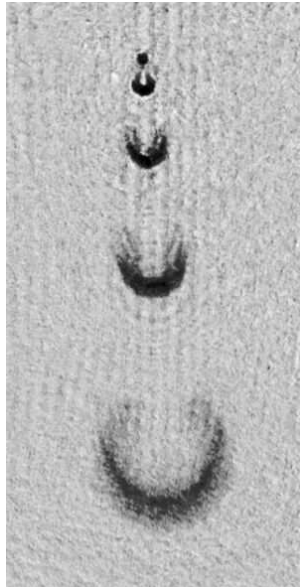


Figure 10. Atom laser pulses realised by repeated pulsed output coupling from trapped Bose-Einstein condensate. Image with courtesy of W. Ketterle, MIT.

results, even in the presence of a slight magnetic field fluctuations, but is intrinsically limited to short output pulses. A significant improvement of the atom laser pulse length was achieved based on a magnetic trap setup optimised for a very quiet magnetic field environment [182]. This enabled the slow output coupling of an entire Bose-Einstein condensate with a fixed radiofrequency, leading to a "quasi-continuous atom laser" beam. The simultaneous output coupling using two radio frequencies in this highly stable setup resulted in two overlapping atom laser beams originating from different positions of the trapped condensate wavefunction [183]. As these positions are given by the trap magnetic field variations and the resonance criteria for rf-induced spinflip transitions, it is possible to test the coherence of different parts of the condensate with this technique. The resulting interference pattern in the according experiment beautifully confirmed the large transverse coherence length of a trapped Bose-Einstein condensate. Fig. 11 shows experimental images on the transverse condensate coherence as a function of temperature. Further experiments clearly demonstrated, that radiofrequency output coupling leads to temporally coherent atom laser beams, which can be used in interferometric applications [184].

A different type of quasi-continuous atom laser was demonstrated based on rapidly pulsed raman output coupling [101]. In this experiment a two photon transition was used to partially transfer the trapped atoms to a different internal and momentum state. The technique is in principle similar to the Bragg diffraction scheme discussed above, but with a two photon transition coupling different internal states. The photon momentum transfer in this scheme allows the extraction of a beam, aiming in any direction at will, from the condensate wavefunction, as opposed to the freely falling beams in the radiofrequency schemes. Using a rapid succession of short raman pulses resulted in spatially overlapping atom laser pulses, which joined to one beam.

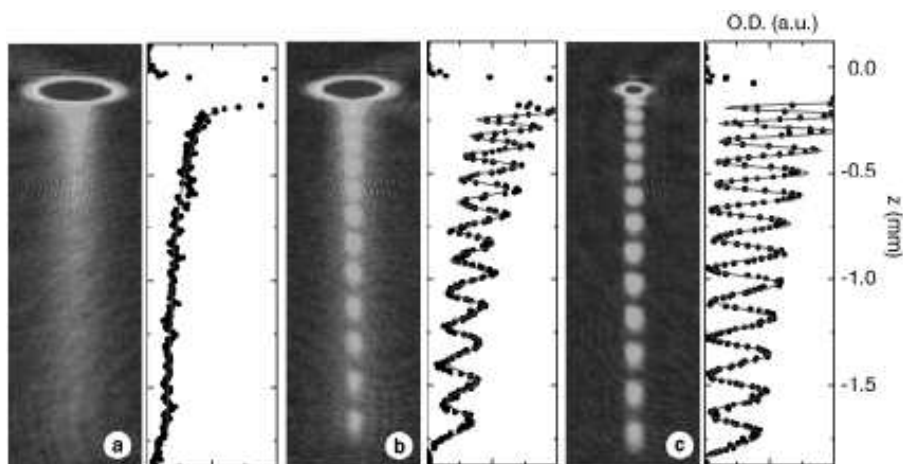


Figure 11. Continuous output coupling of two overlapping atomic beams from different positions of trapped atomic ensembles. The absorption images and the according profiles correspond to a temperature $T > T_c$, $T \leq T_c$ and $T \ll T_c$ (from left to right). The buildup of a coherent matter wavefunction during the Bose-Einstein phase transition is clearly reflected in the visibility of the interference between the two atomic beams. Images with courtesy of I. Bloch, Mainz university and T. W. Hänsch, MPQ.

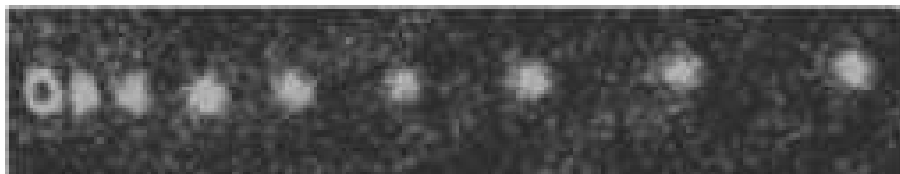


Figure 12. Pulsed atom laser output from a Bose-Einstein condensate (left) stored in an optical lattice. (The image is rotated such that gravity acts from left to right.) Image with courtesy of M. Kasevich, Stanford university.

The analogy between optical and atom laser beams was further extended by the realisation of a "mode-locked" atom laser [185]. The realisation of many atom laser modes was accomplished by first loading a Bose-Einstein condensate into an one-dimensional optical lattice resulting from a retroreflected laser beam in the vertical direction. The resulting condensate was extended over several lattice sites, which were weakly coupled by tunneling through the optical lattice potential barriers. Output coupling due to tunneling from all these potential wells at different heights can be thought of as many overlapping atom laser beams with different frequencies according to their velocities acquired in the gravitational potential. Similar to an optical modelocked laser, in which many resonator modes overlap to form short spatial light pulses, the output of this type of atom laser is intrinsically pulsed, with a pulse separation connected to the optical lattice spacing and the earth gravitational potential.

The continuous development of new trapping schemes and matter wave manipulation tools has led to a variety of further pulsed or quasi-continuous atom

laser realisations, the most recent of which stem from optical traps [186].

5.3. Coherence properties of atom lasers

The idea of an "atom laser" as a matter wave source for experiments, in particular for atom interferometry, has triggered a vivid discussion about the coherence of this device. This question depends on the atom laser mechanism under investigation. For output coupling of matter wave radiation from a trapped Bose-Einstein condensate there was experimental evidence of visible interference fringes [183, 184]. This shows some degree of first order coherence, but the limits of the coherence length are still subject to discussion. From the analogy to the optical laser one would expect the output coupled matter wave to have a larger coherence length than the size of the trapped condensate. In this picture it should depend on the output coupling rate as well as the evaporation rate of the thermal component, replenishing the condensate. Furthermore there are influences due to the width of the output coupling transition and the relative size of the thermal cloud, leading to a phase diffusion process of the condensate wavefunction.

General aspects concerning the coherence properties of continuous atom laser schemes have so far been investigated for quasicontinuous output coupling [184]. Particular coherence aspects connected to continuously pumped atom laser schemes still lack experimental realisations for their confirmation.

5.4. Amplification of coherent matter waves

A major point concerning atom lasers and coherent matter wave sources is the availability of suitable gain media for coherent amplification. The possibility of matter wave amplification by stimulated scattering was beautifully revealed by the detailed investigation of the formation process of a Bose-Einstein condensate itself [45, 75, 187, 188, 189, 140]. This amplification relies on scattering of atoms into the macroscopically occupied mode of the condensate wavefunction. Due to the nature of the scattering process particle number, momentum and energy conservation have to be fulfilled as an essential requirement for the implementation of a coherent matter wave amplifier. Evidence of controllable matter wave amplification was found in a set of spectacular experiments illuminating a Bose-Einstein condensate with a single laser beam [190, 191, 192].

In these experiments amplification of spontaneously scattered photons and the according recoiling matter waves was realised. Under suitable orientation of light polarisation as well as the light incident perpendicular to the long axis of a cigar-shaped Bose-Einstein condensate a regular array of outgoing matter waves emerges, accompanied with directed light beams containing the scattered photons. Matter wave amplification using this and similar schemes is very versatile, not only showing Bragg and Kapitza-Dirac scattering of atoms in one internal state, but also Raman scattering with the involved atoms changing their hyperfine ground state [192]. These processes clearly demonstrate the possibility to use a Bose-Einstein condensate illuminated with one light beam as gain medium for matter wave seeds, but do not provide a controlled seed, i.e. in comparison with a light amplifier they would compare to amplified spontaneous emission (ASE).

A full matter wave amplifier based on the above processes was however realised and characterised by using first a two beam light pulse to extract a small matter wave

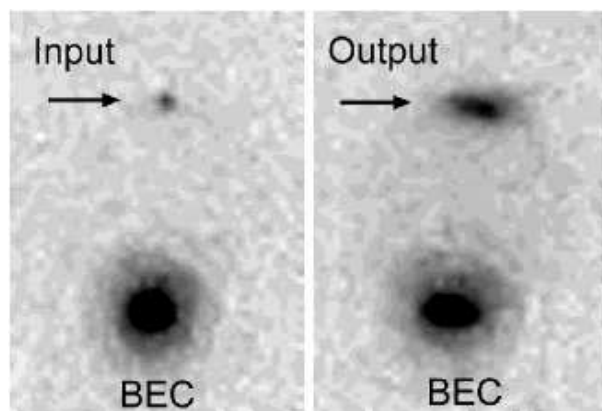


Figure 13. Experimental images on matter wave amplification at MIT. The amplification of a small seed matter wave is provided by a Bose-Einstein condensate illuminated with an appropriate laser beam. The images show the Bose-Einstein condensate and the seeded wave some time after the seed has passed the condensate. The left/right image was taken without/with the laser beam illumination (no amplification/amplification). Images with courtesy of W. Ketterle, MIT.

seed via Bragg scattering from a Bose-Einstein condensate and after that apply a single light beam to turn the same Bose-Einstein condensate into a gain medium [46, 193]. In a series of measurements controlled matter wave amplification using this scheme was clearly demonstrated with typical amplifications of 10-100 (see Fig. 13). Furthermore the coherence of the amplification process was proven by applying a second Bragg scattering pulse after the amplification sequence and investigating the interference fringes, when the resulting and the amplified matter wave are overlapped.

In summary there is a well established tool set for matter wave amplification using Bose-Einstein condensates, its control with light fields as well as the preparation of seed matter waves available, which is only limited by the size of the Bose-Einstein condensate acting as gain medium.

5.5. Future developments

The field of coherent matter wave physics building on Bose-Einstein condensate wavefunctions has seen extraordinary progress in the last years, with many important developments. Nowadays there exist standard techniques for the reliable production of Bose-Einstein condensates as sources of coherent matter waves and for their manipulation. The intensely pursued realisation of a continuous high flux source for coherent matter waves will open this dynamic field for interesting applications and further fundamental experiments. This is in particular true for applications in atom interferometry [10], where one might expect similar progress as after the introduction of the laser in light interferometry.

The creation of high precision sensors based on coherent matter waves is a main motivation for the very active field of atom chips [130, 131]. These devices try to combine the proven but bulky laboratory techniques for the production of coherent matter waves with the miniaturisation and control possibilities offered by

the semiconductor industry. A chip based coherent matter wave sensor would thus greatly improve the versatility of matter wave experiments for high precision measurement applications. Recent investigations in this field concentrate on the coherence properties of 1d waveguides (see Sec. 3.5) and the influence of fluctuations due to the presence of the chip surface close to the guided or trapped matter waves [194, 195, 196, 197, 198, 199, 200, 201, 202].

In summary the field of atom lasers and their uses is only at the beginning of a very promising development. Exciting results such as atom lasers extracted from Bose-Einstein condensates and coherent matter wave amplifiers as well as the establishment of a versatile coherent atom optical tool set represent a solid basis for the future tasks.

6. Nonlinear atom optics with coherent matter waves

Nonlinear atom optics adds new fascinating features to the physics of coherent matter waves. In contrast to light beams coherent matter waves, even in their realisation as nearly ideal dilute atomic gases, exhibit intrinsic nonlinear behaviour. The nonlinearity arises from density dependent interparticle interactions, e.g. the term $g|\phi(\vec{r})|^2$ in the Gross Pitaevskii equation, Eq. (18). Even if these interactions only lead to slight changes of the Bose-Einstein phase transition itself, they add significant new physics to the coherent matter wave itself. The intrinsic nonlinearity gives rise to many fascinating phenomena, such as four wave mixing in analogy to nonlinear optics, solitons in analogy to general nonlinear wave effects and also new couplings, i.e. leading to spin mixing and thus magnetic matter wave effects, to name only a few examples. In the following we will concentrate on these examples and discuss them in more detail.

6.1. Four wave mixing

Nonlinear optics is the basis of intriguing phenomena, such as wave mixing with sum and difference frequency generation and became widely accessible with the invention of the laser as intense and coherent source of light waves. Considering the discussion on analogies between laser radiation and coherent matter waves the question arises, if similar phenomena can arise in these systems. The occurrence of nonlinear phenomena in coherent matter waves seems natural in view of their intrinsic nonlinearity: In respect to the comparison with nonlinear optics the term $g|\phi(\vec{r}, t)|^2\phi(\vec{r}, t)$ describing interactions in the Gross Pitaevskii equation 18 has to be compared to the term $\chi^{(3)}|E|^2E$ representing the interaction of the electric field, E , in a medium with susceptibility $\chi^{(3)}$.

Just as in the discussion on atom lasers and matter wave amplifiers (see above) there is an important distinction between matter and light waves in respect to particle number conservation. While it is possible to convert two photons into a single one with the sum frequency or to make the reverse transformation in optics, the same process is not obvious for matter waves due to their mass. The amount of energy connected to the mass of the atoms constituting the matter waves discussed in this review is far beyond all other energy scales involved and thus naturally enforces particle number conservation. Matter wave mixing experiments are thus limited to special classes of phenomena, e.g. degenerate four wave mixing, which was demonstrated in a beautiful experiment [203] (see Fig. 14). Transformed to an appropriate frame this experiment realised the situation. Two counterpropagating matter waves and one orthogonal

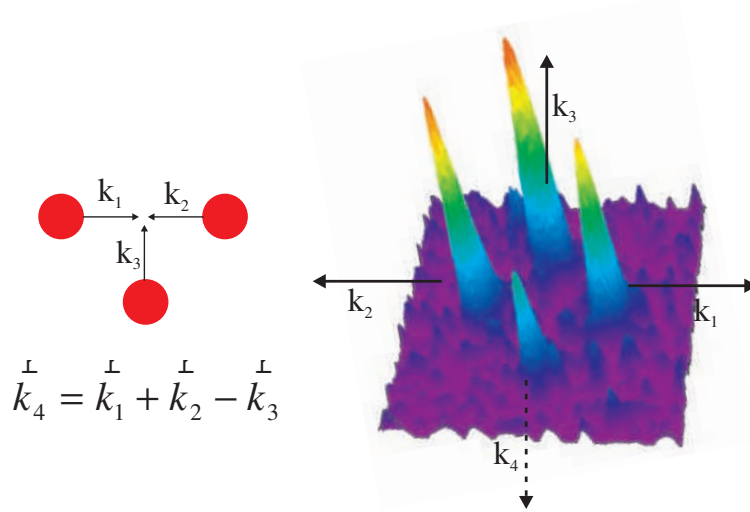


Figure 14. Four wave mixing of matter waves as observed at NIST. Left: schematic view of the collision process leading to four wave mixing and the involved wavevectors. Right: Experimental absorption image of the matter waves after the collision process. Four wave mixing of the three colliding wavepackets gives rise to the appearance of a new fourth wavepacket. Experimental image with courtesy of the National Institute of Standards and Technology, USA.

matter wave, all of equal momentum, interact with each other and give rise to a fourth matter wave. This new matter wave has a wavevector equal to the vectorial sum of the counterpropagating waves (which is zero) minus the wavevector of the orthogonal wave, i.e. it is counterpropagating to this wave $\vec{k}_4 = \vec{k}_1 + \vec{k}_2 - \vec{k}_3$ (see Fig. 14). Even though this image is analogous to the case encountered in nonlinear optics, we want to note again, that this is not true in general. As an example in the above experimental scheme it would not be possible to use a different momentum value for the orthogonal wave, i.e. $k_3 \neq k_1 = k_2$, in order to create variable output frequencies, as routinely performed in nonlinear optics. This is a result of energy and momentum conservation for massive particles and can be most intuitively understood in a particle scattering based picture for the mixing process.

In this approach the counterpropagating matter waves with wavevectors \vec{k}_1 and \vec{k}_2 interact via elastic collisions coupling the waves to a s-wave scattering sphere (only s-wave collisions are involved due to the low relative momenta) (see Fig. 15 (b)). In a single particle picture this sphere results from the quantum mechanical average over many binary collisions. Each binary collision however has to fulfill momentum and energy conservation. Momentum conservation immediately leads to $\vec{k}_1 + \vec{k}_2 = \vec{k}_1' + \vec{k}_2'$ and due to $\vec{k}_1 + \vec{k}_2 = 0$ to $\vec{k}_1' = -\vec{k}_2'$ as well as $\vec{k}_1 = \vec{k}_2$. Energy conservation on the other hand requires $k_1^2 + k_2^2 = k_1'^2 + k_2'^2$ resulting in $k_1 = k_2 = k_1' = k_2'$. The collisional coupling thus can only support equal and opposite momenta for the waves \vec{k}_3 and \vec{k}_4 .

At this point it is important to realise, that the collisional view of the four wave mixing process makes an intriguing connection to matter wave amplification as discussed in section 5.4. The emergence of a clearly visible peak corresponding to $\vec{k}_{\text{new}} = -\vec{k}_3$ instead of a scattering sphere can be interpreted as an amplification

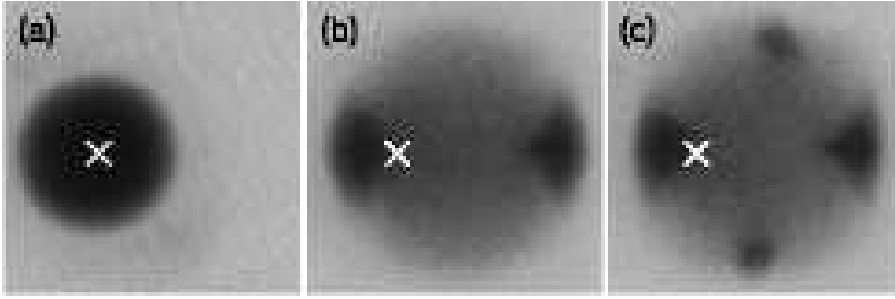


Figure 15. Four wave mixing of matter waves with a small seed and high gain. All images display the ensemble after 43 ms of ballistic expansion. (a) The original Bose-Einstein condensate with a 1% seed (barely visible). (b) After the collision of two matter waves created by Bragg scattering half the original condensate to a higher momentum state. The gray circular background corresponds to amplified spontaneous s-wave scattering events (similar to ASE in laser physics). (c) High gain four wave mixing result after the seed from (a) interacted with the colliding waves from (b). Both the seed and the counterpropagating four wave mixing outcome were significantly amplified and now nearly completely consist of correlated atom pairs. Image from [204] with courtesy of W. Ketterle, MIT.

process of the orthogonal matter wave due to stimulated scattering. Momentum conservation then necessarily requires the emergence of a fourth matter wave with opposite momentum (see Fig. 15). The amplification properties of the four wave mixing process were investigated in detail in [204]. They also point out, that the degenerate matter wave scattering leads to entanglement between the amplified and the new wave components: Each binary scattering event leads to two particles moving in opposite directions with no possibility to decide which of the colliding particles took which way. If the seed wave \vec{k}_3 has relatively small occupation in comparison to its amplified population, then the new and the amplified wave might be imagined to essentially consist of entangled atom pairs.

As a last point we want to stress, that the amplification process in four wave mixing experiments can be interpreted in an analogous way to the amplification using Bragg scattering off a light grating as discussed in section 5.4. Indeed the matter waves with wavenumbers k_1 and k_3 build up a matter wave density grating by which the third matter wave k_2 is scattered as in light optics into the new wave k_4 .

In summary four wave mixing of coherent matter waves represents a fascinating analogy to wave mixing phenomena in nonlinear optics. In addition the entanglement creation connected to the four wave mixing process leads to a new source of entangled particles with promising applications in quantum computing or high resolution interferometry [205, 204].

6.2. Dark solitons

Another class of nonlinear phenomena in matter wave physics consist in solitons as fundamental excitations. Also with the physics of solitons matter wave physics is linked to general nonlinear wave effects, where solitons appear in a wide variety of systems, e.g. in optical fibers or as "Tsunamis" in water. The word soliton denotes the phenomenon of single, i.e. solitary, wavepacket like excitations, which travel with constant shape and without significant dissipation. In more physical terms they are

density variations which self stabilise due to a balance of nonlinear interactions (trying to compress the wavepacket) and dispersive effects (tending to spread the wavepacket)

In a Bose-Einstein condensate matter wave this balance occurs between the nonlinear mean field interaction and quantum pressure. The quantum pressure is related to the kinetic energy associated with the soliton velocity field, and is minimized by widening the spatial extent of a density variation. It is important to note, that this is independent of the nature of the density variation, i.e. whether it is a density maximum or minimum. The possible solitonic matter wave excitations can thus be classified according to the sign of the s-wave scattering length, a , determining whether the interparticle interaction is attractive ($a < 0$) or repulsive ($a > 0$) leading to bright or dark solitons.

A *bright soliton*, i.e. a stable density maximum, can occur for the case of attractive interactions, which tend to further increase density by compressing the maximum and thus balance the spreading effects. Bright solitons and trains of bright solitons have been observed in experiments with bosonic Lithium, having attractive interactions [206, 207]. These experiments are very demanding, as large Bose-Einstein condensates with attractive interactions are in general not stable against collapse. The experimental realisation was possible by tuning the scattering length with a Feshbach resonance, first producing a condensate with repulsive interactions, loading it into a one-dimensional geometry and then switching the interaction to attractive by a change in the magnetic offset field.

A *dark soliton*, i.e. a stable density minimum, is a fundamental excitation for matter waves with repulsive interactions, which are realised in most experiments on Bose-Einstein condensation. Here the quantum pressure spreading effect can be balanced by the repulsive interactions, for the case of a density minimum. The interaction energy would be minimised by filling this minimum, which is by shrinking its spatial extent. In the following we will focus on this kind of soliton which was first experimentally realised at Hannover as well as NIST [138, 137], and later also studied at JILA [208].

For a homogeneous, one dimensional Bose-Einstein condensate matter wave function dark soliton excitations can be found as the following solution of the 1d Gross Pitaevskii equation [209, 210]:

$$\Psi_k(x) = \sqrt{n_0} \left(i \frac{v_k}{c_s} + \sqrt{1 - \frac{v_k^2}{c_s^2}} \tanh \left[\frac{x - x_k}{l_0} \sqrt{1 - \frac{v_k^2}{c_s^2}} \right] \right). \quad (33)$$

In this equation the parameters are the matter wave density n_0 , the position x_k and velocity v_k of the dark soliton, the correlation length $l_0 = (4\pi a n_0)^{-1/2}$, and the speed of sound $c_s = \sqrt{4\pi a n_0} \hbar / m$, where m is the atom mass. Analysing this expression one finds the special case of a so called *black soliton* with zero density at the minimum, if the matter wave phase exhibits a π phase jump at the density kink position. The black soliton is at rest, i.e. $v_k = 0$, while for all other cases the kink in the condensate wave function moves along the condensate, has nonzero density and is associated with a finite phase gradient.

The finite kink velocity of a dark soliton is connected to the gradient in the matter phase distribution $\phi(\vec{r})$, which defines a probability current density. The associated superfluid velocity field $v(\vec{r}) = \frac{\hbar}{m} \nabla \phi(\vec{r})$ leads to a localized peak in the velocity distribution of the matter wave.

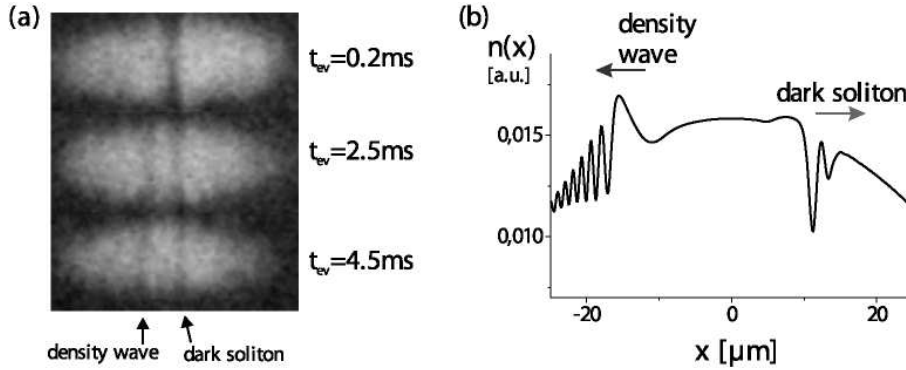


Figure 16. (a) Evolution of a dark soliton in a Bose-Einstein condensate wavefunction. The matter wave evolved in the trapping potential for a time, t_{ev} after phase imprinting. The images were taken after an additional time-of-flight of 4 ms. The matter wave dynamics during this additional time of flight leads to density minima for the dark soliton as well as for an additionally created density wave [138]. (b) Numerical simulation of the density distribution of a dark soliton propagating in a BEC after phase imprinting.

The relatively simple two-valued phase distribution of a dark soliton makes this excitation favourable for the method of phase imprinting as discussed in Sec. 4.2. This method was used for the first experimental realisation of dark soliton excitations in Bose-Einstein condensates [138, 137].

An important aspect is that although dark solitons are only stable in one dimensional or quasi one dimensional systems, they can also be produced in three dimensional near spherical geometries [137, 208]. In these geometries they are however unstable against transverse excitations [210, 211], e.g. their decay into vortex rings was observed in a recent experiment [208].

Fig. 16 shows experimental data and numerical simulations on the propagation of a dark soliton during some evolution time, t_{ev} , in the trap.

In addition to the dark soliton a density wave is created in the phase imprinting process due to the finite optical resolution as compared to the matter wave healing length. The resulting steep light shift potential gradient transfers momentum onto the part of the matter wave, which is at the intended kink position. This reduces the density at the position of the imprinted phase gradient and thus helps in the creation of the kink associated with the dark soliton.

The velocity field due to the phase gradient of the dark soliton is directed opposite to the movement of the density kink. This can be intuitively understood as the movement of the density minimum necessitates a transfer of matter in the opposite direction.

The matter wave flux underlying a dark soliton was analysed using Bragg velocity spectroscopy, i.e. Bragg scattering in the regime of long pulses as discussed in Sec.3.3. In these experiments good agreement with theory was found [39].

The creation of solitons in Bose-Einstein condensates demonstrated fundamental nonlinear excitations in matter waves and represents a nice experimental implementation of the method of phase imprinting. The investigation of solitons as signature of nonlinear excitations depending on the interparticle interactions is

an actual topic in the physics of matter waves. Recent studies demonstrated the possibility use optical lattice geometries in order to modify the effective mass and thus the interactions of the matter waves [212]. With this dispersion management technique it was possible to change the nature of interactions from repulsive to attractive and to observe bright solitons in this regime. Further progress in this area is expected from the realisation of so called discrete solitons in optical lattices, which are an actual topic of theoretical work [213, 214, 215, 216, 217] as well as mixed species solitons.

6.3. Magnetic matter wave effects

The intrinsic nonlinear interactions of matter waves not only gives rise to the fascinating nonlinear single state effects discussed above, but opens a wide variety of new phenomena based on an inter-state coupling in multi-component condensates. Multi-component matter waves are composed of atoms with multiple internal states, e.g. multiple hyperfine states or multiple magnetic quantum states in atoms with non-zero total angular momentum.

In the typical magnetic trap arrangement for the creation of Bose-Einstein condensates the additional degrees of freedom due to the internal atomic states are frozen by energetic restrictions. Once released by hf coupling [218] or by storage in a state-independent optical dipole trap [219] magnetic effects and intriguing multi-state dynamics as well as new thermalisation phenomena become visible.

Experiments on coherent multi-component matter waves with spin degree of freedom were performed in two different systems. So called spinor condensates were first realised with optically trapped ^{23}Na in the $F=1$ hyperfine state [219, 220, 36, 221], while at the same time a different class of multi-component system was realised by coupling the magnetically trapped $F = 1, m_F = -1$ and $F = 2, m_F = 1$ hyperfine states of ^{87}Rb [218]. This system is analogous to an effective spin 1/2 system and shows fascinating mixing and demixing effects [222]. Long intrinsic inter-state coherence times up to several seconds were found [85, 223]. In recent experiments this system was used for various studies on spin transport, coherence and decoherence phenomena, in particular with respect to interactions with the normal component [224, 225, 226, 227]. Fig. 17 shows an example of spin domain formation, which was studied in detail in [226].

Recently studies on $F = 2$ ^{87}Rb spinor condensates were performed [228] that extend the multi-component physics to five states and offer additional rich structures.

Optically trapped spinor condensates offer the possibility of collisional coupling, which gives rise to intrinsic magnetic properties of the system and opens intriguing new possibilities for the study of finite temperature phenomena.

The magnetic properties of coherent matter waves are typically considered for a single hyperfine state, e.g. denoted by the total single particle spin F . They give rise to a characteristic distribution of the m_F -components, i.e. the spin orientations projected on a quantisation axis, and can be classified similar to solid state magnetic effects.

Although studies on dipolar quantum gases, where magnetic (or electric) dipole-dipole interactions play a dominant role, are an actively pursued field [229, 230, 231, 232, 233], most experiments deal with matter wave systems dominated by collisional mean field interactions. In the following we will concentrate on these systems, ruled by a spin-dependence of the molecular potential curves which are involved in the collisional interaction. The interactions can be classified most intuitively by first

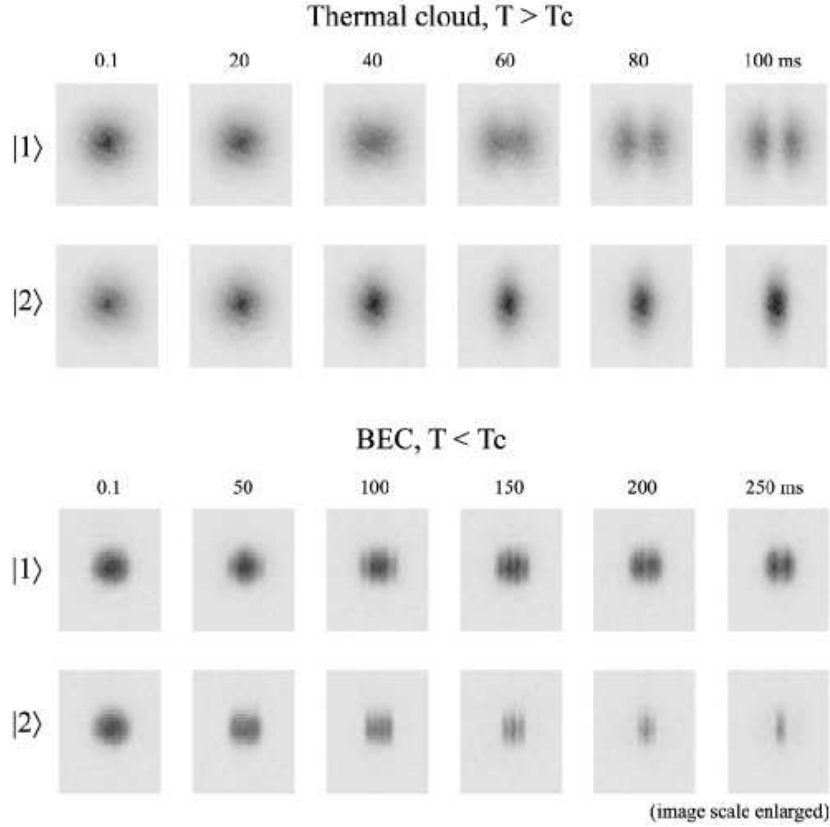


Figure 17. Dynamics of the component separation and domain formation in a quasi spin-1/2 spinor gas (states $|1\rangle$ and $|2\rangle$), for the case of a thermal gas ($T > T_c$) and a nearly pure Bose-Einstein condensate ($T < T_c$). This example shows the different timescales for spin transport for the two regimes, which are again significantly modified in a Bose-Einstein condensate with significant normal component [226]. Image with courtesy of E. A. Cornell, JILA, Boulder

considering the collision of two particles, each with total spin F [234, 235, 236]. The two-particle collision now only depends on the total two-particle spin f , which can take values from $0..2F$ depending on the orientation of the single particle spins. Note that only even values of f occur due to bose symmetry. The resulting two particle interaction potential can thus in principle be divided into the corresponding contributions by the introduction of the s-wave scattering lengths a_f for the different two-particle spin collisions [234, 235]:

$$\hat{V}(\mathbf{r}_1 - \mathbf{r}_2) = \delta(\mathbf{r}_1 - \mathbf{r}_2) \sum_{f=0}^{2F} \frac{4\pi\hbar^2 a_f}{m} \hat{P}_f. \quad (34)$$

Here \hat{P}_f is the projection operator onto total spin f and m is the mass of a single atom. A further simplification concerning the experimentally relevant case of a coherent matter wave with particle spin $F = 1, 2$ finally results in the following spin-dependent

mean field energy contributions:

$$K_{spin} = c_1 \langle \mathbf{F} \rangle^2 + \frac{4}{5} c_2 |\langle s_- \rangle|^2 - \tilde{p} \langle F_z \rangle - q \langle F_z^2 \rangle. \quad (35)$$

In this expression $\langle \mathbf{F} \rangle$, $\langle F_z \rangle$ and $\langle s_- \rangle$ denote the expectation values for the single particle spin vector, its z component and the spin-singlet pair amplitude.

The parameters c_1 and c_2 characterise the magnetic properties of the system and are essentially given by linear combinations of the spin-dependent s-wave scattering lengths. For $F=1$ systems $c_1 = \frac{4\pi\hbar^2}{m} \times \frac{a_2 - a_0}{3} n$ and $c_2 = 0$, while for $F=2$ systems $c_1 = \frac{4\pi\hbar^2}{m} \times \frac{a_4 - a_2}{7} n$ and $c_2 = \frac{4\pi\hbar^2}{m} \times \frac{7a_0 - 10a_2 + 3a_4}{7} n$, with the particle density n .

Considering only these parameters the spinor systems can be classified into antiferromagnetic (or polar), ferromagnetic and cyclic behaviour. The first two phases occur for both $F = 1$ and $F = 2$ systems, while the cyclic phase needs the additional degrees of freedom only offered in the $F = 2$ system. An antiferromagnetic or polar system shows miscibility of the $m_F = -F$ and $m_F = +F$ spinor components, while they spatially separate for a ferromagnetic system. The cyclic phase supports a mixture of the $m_F = -2$, $m_F = 0$ and $m_F = +2$ spins [236]. The corresponding ground state matter wave distributions additionally depend on experimental parameters, in particular the magnetic offset field and the magnetic field gradient. Detailed phase diagrams taking these effects into account can be found for $F = 1$ systems in [36].

One important point we want to emphasize for atomic systems dominated by the above interactions (negligible dipole-dipole interactions) is that the total spin projection on the quantisation axis is conserved in a two-particle scattering event. This introduces important differences for spin dynamics in coherent matter waves as compared to condensed matter systems. In condensed matter the spin degree of freedom is coupled to other degrees of freedom of the bulk system, which can cause spin flip processes and typically limits coherent dynamics.

In the spinor coherent matter waves discussed above spin dynamics is fully due to their intrinsic quantum mechanical interactions. Consequently spin dynamics in $F = 1$ spinor gases is determined by the process $| - 1 \rangle + | + 1 \rangle \leftrightarrow | 0 \rangle + | 0 \rangle$, (denoting the states by their m_F -component for simplicity). Although similar rules apply for $F = 2$ systems, the availability of 5 spin components allows much more complex dynamics in this case.

A fascinating set of experiments investigated the spinor properties and dynamics of the $F = 1$ state of ^{23}Na [237, 36]. These experiments showed that this state behaves antiferromagnetic and studied the corresponding phase diagram. Miscible and immiscible spin mixtures were produced and tunneling processes during their spatial rearrangement were studied [238]. Furthermore metastability and delay effects were observed in spinor dynamics [220]. Recent experiments showed, that the ^{23}Na system shows severe limitations for studies of the $F = 2$ spinor system due to rapid hyperfine loss processes [239].

The first studies on a $F = 2$ spinor system were achieved in ^{87}Rb (see Fig 18) showing intriguing spin dynamics with evidence for coherent oscillations, condensate melting thermalisation effects and an antiferromagnetic ground state behaviour, close to the cyclic phase with metastable states belonging to this phase [228]. Furthermore it was shown that the ^{87}Rb $F = 1$ state behaves ferromagnetic [240, 228].

In conclusion the nonlinear interstate coupling in matter waves gives rise to new fascinating phenomena and magnetic properties. Recent experiments provide a variety

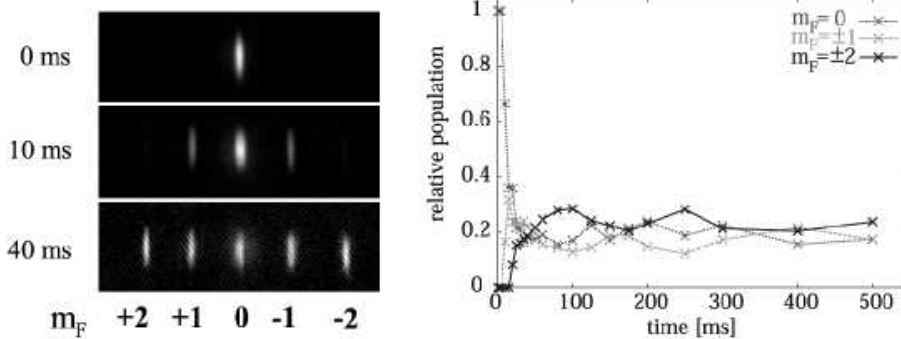


Figure 18. Example for $F=2$ spin dynamics starting with a matter wave prepared in the $m_F = 0$ state. The absorption images on the left show the temporal evolution of the individual spin components, which overlap in the trap but are separated by a Stern-Gerlach setup for the images. First the ± 1 components are populated and only later also the ± 2 spin components. This behaviour is also reflected in the graph on the right, which furthermore shows oscillatory behaviour in the magnetic dynamics of the quantum gas.

of rich spinor systems, with exciting physics to be explored. These systems offer promising extension possibilities by new matter wave species (e.g. $F = 3$ and $F = 4$ in ^{85}Rb and ^{133}Cs) but also by coherent coupling of different hyperfine states or tuning with recently observed interstate Feshbach resonances [241].

7. Guiding structures and optical elements for coherent matter waves

One main point of interest in coherent matter waves lies in their application, in particular in high precision sensors for fundamental physics as well as commercial tasks. These prospects are strongly supported by the analogies with optical laser beams but the mass and internal atomic structure lead to fundamental differences. These differences open new prospects for applications, but also require adapted strategies for matter wave manipulation. In terms of counteracting gravitational acceleration and prolonging observation times waveguides for matter waves seem highly promising. In this respect it is desirable to achieve guiding structures with high transverse confinement, as this enhances shielding from external noise and facilitates single transverse mode guiding. In addition the coherent manipulation of matter waves is a nontrivial task and requires considerable investigation.

7.1. Magnetic guides

Magnetic guiding structures for matter waves have been under research from the beginning of atom optics [130]. They rely on the same principles (i.e. the Zeeman energy shift of suitable atomic sublevels) as magnetic traps commonly used in Bose-Einstein condensation experiments. Magnetic matter waveguides have been demonstrated with different geometries, e.g. in wire-lined hollow fibers [242] and along current carrying wires [243, 244, 245]. The latter realisation is particularly well suited for miniaturisation and commonly used in various atom chip designs. It relies on the creation of a two-dimensional magnetic quadrupole field by combining the

magnetic field of a current carrying wire with a homogeneous offset field. The scaling of the field gradient with the wire dimensions and the distance from the wire results in stronger possible confinement for miniaturised setups as an advantage for atom chip designs. A variety of elongated traps and guiding structures have been realised with this design [246, 247, 248, 249, 250, 251, 252, 253, 254, 255]. Transverse confinements with an energy spacing between ground and first excited state up the h times 100 kHz range can nowadays be achieved and trapping frequencies up to the MHz range seem feasible in the near future [256].

The proximity of a room temperature surface in the miniaturised atom chip setups introduces new heating effects, which were proposed by [194, 195, 198, 202] and also recently investigated in several experiments [199, 200, 201]. The main effects arise from magnetic fields due to thermal current noise in metallic substrates and evanescent electromagnetic waves above dielectric substrates. The latter effect is much smaller and does not seem to limit current technology but metallic surfaces were found to induce significant heating and trap loss for samples at close distance.

Further influences on guided or trapped atomic samples were found due to the current carrying wire itself [196, 197, 254]. These effects are found to be connected to the current flow, which might be made irregular by small fabrication irregularities and/or crystal grain boundaries inside the conductor.

Wire based guides and atom chips are very versatile devices with many promising applications. The achievement of significant further miniaturisation is an actively pursued technological task, which has to take into account fundamental surface induced heating effects as well as find suitable materials and processes to ensure regular current flow in the guiding wire.

7.2. Optical guides

Optical guides represent a second promising class of waveguides for coherent matter waves. They are based on the dipole potential, i.e. the ac Stark shift of the atomic states, induced by the interaction of the atoms with laser light with a frequency far detuned from the atomic resonance (see e.g. [257]). In a simple model the dipole potential is given by [257]:

$$U_{\text{dip}}(\vec{r}) = -\frac{3\pi c^2}{2\omega_0^3} \left(\frac{\Gamma}{\omega_0 - \omega} + \frac{\Gamma}{\omega_0 + \omega} \right)^2 I(\vec{r}). \quad (36)$$

In this equation $\omega_0/2\pi$ is the atomic resonance frequency, $\omega/2\pi$ is the laser frequency and Γ is the damping rate corresponding to the spontaneous decay rate of the upper level. typical depth of dipole potential traps and guides correspond to μK to mK , if expressed as temperatures.

Light can guide atoms in a very flexible way and a high confinement not necessarily relies on proximity to surfaces possibly leading to heating effects.

A straightforward method for the realisation of an optical matter wave guide is to rely on the potential created by a freely propagating laser beam. The detuning of the laser frequency versus the atomic resonances determines, whether the atoms are confined at positions of high (for red detuning, i.e. laser frequency below the atomic resonance frequency) or low (for blue detuning, i.e. laser frequency above the atomic resonance frequency) light intensity.

The case of red detuning was mainly used for the realisation of matter wave traps [258, 259, 260, 219] in the focus of a laser beam. The trapping effect instead

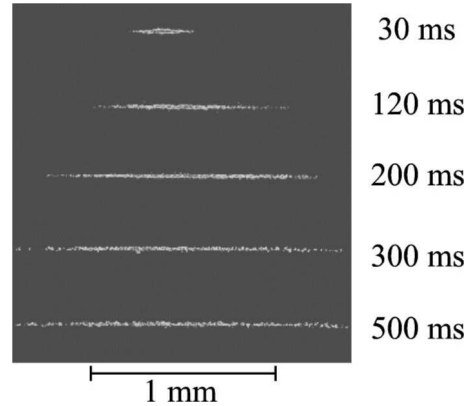


Figure 19. Expansion of a Bose-Einstein condensate inside a doughnut-shaped, far blue detuned light field acting as a matter waveguide [104].

of a pure guide is due to the propagation rules for the evolution of a gaussian laser beam. These rules lead to a stronger divergence of the beam the smaller its focus is. In other words creating a strong transverse confinement by tightly focussing the trapping beam, will lead to an additional axial intensity gradient, which provides a confinement in beam direction. This effect can be minimised by the use of weakly focussed laser beams of high power, but is limited by the available lasers.

Optical waveguides based on a hollow blue detuned laser beam [261, 262], creating a repulsive potential tube for were demonstrated for thermal atoms [263, 264, 265, 266, 267, 268, 269, 270] and coherent matter waves [104]. In [104] a TEM_{00} mode laser beam was transformed into a doughnut-shaped hollow TEM_{01}^* laser beam using a blazed-grating phase hologram. The beam parameters were chosen as to lead to a Rayleigh range on the order of 1 mm, which has to be compared to the initial $100 \mu\text{m}$ size of the Bose-Einstein condensate wavefunction loaded into this guide. This resulted in a slight longitudinal potential hill in the guide as opposed to the potential minimum in red detuned beams. Fig. 19 shows the slow spreading and propagation of a matter wave in this guiding geometry. It was shown, that this spreading is consistent with a transformation of mean field energy into one dimensional kinetic energy along the guide direction. Furthermore Bragg interferometric measurements demonstrated the coherence of the sample after some expansion time inside the guide.

Note that in contrast to the above low temperature coherence measurements, phase fluctuations occur at finite temperatures in these elongated geometries and pose severe limitations on applications (see Sec. 3.5). Successful guided measurement applications seem to require operation at temperatures much below typical Bose-Einstein phase transition temperature.

Other actively pursued methods for the realisation of optical waveguides concentrate on integration and flexible geometries. One important scheme relies on the guidance of atoms in light fields themselves guided in hollow fibers [271, 272, 273, 274, 275, 276, 277, 278]. This promises to remove the constraints of gaussian optics for freely propagating beams and to realise long, curved guiding structures with spatially constant and high confinement. Successful guiding was demonstrated by confining atoms in the evanescent field of blue detuned light modes guided in the glass fiber

tube. Technical limits of this technique lie in speckle patterns inside the fiber due to multimode operation, which lead to heating and atom loss. Furthermore suitable loading schemes funneling the atoms into the repulsive laser field have to be applied. A more natural loading seems possible with red detuned guiding light fields, but these experience severe losses inside conventional hollow fibers. The recent invention of hollow photonic crystal fibers might change this situation in future experiments.

New approaches also combine atom chip technology with optical atom guiding [279]. Recent experiments realised trapping and guiding of atoms in light fields shaped with microlens arrays and cylindrical microlenses [131, 280]. These experiments also demonstrated integrated beamsplitters and interferometric setups.

Optical atom guiding in its various forms shows high flexibility and comparable confinement strength as its magnetic counterpart. Ongoing technological developments, in particular microoptics and photonic crystal materials offer promising prospects for reliable coherent matter waveguides.

7.3. Mirrors and beamsplitters

The ability to manipulate and control coherent matter waves relies on the availability of suitable optical elements [281]. In comparison to light optics, the situation in matter wave optics is complicated by several aspects. Some intrinsic points are the different dispersion relation for matter waves, which often leads to velocity dependent, i.e. dispersive processes. Furthermore the interparticle interaction causes nonlinear processes to influence matter wave dynamics at high densities.

In addition to the guiding structures for matter waves mirrors and beamsplitters as basic optical elements are required for the implementation of applications such as interferometric measurements. These elements have to preserve the coherence of the matter waves, i.e. to avoid spontaneous processes in light based realisations. In principle all atom optical elements are either based on suitable potential geometries, e.g. short range repulsive potentials for the realisation of mirrors, or on coherent atom light interactions changing the momentum and/or the internal state of the underlying atoms. The potentials are typically realised with light fields or magnetic fields.

The reflection of atoms with relatively high kinetic energy has been demonstrated using steep potentials realised with evanescent waves [282, 283, 284, 285, 286, 287] and periodic magnetic surfaces [288, 289, 290, 291, 292, 293, 294, 295, 296, 297, 298]. These elements however critically depend on their surface roughness, which often hinders a purely specular reflection.

These aspects can be relatively well controlled by the reflection of coherent matter waves from flat light fields [95] but in this case the gradient of the light field potential is weaker leading to a "softer" mirror compared to evanescent waves. As an advantage these mirrors do not require the presence of a surface, i.e. they can also transmit matter waves.

A different type of "soft" mirror has been demonstrated for Bose-Einstein condensates and atom-lasers with magnetic fields [299].

Very controlled and non-dispersive mirrors as well as variable beamsplitters have been realised using Bragg reflection in the short pulse regime (see Sec. 3.3 and Sec. 8.1) as well as Raman reflection [10]. Raman reflection is similar to the Bragg process discussed above, but in this case the internal atomic state is changed during the atom-laser interaction. Due to their high reliability and non-dispersive character these matter wave optical elements are used in most coherent matter wave interferometric

schemes which will be discussed in the next section. Their main drawback lies in the small possible momentum transfer, limited to a few photon recoil momenta.

Guiding structures open a new way to realise a beamsplitter by splitting a matter wave guide in two new branches [300, 280]. The question on the coherence properties of this new type of beamsplitter and their possible use in interferometric structures is currently under investigation [301, 302]

The search for coherent high momentum transfer non-dispersive matter wave optical elements is still an active field of research, which has strong impact on future applications.

8. Atom interferometry with coherent matter waves

There are many expectations connected to the introduction of coherent matter waves into high precision interferometric measurements. These expectations are supported by the analogy to light optics and the rapid gain in sensitivity after the invention of the laser as source of coherent light waves. The interest in atom interferometric sensors stems from the high sensitivity which can be realised with these instruments. State-of-the-art atom interferometers are among the most precise sensors for the measurement of frequency, rotations, gravity and gravity gradients [10, 303, 12, 304, 305, 306, 307, 308, 309, 310, 311] even with a thermal atom source. The prospect of significant further sensitivity increases due to the implementation of a coherent matter wave source is connected to several issues, which are under active investigation.

First of all the progress in light interferometry with the invention of the laser is to a great part due to an increase in photon flux in the interfering mode. Modern atom interferometric schemes are able to extract a signal from entire thermal ensembles of atoms, given that their momentum and spatial spread is not too large. In this respect a coherent matter wave source has to compete with thermal atom sources which nowadays typically have many orders of magnitude higher flux. Thermal atom beam sources achieve a typical flux of 10^{14} atoms/s and laser cooled sources achieve in the range of 10^9 atoms/s, while Bose-Einstein condensates can typically be created with up to 10^7 atoms every 10s, thus leading to a coherent matter wave flux of 10^6 atoms/s. The increase of coherent matter wave flux is a major topic in nowadays coherent matter wave research, i.e. by the development of novel atom laser sources discussed in Sec. 5.

Another important point are evolution time limitations due to the influence of gravity on all kind of matter wave interferometer. In many interferometric setups an increase in evolution time, i.e. the time between splitting and recombining the interfering wave packets, leads to a higher sensitivity. The precision of atom interferometric measurements could be significantly increased using a longer evolution time, which is mainly limited by two factors: the spreading of the wave packet and the free fall trajectory used in state-of-the-art instruments. One of the main tasks is to exploit the superiority of coherent matter waves in terms of their heisenberg limited momentum spread, which becomes an advantage for evolution times of several seconds. In order to obtain these times in the well understood free fall interferometers, it seems promising to build a gravity free, i.e. space bound, instrument. Another main route to enlarge the evolution time consists in various efforts to develop matter wave guiding structures as discussed in Sec. 7. Both routes are actively pursued in nowadays experimental activities.

Further promising attempts to reach increased precision with matter wave interferometric sensors concentrate on obtaining Heisenberg limited sensitivity, i.e. sensitivity going with $\frac{1}{N}$ instead of the poissonian limit $\frac{1}{\sqrt{N}}$, with the number of interfering particles N . There are several proposals to prepare squeezed and/or entangled matter wave states which show the according interference [205, 312, 313, 314, 315, 316, 204, 317, 318, 319]. Recent experiments demonstrated number squeezing of coherent matter waves [81, 82] as an important step towards Heisenberg limited atom interferometry.

In the following we will discuss the implementation of atom interferometers based on Bose-Einstein condensates as coherent matter wave source. It is important to note, that all these interferometers are based on single particle interference. Even if a macroscopically occupied Bose-Einstein condensate wavefunction is used as a source, the beamsplitting process relies on single particle processes. This is in analogy to optical setups using laser sources, which are also based on single photon processes.

8.1. Bragg atom interferometers with BEC

The current development of atom interferometers based on coherent matter waves aims at several fundamental issues: using the low momentum spread, understanding and controlling interparticle interactions and reaching Heisenberg limited sensitivity.

One of the first interferometric schemes implemented with Bose-Einstein condensates relies on Bragg diffraction for the mirrors and beamsplitters [103, 96, 104]. This method (see Sec. 3.3) with a typical two photon momentum transfer is especially interesting for matter waves with a narrow momentum spread. The momentum spread of a Bose-Einstein condensate wavefunction can be easily made smaller than the Bragg diffraction momentum transfer. It is thus possible to not only split the wavefunction in momentum but also in real space, resulting in interferometers with well separated paths. This allows to modify the phase along one of the paths with suitable light pulses [137].

Bragg interferometers have been used in studies of the phase evolution of BECs [103] as well as their coherence properties [104, 123], in which they show clear signatures of the nonlinear interparticle interactions of the dense matter waves as well as phys fluctuations for finite temperatures.

A Bragg interferometer scheme is exemplarily shown in Fig. 20.

The above scheme with different evolution times between Bragg pulses results in an open interferometer. In this case Bose-Einstein condensates passing through this interferometer will be only partially overlapped in the output ports. The resulting interference signal allows a measurement of the condensate autocorrelation function [103], which is modified by interparticle interactions in the first stages of expansion after release from the trap.

For the case that one is mainly interested in the spatial coherence of the matter wave function, a simplified $\frac{\pi}{2}$ - $\frac{\pi}{2}$ pulse configuration can be employed [104]. The first pulse splits the matter wave, which is recombined by the second pulse after a variable time, which defines the relative spatial shift of the interfering wavepackets. This enables the measurement of the matter wave coherence length.

The advantage of coherent matter waves in Bragg interferometric schemes is not only due to the low momentum spread allowing separated path interferometers, but is also reflected in the clearly visible large scale density modulations in the output ports. An advanced concept employing new readout schemes based on this feature was

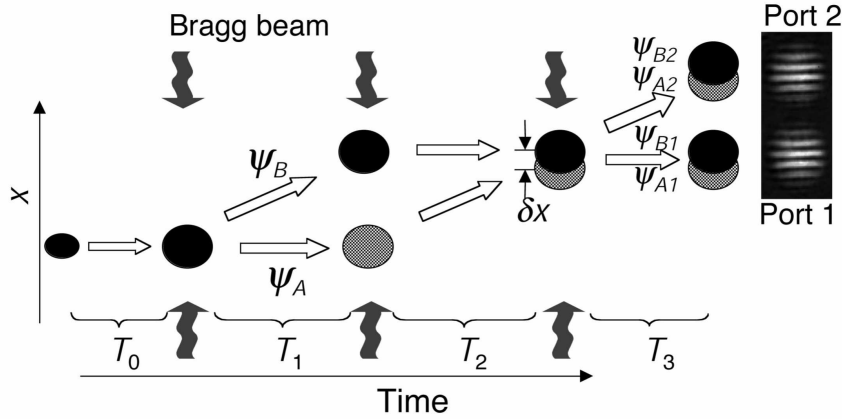


Figure 20. Bragg pulse interferometer based on a $\frac{\pi}{2} - \pi - \frac{\pi}{2}$ scheme. A free falling Bose-Einstein condensate wavefunction is subjected to three Bragg pulses. The first pulse is a $\frac{\pi}{2}$ pulse splitting the condensate wavefunction into an equal superposition of two different momentum states, leading to a subsequent spatial separation of the wavepackets. The second pulse is a π pulse inverting the states and thus acting as a mirror. The third pulse is another $\frac{\pi}{2}$ beamsplitter pulse, recombining the wavepackets. Interference leads to varying populations of the two different momentum state output ports. These wavepackets in these ports are spatially separated after some time of flight and can be individually detected. If the times between the Bragg pulses is equal, e.g. $t_1 = t_2$ the interferometer is closed and varying the interference phase leads to oscillation of the whole cloud between the output ports. For the case of $t_1 \neq t_2$, as in the example given here, the clouds will only have partial overlap at the second beamsplitter making the observation of the phase distribution of the condensate wavefunction possible [103]. Image with courtesy of National Institute of Standards and Technology, USA.

recently demonstrated in a slightly different interferometer type [320]. The scheme used in this experiment employs a Kapitza Dirac pulse for initial splitting of the matter wave, i.e. a very short standing wave light pulse leading to three momentum states [321]. A second order Bragg pulse after some evolution time, T , redirects the split wavepackets towards each other such that they pass through each other at time $2T$. During this passage the coherent wavepackets interfere and show the periodic buildup and decay of a matter wave density grating. One intriguing feature of the interferometer scheme is that the readout traces the reflection of an appropriate laser beam off this density grating in time. This allows to determine the interferometer phase in a single run, i.e. with one wavepacket passing through. This interferometer demonstrates high potential for precision measurements of $\frac{\hbar}{m}$. It is important to note that it only exploits the low momentum spread of the Bose-Einstein condensate wavefunction but does not rely on its coherence properties.

8.2. Interferometers of Ramsey type

Ramsey-type interferometers make use of the internal atomic degrees of freedom in order to split manipulate and recombine a wavepacket [10]. The coupling can be realised with or without momentum transfer, depending on the chosen

interaction. Ramsey-type interferometers have the advantage, that the different paths of the wavepackets inside the interferometer as well as the two output ports are represented by different internal states. As a consequence neither a phase shift in one interferometer arm nor the detection of the interferometry signal require a spatial separation of the interfering wavepackets but only state selective interactions. This feature makes Ramsey-type matter wave interferometers very versatile and useful even for thermal ensembles. They are implemented in most types of modern atom interferometric precision sensors [10].

The high technological importance of this type of interferometer gives rise to great interest concerning possible improvements with coherent matter wave sources. A straightforward improvement lies again in the low momentum spread, which allows a longer evolution times with well defined trajectories. This essentially enhances the flux along the desired pathways and minimises broadening effects, which arise due to different phase contributions along different paths or due to matter waves with different wavelength contributing to the signal. In this sense these improvements are analogous to the advantages of a laser source in optics.

The first implementation of a coherent matter wave Ramsey interferometer was realised with a magnetically trapped Bose-Einstein condensate at JILA [85]. In this experiment a ^{87}Rb condensate was prepared in the $|F = 1, m_F = -1\rangle$ state and coupled to the $|F = 2, m_F = 1\rangle$ state with two combined microwave and radiofrequency fields. The interferometer scheme consisted in two $\frac{\pi}{2}$ pulses (each transferring 50% of the population of one component into the other component and thus acting as 50% beamsplitter) separated by a variable evolution time. One aim of this experiment was to study the effect of interparticle interactions on the phase evolution of the interfering paths, in particular looking for phase diffusion processes. It was found, that the two matter wave components tend to spatially separate due to their interactions, which in the trapping fields leads to damped oscillatory motion relative to each other. The phase evolution of the internal state superposition however remained trackable without significant visible diffusion. This result shows that the coherent evolution of a superposition of the internal hyperfine ground states is not quickly destroyed due to interparticle interaction and relative spatial movement of the two components.

The interparticle interaction has however an important effect on the frequency of the hyperfine transition. The density dependent mean field energy difference for particles in one versus the other spin state results in a position dependent shift of the resonance frequency of the trapped ensemble.

The density dependence of the transition frequency difference was employed in precise measurements of the difference of the scattering lengths of the two involved spin components [225, 239]. In similar experiments with fermionic gases it was further shown, that these stay noninteracting during the interferometric sequence. In this respect incoherent fermionic matter waves are better suited for high precision measurements, if the Fermi momentum spread of the sample can be tolerated.

A further experiment with the ^{87}Rb quasi-spin 1/2-system investigated the influence of a position dependent Rabi-frequency [223]. In this case a linearly varying Rabi detuning was achieved by a slight spatial offset of the centers of the $|F = 1, m_F = -1\rangle$ component and the $|F = 2, m_F = 1\rangle$ component. Coupling of the two components for several Rabi oscillation cycles results in a complicated phase pattern inscribed into the condensate wavefunction, which was studied in detail in [223].

The optimisation of interferometric schemes with respect to the advantages of noninteracting fermionic atoms or low momentum spread coherent bosonic matter waves is under current investigation.

8.3. Advanced concepts for atom optics with coherent matter waves

The above matter wave interferometric schemes only make indirect use of coherent matter waves by exploiting the possible low momentum spread to reach high flux also for very long evolution times. The resulting interferometry signal relies on single particle interference effects. Its signal to noise ratio is limited by counting statistics to a value proportional to $\frac{1}{\sqrt{N}}$ with the number, N , of detected particles. Advanced concepts aim at an increasing matter wave interferometer sensitivity to the Heisenberg limit $\frac{1}{N}$. This might be achieved by using squeezed matter waves similar to analogous concepts in light optics or by arrangements employing entangled particles or two coherent matter wave sources as discussed above.

Experimentally important progress towards squeezed matter waves has been made in optical lattice geometries, where number squeezing has been observed [81, 82]. In [81] a Bose-Einstein condensate is loaded into a 1d standing wave optical dipole potential, coherently distributing the condensate wavefunction over ≈ 30 lattice sites. The intensity of the light field is used to control the confinement at each site and the tunneling rate between adjacent sites. For very high intensities the limit of negligible tunneling versus the on site interparticle interaction is reached. This leads to a quantum phase transition to an insulating state similar to the Mott insulator discussed in Sec. 9.3. The special feature of this state is that the number of atoms in each individual potential well is fixed to a precise value, i.e. the atom number is squeezed. As the atom number is intrinsically related to the phase uncertainty by a phase-number uncertainty relation, the phase shows maximum uncertainty in this state. The transition to the number squeezed state with high phase uncertainty is clearly visible in the loss of interference contrast of the matter wavepackets, when released from the optical lattice (see Fig. 21).

One idea is to enhance the sensitivity of interferometric measurements by transforming this number squeezed state into a phase squeezed state. This phase squeezed state can then be employed in a contrast interferometer scheme to reach Heisenberg limited sensitivity [205]. First experiments using fast intensity changes of the optical lattice state oscillations from number squeezing to phase squeezing, which open interesting perspectives for the realisation of such a scheme.

Furthermore it should be noted, that the progress in manipulating the external and internal degrees of freedom of matter waves enables the creation of entangled atomic pairs due to collisional processes [313, 204, 322]. Feeding a matter wave interferometer with these entangled pairs represents another way of reaching Heisenberg limited sensitivity (see e.g. [323]).

Modern atom interferometric schemes allow highest precision in several types of measurements but typically do not directly benefit from the coherence of a matter wave source. The optimum configuration and possible improvements with novel coherent sources is subject of ongoing research. Furthermore the high experimentally achievable control over matter wave internal and external dynamics opens new possibilities for reaching ultimate sensitivity with adapted sources.

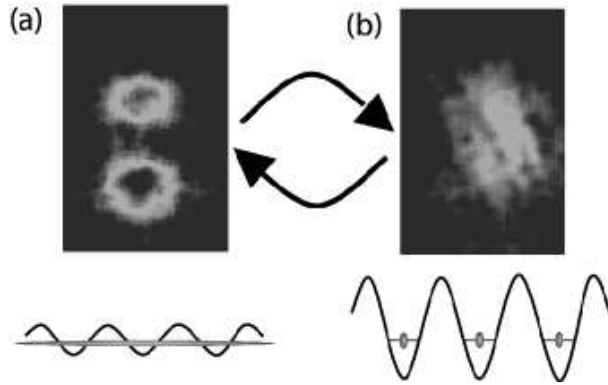


Figure 21. Transition from a coherent matter wave state (a) to a number squeezed state (b) with Bose-Einstein condensates loaded into an optical lattice. The absorption images show the interference/disappearance of interference, appearing when the matter wave is released from the lattice potential. The lower pictures show schematically how the matter wave distributes in the optical lattice, from delocalised to localised. Note that the transition is reversible. Experimental images with courtesy of M. Kasevich, Stanford university.

9. Coherent matter waves in optical lattices

The combination of coherent matter waves with periodic potential structures opens a new quality in controlled matter wave manipulation and in the realisation of model systems for condensed matter phenomena. Optical lattices created from interfering laser beams are defect-free periodic potentials with easily tunable parameters. Depending on the number and the geometry of interfering lasers 1d, 2d or 3d lattices can be created with different symmetries [324]. Changing the laser intensity the system can be tuned from the tight binding model to a free sample, relative laser frequency detuning allows to exert precise accelerations on the sample and different frequency or different polarisation lattices can shift the relative position of different components in multi-component matter waves in a controlled way.

9.1. Coherent phenomena

The adiabatic transfer of a Bose-Einstein condensate into a periodic potential as created by an optical lattice gives rise to a macroscopic population of the lowest momentum state in the lowest Bloch band [325, 326]. If tunneling between lattice sites is not negligible, i.e. the Mott insulator regime is not realised, the coherence of the matter wave will be preserved. This coherence leads to various interference effects, e.g. in transport phenomena and in free expansion after switching off the lattice potential. The possibility to project the momentum distribution of the matter wave inside the lattice onto free space momentum states by abruptly switching off the optical potentials offers unique possibilities to study coherent effects in crystal lattices. This type of investigation of condensed matter phenomena opens new pathways, which are not accessible in real condensed matter systems. The interference structure obtained some time after switching off a 3d optical lattice (see Fig. 22) can be interpreted in several ways: First one can use a condensed matter approach in considering the pattern as the momentum distribution of the lowest state in the first Brillouin zone (Fig. 22

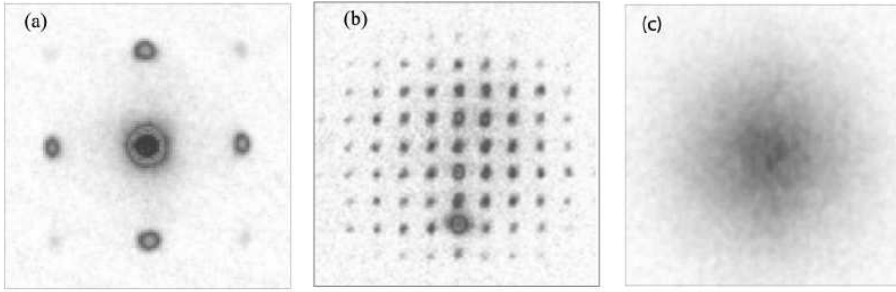


Figure 22. Interference of coherent matter waves interacting with a three dimensional optical lattice. The absorption images were taken after a time of flight period, such that the visible distribution corresponds to the momentum distribution of the ensemble. (a) Interference peaks from a matter wave adiabatically loaded into the lattice, which was then abruptly switched off. In this case only a few momentum components are occupied. (b) Interferences for a matter wave subjected to a pulsed optical lattice potential with many occupied momentum components. (c) Same as (a) but with a high optical lattice confinement, leading to a Mott insulator state (see Sec. 9.3). In this state the inter-site coherence is completely lost and the image shows no interferences. Note that the momentum separation of the peaks in (a) and (b) is the same, only the scales are different. (c) uses the same scale as (a). Images with courtesy of I. Bloch, Mainz university and T. W. Hänsch, MPQ.

(a)). The crystal momentum distribution peaked at zero momentum is periodically repeated in free space momentum space with a spacing proportional to the inverse lattice period.

A second picture of the process comes from the analogy to wave diffraction by periodic structures, e.g. Laue peaks from electron diffraction by crystal structures. The idea is to associate the matter wave inside the optical lattice with waves passing through a crystal and later interfere. This picture clearly incorporates interference effects but it should be noted that it rather corresponds to a pulsed matter waver - optical lattice interaction (Fig. 22 (b)).

The above ideas also hold for the case of a 1d optical lattice, where an analogy to laser beam diffraction off a periodic grating can be made. Recent experiments have analysed the according matter wave interference structure and found similar structures to the ones obtained in optical grating diffraction experiments [98] (see Fig. 23). These structures can be modified by moving or accelerating the lattice. Accelerating a lattice to a certain velocity corresponds to imposing a linear phase gradient across the matter wave. In the optics picture this mimics a laser beam incident on a diffraction grating with a non-orthogonal angle between grating and laser propagation direction. This regime has first been explored by the group of M. Kasevich at Yale university with a 1d lattice oriented in the direction of gravity and might be useful for high precision measurements of accelerations.

9.2. Bloch oscillations and Josephson junctions

Bloch oscillations are a paradigm of condensed matter physics and intrinsic to the Bloch lattice model. The acceleration of particles in the lowest momentum states of a perfect lattice leads to an increase in crystal momentum until the border of the first

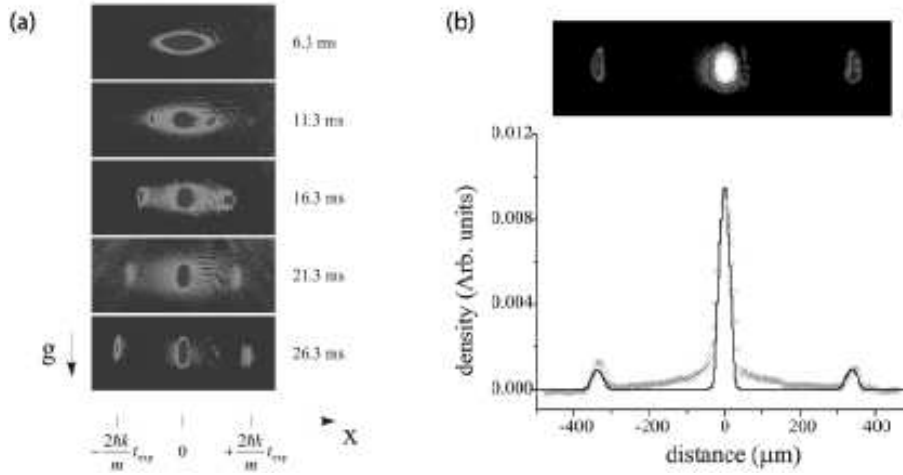


Figure 23. Interference structures of a coherent matter wave released from a one dimensional optical lattice (which is abruptly switched off). (a) Time of light development of the ensemble with the buildup of interferences between the different momentum components. (b) Comparison of the interference profile with the theoretical prediction for an array of expanding condensates [98]. Images with courtesy of M. Inguscio, LENS, Florence.

Brillouin zone is reached. A further acceleration leads to the transfer of the particles to the opposite border of the Brillouin zone with the inverse momentum. From there the particles start again gaining crystal momentum, until they reach the border of the Brillouin zone another time and everything starts over. Applying a constant force to particles confined in an ideal lattice thus leads to a sawtooth-like periodic increase and inversion of momentum.

In a matter wave picture the acceleration corresponds to an increase of the wavenumber of the particles. The border of the Brillouin zone is reached, when this wavenumber equals the π over the lattice period. In other terms the Bragg scattering condition for the matter waves to be reflected by the lattice is fulfilled and the velocity of the matter wave is inverted.

Due to lattice defects and phonon excitations Bloch oscillations are very difficult to observe in condensed matter systems. The implementation of an atom optical model system with atomic particles in a practically defect-free optical lattice has changed this situation and enabled the observation of matter wave Bloch oscillations [327]. The first experiments were based on laser-cooled thermal ensembles and no spatial information on the Bloch oscillations could be obtained. In recent experiments based on coherent matter waves both the momentum as well as the spatial evolution of the wavepackets were investigated [135]. With these experiments the intrinsic features of Bloch oscillations became clearly visible in time of flight images.

While Bloch oscillations typically occur in relatively shallow lattices with significantly broadened conduction bands the related physics of Josephson junctions is based on tunneling through a relatively high barrier as might be realised in a deep lattice. Both regimes give rise to oscillatory behaviour and a smooth crossover can be expected in the lattice realisation.

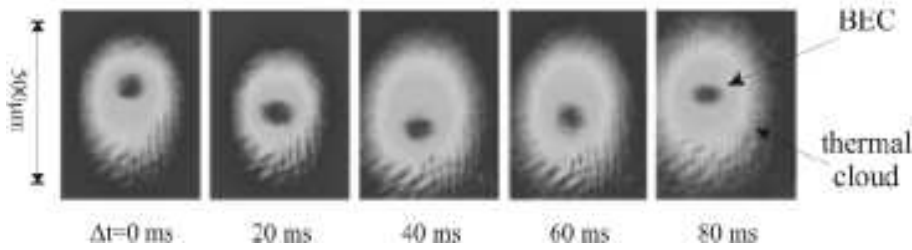


Figure 24. Motion of a Bose-Einstein condensate with significant normal component (“thermal cloud”) in a one dimensional optical lattice with superposed harmonic oscillator potential. In the beginning the Bose-Einstein condensate was displaced from the minimum of the harmonic potential. Due to the optical lattice only coherent tunneling currents are possible, resulting in an oscillatory motion of the condensate wavefunction, while the normal component remains fixed in space. Image with courtesy of M. Inguscio, LENS, Florence.

In experiment a vertical array of Josephson junctions was realised by loading a vertical 1d optical lattice with a Bose-Einstein condensate [185]. This setup incorporates output coupling of the matter wave due to tunneling through the potential barriers and thus realises an atom laser. Due to the gravitational potential difference the phase between different sites increases linearly, which leads to an oscillating Josephson current. The atom laser output is pulsed according to this oscillation. The atom laser repetition frequency is a means to measure gravity with prospects for high precision measurements.

Another fascinating feature of Josephson tunneling was demonstrated by comparing the movement of the normal (thermal) component and the wavefunction of a Bose-Einstein condensate [328]. A Bose-Einstein condensate with significant normal component was loaded into a 1d optical lattice with a superposed harmonic oscillator potential. The lattice potential was relatively high compared to the temperature of the sample but still allowed significant tunneling. The motion of the ensemble was investigated after a sudden displacement of the harmonic oscillator potential minimum. The “classical” normal component was essentially confined to its original position, while the superfluid condensate wavefunction fulfilled oscillations due to coherent Josephson tunneling through the potential barriers. An analysis of the potential dependend oscillation period is in agreement with the prediction from Josephson junction theory [329]. This experiment shows the extraordinary properties of superfluidity in an impressive way and is analogous to experiments on the flow of superfluid helium in porous vycor.

9.3. Mott insulator transition

The recent observation of the superfluid to Mott insulator quantum phase transition demonstrates the power of coherent matter waves in optical lattices as model system for condensed matter phenomena in an impressive way [82]. A quantum phase transition is special in the sense, that it is driven by quantum instead of classical fluctuations. Furthermore it is based on a competition between two different contributions in the hamiltonian of the system instead of a competition between inner energy and entropy [330].

The superfluid to Mott insulator transition of coherent matter waves in an optical lattice is driven by the competition between on-site interparticle interactions and the tunnel coupling of adjacent sites. The system consists of bosonic atoms in a relatively deep 3d optical lattice, such that site-to-site motion is solely based on tunneling processes. The according second quantised hamiltonian in the Bose-Hubbard model [331] without external confinement is given by [82]

$$H = -J \sum_{\langle i,j \rangle} \hat{a}_i^\dagger \hat{a}_j + \frac{1}{2} U \sum_i \hat{n}_i (\hat{n}_i - 1). \quad (37)$$

The number operator $\hat{n}_i = \hat{a}_i^\dagger \hat{a}_i$ is defined by the bosonic operators \hat{a}_i^\dagger and \hat{a}_i creating or annihilating a particle at lattice site i . The energy scales of the tunneling and interaction are given by the hopping matrix element J and the on-site interaction matrix element U (see [82]).

In the limit of high tunneling as compared to the on-site interaction, $\frac{J}{U} \gg 1$, long range coherence can be maintained. The many-body ground state wavefunction is then given by a multiple occupied single particle wavefunction similar to the case of a harmonically trapped Bose-Einstein condensate. Due to the long range coherence this state corresponds to a superfluid inside the optical lattice (see Fig. 22 (a)).

In the opposite limit, $\frac{J}{U} \ll 1$, in which tunneling is negligible long range coherence is lost and the particles become localised at single lattice sites. For commensurate fillings the many body ground state is represented by a product wavefunction of single site Fock state wavefunctions with exactly the same particle number at each site. In this sense this regime again realises particle number squeezing as discussed in section 8.3. In this interpretation the total phase uncertainty due to phase fluctuations in between different sites suppresses transport and the system becomes an insulator (see Fig. 22)(c)).

The transition from superfluid tunneling transport to an insulator regime can also intuitively be explained in a picture based on the energy levels of the individual wells. Considering one atom per lattice site, the lowest energy level of each site will be singly occupied. Furthermore, regarding the entire optical crystal system, there will be an energy band formed by the combination of all these local energy levels with a broadening according to the inter-site tunneling. Transport of atoms from one lattice site to another would in a first step lead to a double occupancy of one site. In this case the local energy level would be shifted by the inter-particle interaction energy, U . Following energetic considerations transport can only occur, if the tunnel broadening is larger than the interparticle interaction term, i.e. $J > U$. The Mott insulator state is reached when the tunneling energy cannot account for the interaction energy difference any more, $J < U$.

In addition this simplified intuitive picture directly leads to the occurrence of an energy gap for transport excitation of the sample, once the insulating state is reached. The experimental investigation of the above superfluid to Mott insulator transition [82] confirmed this energy gap and its dependence on the relative values of tunneling matrix element and interaction energy.

The very clean realisation of the Mott insulator starting with coherent matter waves in an optical lattice was a milestone in modelling condensed matter phenomena. In this sense the well controlled systems for coherent matter wave creation and control represent an analog quantum computer which directly maps one hamiltonian onto another.

In addition the ultimate control over single atoms reached in the above experiment was further extended to different internal states with controllable interactions [332, 333] new interferometer schemes and multi-particle entanglement at will [322]. This paves the way for new types of matter wave sensors, quantum computers and controlled quantum chemistry.

10. Concluding remarks

This article is intended to give a representative overview of the field of coherent matter waves with emphasis on the physics with this new type of system. Due to the rapid developments and the explosion in activities and publications following the first realisation of Bose-Einstein condensation in dilute atomic gases a comprehensive coverage of the entire field is beyond the scope of a single review article. For further information we refer the reader to the available books [40, 41, 42, 43, 44] and review articles with different emphasis [28, 29, 30, 31, 32, 33, 34, 35, 36, 37, 16, 38, 39].

We have shown that the ability to produce macroscopically occupied matter wave functions via Bose-Einstein condensation is the basis for many new insights into the physics of coherent matter waves. For the first time it is now possible to directly image the probability distribution of a matter wavefunction onto a CCD camera. Although this distribution is integrated along the detection direction one obtains spatially resolved two dimensional information, which greatly influenced our understanding of quantum physics.

As an example discussed in Sec. 3.2, this spatial resolution enabled the observation of the interference between two Bose-Einstein condensate wavefunctions in a single shot. The intense theoretical discussion on this interference pattern established new views on how Fock state wavefunctions with total phase uncertainty can nevertheless interfere, e.g. by the establishment of a relative phase during the detection process.

In addition the spatial resolution can also be used for local manipulations of the quantum mechanical wave function, e.g. by phase imprinting discussed in Sec. 4.2. This novel access to quantum physics demonstrated its power in the creation of dark matter wave solitons as basic nonlinear excitation in these systems. Further examples of the local manipulation of the condensate wavefunction are the demonstration of its superfluid character and the creation of quantised vortices.

These examples are just the starting point for the field of quantum engineering with coherent matter waves which promises many more insights into the quantum world.

As an important point for future developments we discussed the achievements and new schemes in the development of new sources for coherent matter waves. One major goal in this respect is the realisation of a continuous atom laser with high flux. Next to experimental activities to reach this goal there are ongoing studies on the coherence properties of such a device. First experimental studies on coherence of an atom laser source were already possible based on pulsed or quasi-continuous atom lasers. These were realised by controlled output coupling of Bose-Einstein condensates confined in a trapping potential.

We presented several intriguing aspects connected to the nonlinearity intrinsic to matter waves due to the interparticle interactions. These aspects highlight the analogy to optical laser fields, with phenomena such as four wave mixing and solitons. The interactions connecting the internal atomic spin degrees of freedom however also allow novel effects, such as magnetism and coherent spin oscillations, in these fascinating

quantum gases. Further novel developments aim at two-particle entanglement created during the nonlinear matter wave interactions.

As a further point we discussed the status of development of coherence preserving atom optical elements, necessary to manipulate coherent matter waves. In particular we concentrated on optical and magnetic approaches to guiding structures as well as different types of mirrors and beamsplitters.

We note in this article that many promising applications for coherent matter waves, such as high precision measurements, primarily require a high flux. For state-of-the-art interferometric setups the main benefit from the coherence properties is the brightness of the source. As discussed in Sec. 8 there are however limitations due to the gravitational acceleration, which in practise limit the evolution time, such that the gain versus a thermal source is relatively small. Furthermore the one has to control intrinsic nonlinearity of nowadays relatively dense coherent matter wave sources in order to achieve high precision interferometric measurements.

We discussed several types of atom interferometric setups realised with Bose-Einstein condensate wavefunctions, in particular Bragg and Raman interferometer schemes. These setups presented important steps towards the understanding of the behaviour of coherent matter waves in interferometric applications. In addition they added significant information on the coherence properties and phase of the condensate wavefunction. We also discussed experiments and ideas on advanced approaches to coherent matter wave interferometry, which make use of guiding structures, squeezing or multi-particle entanglement.

As final points we concentrated on recent achievements with coherent matter waves in optical lattices. These systems are particularly interesting in terms of model systems for condensed matter phenomena. Phenomena such as Bloch oscillations, Josephson currents and Mott insulator phases have been realised in a very clean way. They mark the beginning of this novel direction in physics with coherent matter waves.

Another important aspect of matter wave systems inside optical lattice structures lies in the further increased control one can exert over the system. We discussed progress towards moving single atoms at will in momentum and position space, letting them interact in a well defined way and detecting their individual state.

In summary the physics of coherent matter waves rapidly grows into diverse fields. Starting from fundamental insights into the quantum world we find fascinating analogies to coherent and nonlinear optics, promising applications in high precision measurements, intriguing possibilities to model condensed matter phenomena and novel prospects for quantum computation. Although several basic features have been investigated the whole field is still at the beginning of many interesting developments and clearly continues to expand. One can expect exciting results and fundamental new physics in near future in the area of the physics with coherent matter waves.

- [1] L. deBroglie. *Ann. Phys.*, 3:22, 1925.
- [2] C. Davisson and L. H. Germer. Diffraction of electrons by a crystal of nickel. *Phys. Rev.*, 30:705, 1927.
- [3] C. J. Bordé. *Phys. Lett. A*, 140:10, 1989.
- [4] O. Carnal and J. Mlynek. Young's double-slit experiment with atoms: A simple atom interferometer. *Phys. Rev. Lett.*, 66:2689, 1991.
- [5] D. W. Keith, C. R. Ekstrom, Q. A. Turchette, and D. E. Pritchard. An interferometer for atoms. *Phys. Rev. Lett.*, 66:2693, 1991.
- [6] F. Riehle and T. Kisters, A. Witte, J. Helmcke, and C. J. Bordé. Optical Ramsey spectroscopy in a rotating frame: Sagnac effect in a matter-wave interferometer. *Phys. Rev. Lett.*, 67:177, 1991.

- [7] M. Kasevich and S. Chu. Atomic interferometry using stimulated raman transitions. *Phys. Rev. Lett.*, 67:181, 1991.
- [8] D. S. Weiss, B. C. Young, and S. Chu. Precision measurement of the photon recoil of an atom using atomic interferometry. *Phys. Rev. Lett.*, 70:2706, 1993.
- [9] T. L. Gustavson, P. Bouyer, and M. A. Kasevich. Precision rotation measurements with an atom interferometer gyroscope. *Phys. Rev. Lett.*, 78:2046, 1997.
- [10] P. R. Berman, editor. *Atom interferometry*. Academic Press, 1997.
- [11] M. J. Snadden, J. M. McGuirk, P. Bouyer, K. G. Haritos, and M. A. Kasevich. Measurement of the earth's gravity gradient with an atom interferometer-based gravity gradiometer. *Phys. Rev. Lett.*, 81:971, 1998.
- [12] T. L. Gustavson, A. Landragin, and M. A. Kasevich. *Class. Quant. Gravity*, 17:2385, 2000.
- [13] M. H. Anderson, J. R. Ensher, M. R. Matthews, C. E. Wieman, and E. A. Cornell. Observation of Bose-Einstein condensation in a dilute atomic vapor. *Science*, 269(0):198, 1995.
- [14] K. B. Davis, M.-O. Mewes, M. R. Andrews, N. J. van Druten, D. S. Durfee, D. M. Kurn, and W. Ketterle. Bose-Einstein condensation in a gas of sodium atoms. *Phys. Rev. Lett.*, 75(22):3969, 1995.
- [15] C. C. Bradley, C. A. Sackett, J. J. Tollett, and R. G. Hulet. Evidence of Bose-Einstein condensation in an atomic gas with attractive interactions. *Phys. Rev. Lett.*, 75(9):1687, 1995. *ibid.* **79**, 1170 (1997).
- [16] E. A. Cornell and C. E. Wieman. Nobel lecture: Bose-Einstein condensation in a dilute gas, the first 70 years and some recent experiments. *Rev. Mod. Phys.*, 74(3):875, 2002.
- [17] W. Ketterle. Nobel lecture: When atoms behave as waves: Bose-Einstein condensation and the atom laser. *Rev. Mod. Phys.*, 74:1131, 2002.
- [18] M. R. Andrews, C. G. Townsend, H.-J. Miesner, D. S. Durfee, D. M. Kurn, and W. Ketterle. Observation of interference between two Bose-Einstein condensates. *Science*, 275(0):637, 1997.
- [19] S. N. Bose. Plancks Gesetz und Lichtquantenhypothese. *Z. Phys.*, 26(3):178, 1924.
- [20] A. Einstein. Quantentheorie des einatomigen idealen Gases. Zweite Abhandlung. *Sitzungber. Preuss. Akad. Wiss.*, 1925:3, 1925.
- [21] F. London. On the Bose-Einstein condensation. *Phys. Rev.*, 54(0):947, 1938.
- [22] Fritz London. The λ -phenomenon of liquid helium and the Bose-Einstein degeneracy. *Nature*, 141(3571):643, 1938.
- [23] William C. Stwalley and L. H. Nosanow. Possible "new" quantum systems. *Phys. Rev. Lett.*, 36(15):910, 1976.
- [24] I. F. Silvera and J. T. M. Walraven. Stabilization of atomic hydrogen at low temperature. *Phys. Rev. Lett.*, 44(3):164, 1980.
- [25] W. N. Hardy, M. Morrow, R. Jochemsen, and A. J. Berlinsky. Magnetic resonance of atomic hydrogen at low temperatures. *Physica*, 109/110B(0):1964, 1982.
- [26] Harald F. Hess, David A. Bell, Gregory P. Kochanski, Richard A. Cline, Daniel Kleppner, and Thomas J. Greytak. Observation of three-body recombination in spin-polarized hydrogen. *Phys. Rev. Lett.*, 51(6):483, 1983.
- [27] B. R. Johnson, J. S. Denker, N. Bigelow, L. P. Lévy, J. H. Freed, and D. M. Lee. Observation of nuclear spin waves in spin-polarized atomic hydrogen gas. *Phys. Rev. Lett.*, 52(17):1508, 1984.
- [28] E. Cornell. Very cold indeed: The nanokelvin physics of Bose-Einstein condensation. *J. Res. Natl. Inst. Stand. Tech.*, 101(4):419, 1996.
- [29] K. Burnett. Ultracold interactions and mean-field theory of Bose-Einstein condensates. In M. Inguscio, S. Stringari, and C. E. Wieman, editors, *Proceedings of the International School of Physics - Enrico Fermi*, page 265. IOS Press, 1999.
- [30] E. A. Cornell, J. R. Ensher, and C. E. Wieman. Experiments in dilute atomic Bose-Einstein condensation. In M. Inguscio, S. Stringari, and C. E. Wieman, editors, *Proceedings of the International School of Physics - Enrico Fermi*, page 15. IOS Press, 1999.
- [31] W. Ketterle, D. S. Durfee, and D. M. Stamper-Kurn. Making, probing and understanding Bose-Einstein condensates. In M. Inguscio, S. Stringari, and C. E. Wieman, editors, *Proceedings of the International School of Physics - Enrico Fermi*, page 67. IOS Press, 1999.
- [32] F. Dalfovo, S. Giorgini, L. P. Pitaevskii, and S. Stringari. Theory of Bose-Einstein condensation in trapped gases. *Rev. Mod. Phys.*, 71(3):463, 1999.
- [33] A. Griffin. A brief history of our understanding of BEC: From Bose to Beliaev. In M. Inguscio, S. Stringari, and C. E. Wieman, editors, *Proceedings of the International School of Physics - Enrico Fermi*, page 1. IOS Press, 1999.
- [34] K. Helmerson and W. D. Phillips. Cooling, trapping and manipulation of neutral atoms and

- BEC by electromagnetic fields. In M. Inguscio, S. Stringari, and C. E. Wieman, editors, *Proceedings of the International School of Physics - Enrico Fermi*, page 391. IOS Press, 1999.
- [35] Ph. W. Courteille, V. S. Bagnato, and V. I. Yukalov. Bose-Einstein condensation of trapped atomic gases. *Laser Phys.*, 11.
- [36] D. M. Stamper-Kurn and W. Ketterle. Spinor condensates and light scattering from Bose-Einstein condensates. In R. Kaiser, C. Westbrook, and F. David, editors, *Coherent Atomic Matter Waves - Les Houches Summer School Session LXXII*, page 137. Springer, 2001.
- [37] W. Ketterle and S. Inouye. Collective enhancement and suppression in bose-einstein condensates. *Compte rendus de l'académie des sciences, Serie IV - Physique Astrophysique*, 2:339, 2001.
- [38] Eric A. Cornell and Carl E. Wieman. Bose-Einstein condensation in a dilute gas: The first 70 years and some recent experiments (Nobel Lecture). *Chem. Phys. Chem.*, 3:476, 2002.
- [39] K. Bongs, S. Burger, D. Hellweg, M. Kottke, S. Dettmer, T. Rinkleff, L. Cacciapuoti, J. Arlt, K. Sengstock, and W. Ertmer. Spectroscopy of dark soliton states in Bose-Einstein condensates. *J. Opt. B: Quantum Semiclass. Opt.*, 5:124, 2003.
- [40] A. Griffin, D. W. Snoke, and S. Stringari. *Bose-Einstein Condensation*. Cambridge University Press, 1995.
- [41] S. Martellucci, A. N. Chester, and A. Aspect. *Bose-Einstein Condensates and Atom Lasers*. Plenum Publishing Corporation, 2000.
- [42] C. Savage and P. D. Mukunda. *Bose-Einstein Condensation: From Atomic Physics to Quantum Fields*. World Scientific Publishing Company, 2001.
- [43] C. J. Pethick and H. Smith. *Bose-Einstein Condensation in Dilute Gases*. Cambridge University Press, 2002.
- [44] L. P. Pitaevskii and S. Stringari. *Bose-Einstein Condensation (The International Series on Monographs on Physics)*. Oxford University Press, 2003.
- [45] H.-J. Miesner, D. M. Stamper-Kurn, M. R. Andrews, D. S. Durfee, S. Inouye, and W. Ketterle. Bosonic stimulation in the formation of a Bose-Einstein condensate. *Science*, 279(0):1005, 1998.
- [46] S. Inouye, T. Pfau, S. Gupta, A. P. Chikkatur, A. Görlitz, D. E. Pritchard, and W. Ketterle. Phase-coherent amplification of atomic matter waves. *Nature*, 402:641, 1999.
- [47] V. V. Goldman, Isaac F. Silvera, and Anthony J. Leggett. Atomic hydrogen in an inhomogeneous magnetic field: Density profile and Bose-Einstein condensation. *Phys. Rev. B*, 24(5):2870, 1981.
- [48] D. A. Huse and E. D. Siggia. The density distribution of a weakly interacting Bose gas in an external potential. *J. Low Temp. Phys.*, 48(1/2):137, 1982.
- [49] V. Bagnato, D. E. Pritchard, and D. Kleppner. Bose-Einstein condensation in an external potential. *Phys. Rev. A*, 35:4354, 1987.
- [50] R. K. Pathria. Bose-Einstein condensation of a finite number of particles confined to harmonic traps. *Phys. Rev. A*, 58(2):1490, 1998.
- [51] J. R. Ensher, D. S. Jin, M. R. Matthews, C. E. Wieman, and E. A. Cornell. Bose-Einstein condensation in a dilute gas: Measurement of energy and ground-state occupation. *Phys. Rev. Lett.*, 77(25):4984, 1996.
- [52] M.-O. Mewes, M. R. Andrews, N. J. van Druten, D. M. Kurn, D. S. Durfee, and W. Ketterle. Bose-Einstein condensation in a tightly confining dc magnetic trap. *Phys. Rev. Lett.*, 77(3):416, 1996.
- [53] F. Gerbier, J. H. Thywissen, S. Richard, M. Hugbart, P. Bouyer, and A. Aspect. Critical temperature of a trapped, weakly interacting Bose gas. *Phys. Rev. Lett.*, 92:030405, 2004.
- [54] M. Gajda and K. Rzążewski. Fluctuations of bose-einstein condensate. *Phys. Rev. Lett.*, 78:2686, 1997.
- [55] P. Navez, D. Bitouk, M. Gajda, Z. Idziaszek, and K. Rzążewski. Fourth statistical ensemble for the Bose-Einstein condensate. *Phys. Rev. Lett.*, 79(10):1789, 1997.
- [56] M. Wilkens and C. Weiss. *J. Mod. Opt.*, 44:1801, 1997.
- [57] N. L. Balazs and T. Bergeman. Statistical mechanics of ideal Bose atoms in a harmonic trap. *Phys. Rev. A*, 58(3):2359, 1998.
- [58] M. Holthaus, E. Kalinowski, and K. Kirsten. *Ann. Phys. (N.Y.)*, 270:198, 1998.
- [59] Z. Idziaszek, M. Gajda, P. Navez, M. Wilkens, and K. Rzążewski. Fluctuations of the weakly interacting Bose-Einstein condensate. *Phys. Rev. Lett.*, 82(22):4376, 1999.
- [60] P. Borrmann, J. Harting, O. Mülken, and E. R. Hilf. Calculation of thermodynamic properties of finite Bose-Einstein systems. *Phys. Rev. A*, 60(2):1519, 1999.
- [61] V. V. Kocharovskiy, V. V. Kocharovskiy, and Marlan O. Scully. Condensate statistics in

- interacting and ideal dilute Bose gases. *Phys. Rev. Lett.*, 84(11):2306, 2000.
- [62] V. V. Kocharovskiy, Marlan O. Scully, Shi-Yao Zhu, and M. Suhail Zubairy. Condensation of N bosons. II. Nonequilibrium analysis of an ideal Bose gas and the laser phase-transition analogy. *Phys. Rev. A*, 61:023609, 2000.
- [63] V. V. Kocharovskiy, V. V. Kocharovskiy, and Marlan O. Scully. Condensation of N bosons. III. Analytical results for all higher moments of condensate fluctuations in interacting and ideal dilute Bose gases via the canonical ensemble quasiparticle formulation. *Phys. Rev. A*, 61:053606, 2000.
- [64] M. Holthaus, K. T. Kapale, and M. O. Scully. Influence of boundary conditions on statistical properties of ideal Bose-Einstein condensates. *Phys. Rev. E*, 65:036129, 2002.
- [65] H. Xiong, S. Liu, G. Huang, and Z. Xu. Canonical statistics of trapped ideal and interacting Bose gases. *Phys. Rev. A*, 65:033609, 2002.
- [66] E. P. Gross. *J. Math. Phys.*, 4:915, 1963.
- [67] L. P. Pitaevskii. *Sov. Phys. JETP*, 13:451, 1961.
- [68] A. L. Fetter. *Ann. Phys.*, 70:67, 1972.
- [69] N. Bogoliubov. *J. Phys.*, 11:23, 1947.
- [70] N. P. Proukakis and K. Burnett. Generalized mean fields for trapped atomic Bose-Einstein condensates. *J. Res. Natl. Inst. Stand. Tech.*, 101(4):457, 1996.
- [71] C. W. Gardiner and P. Zoller. Quantum kinetic theory: A quantum kinetic master equation for condensation of a weakly interacting Bose gas without a trapping potential. *Phys. Rev. A*, 55(4):2902, 1997.
- [72] C. W. Gardiner, P. Zoller, R. J. Ballagh, and M. J. Davis. Kinetics of Bose-Einstein condensation in a trap. *Phys. Rev. Lett.*, 79(10):1793, 1997.
- [73] D. A. W. Hutchinson, E. Zaremba, and A. Griffin. Finite temperature excitations of a trapped Bose gas. *Phys. Rev. Lett.*, 78(10):1842, 1997.
- [74] C. W. Gardiner and P. Zoller. Quantum kinetic theory. III. Quantum kinetic master equation for strongly condensed trapped systems. *Phys. Rev. A*, 58(1):536, 1998.
- [75] C. W. Gardiner, M. D. Lee, R. J. Ballagh, M. J. Davis, and P. Zoller. Quantum kinetic theory of condensate growth: Comparison of experiment and theory. *Phys. Rev. Lett.*, 81(24):5266, 1998.
- [76] S. Choi, S. A. Morgan, and K. Burnett. Phenomenological damping in trapped atomic Bose-Einstein condensates. *Phys. Rev. A*, 57(5):4057, 1998.
- [77] M. Rusc and K. Burnett. Mean-field theory for excitations of trapped Bose condensates at finite temperatures. *Phys. Rev. A*, 59(5):3851, 1999.
- [78] E. Zaremba, T. Nikuni, and A. Griffin. Dynamics of trapped Bose gases at finite temperatures. *J. Low Temp. Phys.*, 116(3/4):277, 1999.
- [79] C. W. Gardiner and P. Zoller. Quantum kinetic theory. V. Quantum kinetic master equation for mutual interaction of condensate and noncondensate. *Phys. Rev. A*, 61:033601, 2000.
- [80] M. Gajda, K. Góral, and K. Rzążewski. Thermodynamics of an interacting trapped Bose-Einstein gas in the classical field approximation. *Phys. Rev. A*, 66:051602, 2002.
- [81] C. Orzel, A. K. Tuchman, M. L. Fenselau, M. Yasuda, and M. A. Kasevich. Squeezed states in a Bose-Einstein condensate. *Science*, 291(5512):2386, 2001.
- [82] M. Greiner, O. Mandel, T. Esslinger, T. W. Hänsch, and I. Bloch. Quantum phase transition from a superfluid to a Mott insulator in a gas of ultracold atoms. *Nature*, 415:39, 2002.
- [83] M. Erhard, H. Schmaljohann, J. Kronjäger, K. Bongs, and K. Sengstock. Bose-Einstein condensation at constant temperature. *cond-mat/*, 0402003, 2004.
- [84] E. A. Burt, R. W. Ghrist, C. J. Myatt, M. J. Holland, E. A. Cornell, and C. E. Wieman. Coherence, correlations, and collisions: What one learns about Bose-Einstein condensates from their decay. *Phys. Rev. Lett.*, 79(3):337, 1997.
- [85] D. S. Hall, M. R. Matthews, C. E. Wieman, and E. A. Cornell. Measurements of relative phase in two-component Bose-Einstein condensates. *Phys. Rev. Lett.*, 81(8):1543, 1998.
- [86] M. Naraschewski and R. J. Glauber. Spatial coherence and density correlations of trapped Bose gases. *Phys. Rev. A*, 59:4595, 1999.
- [87] M. Naraschewski, H. Wallis, A. Schenzle, J. I. Cirac, and P. Zoller. Interference of Bose condensates. *Phys. Rev. A*, 54(3):2185, 1996.
- [88] T. Wong, M. J. Collett, and D. F. Walls. Interference of two Bose-Einstein condensates with collisions. *Phys. Rev. A*, 54(5):R3718, 1996.
- [89] J. Javanainen and S. M. Yoo. Quantum phase of a Bose-Einstein condensate with an arbitrary number of atoms. *Phys. Rev. Lett.*, 76(2):161, 1996.
- [90] W. Hoston and L. You. Interference of two condensates. *Phys. Rev. A*, 53(6):4254, 1996.
- [91] A. Röhrl, M. Naraschewski, A. Schenzle, and H. Wallis. Transition from phase locking to the

- interference of independent Bose condensates: Theory versus experiment. *Phys. Rev. Lett.*, 78(22):4143, 1997.
- [92] Y. Castin and J. Dalibard. Relative phase of two Bose-Einstein condensates. *Phys. Rev. A*, 55(6):4330, 1997.
- [93] J. Javanainen and M. Wilkens. Phase and phase diffusion of a split Bose-Einstein condensate. *Phys. Rev. Lett.*, 78(25):4675, 1997.
- [94] M. Kozuma, L. Deng, E. W. Hagley, J. Wen, R. Lutwak, K. Helmerson, S. L. Rolston, and W. D. Phillips. Coherent splitting of Bose-Einstein condensed atoms with optically induced Bragg diffraction. *Phys. Rev. Lett.*, 82(5):871, 1999.
- [95] K. Bongs, S. Burger, G. Birkl, K. Sengstock, W. Ertmer, K. Rzążewski, A. Sanpera, and M. Lewenstein. Coherent evolution of bouncing Bose-Einstein condensates. *Phys. Rev. Lett.*, 83(18):3577, 1999.
- [96] Y. Torii, Y. Suzuki, M. Kozuma, T. Sugiura, T. Kuga, L. Deng, and E. W. Hagley. Mach-Zehnder Bragg interferometer for a Bose-Einstein condensate. *Phys. Rev. A*, 61:041602(R), 2000.
- [97] F. Minardi, C. Fort, P. Maddaloni, M. Modugno, and M. Inguscio. Time-domain atom interferometry across the threshold for Bose-Einstein condensation. *Phys. Rev. Lett.*, 87(17):170401, 2001.
- [98] P. Pedri, L. Pitaevskii, S. Stringari, S. Burger, C. Fort, F. S. Cataliotti, P. Maddaloni, F. Minardi, and M. Inguscio. Expansion of a coherent array of Bose-Einstein condensates. *Phys. Rev. Lett.*, 87:220401, 2001.
- [99] J. Stenger, S. Inouye, A. P. Chikkatur, D. M. Stamper-Kurn, D. E. Pritchard, and W. Ketterle. Bragg spectroscopy of a Bose-Einstein condensate. *Phys. Rev. Lett.*, 82(23):4569, 1999.
- [100] P. J. Martin, B. G. Oldaker, A. H. Miklich, and D. E. Pritchard. Bragg scattering of atoms from a standing light wave. *Phys. Rev. Lett.*, 60:515, 1988.
- [101] E. W. Hagley, L. Deng, M. Kozuma, J. Wen, K. Helmerson, S. L. Rolston, and W. D. Phillips. A well-collimated quasi-continuous atom laser. *Science*, 283:1706, 1999.
- [102] E. W. Hagley, L. Deng, M. Kozuma, M. Trippenbach, Y. B. Band, M. Edwards, M. R. Doery, P. S. Julienne, K. Helmerson, S. L. Rolston, and W. D. Phillips. Measurement of the coherence of a Bose-Einstein condensate. *Phys. Rev. Lett.*, 83(16):3112, 1999.
- [103] J. E. Simsarian, J. Denschlag, Mark Edwards, Charles W. Clark, L. Deng, E. W. Hagley, K. Helmerson, S. L. Rolston, and W. D. Phillips. Imaging the phase of an evolving Bose-Einstein condensate wave function. *Phys. Rev. Lett.*, 85(10):2040, 2000.
- [104] K. Bongs, S. Burger, S. Dettmer, D. Hellweg, J. Arlt, W. Ertmer, K. Sengstock, and W. Ertmer. Waveguide for Bose-Einstein condensates. *Phys. Rev. A*, 63:031602(R), 2001.
- [105] Yu. Kagan, E. L. Surkov, and G. V. Shlyapnikov. Evolution of a Bose-condensed gas under variations of the confining potential. *Phys. Rev. A*, 54(3):R1753, 1996.
- [106] Y. Castin and R. Dum. Bose-Einstein condensates in time-dependent traps. *Phys. Rev. Lett.*, 77(27):5315, 1996.
- [107] Yu. Kagan, B. V. Svistunov, and G. V. Shlyapnikov. Kinetics of Bose condensation in an interacting Bose gas. *Sov. Physics JETP*, 74:279, 1992.
- [108] Yu. Kagan and B. V. Svistunov. Kinetics of the onset of long-range order during Bose condensation in an interacting gas. *Sov. Phys. JETP*, 78(2):187, 1994.
- [109] Yu. Kagan. Kinetics of Bose-Einstein condensate formation in an interacting Bose gas. In A. Griffin, D. W. Snoke, and S. Stringari, editors, *Bose-Einstein Condensation*, page 202. Cambridge University Press, 1995.
- [110] N. J. van Druten and Wolfgang Ketterle. Two-step condensation of the ideal Bose gas in highly anisotropic traps. *Phys. Rev. Lett.*, 79(4):549, 1997.
- [111] H. Monien, M. Linn, and N. Elstner. Trapped one-dimensional Bose gas as a Luttinger liquid. *Phys. Rev. A*, 58(5):R3395, 1998.
- [112] M. Olshanii. Atomic scattering in the presence of an external confinement and a gas of impenetrable bosons. *Phys. Rev. Lett.*, 81(5):938, 1998.
- [113] D. S. Petrov, M. Holzmann, and G. V. Shlyapnikov. Bose-einstein condensation in quasi-2d trapped gases. *Phys. Rev. Lett.*, 84:2551, 2000.
- [114] D. S. Petrov, G. V. Shlyapnikov, , and J. T. M. Walraven. Regimes of quantum degeneracy in trapped 1d gases. *Phys. Rev. Lett.*, 85:3745, 2000.
- [115] Yu. Kagan, V. A. Kashurnikov, A. V. Krasavin, N. V. Prokof'ev, and B. V. Svistunov. Quasicondensation in a two-dimensional interacting Bose gas. *Phys. Rev. A*, 61:043608, 2000.
- [116] J. O. Andersen and H. Haugerud. Ground state of a trapped Bose-Einstein condensate in two dimensions: Beyond the mean-field approximation. *Phys. Rev. A*, 65:033615, 2002.

- [117] U. Al Khawaja, J. O. Andersen, N. P. Proukakis, and H. T. C. Stoof. Low dimensional bose gases. *Phys. Rev. A*, 66:013615, 2002.
- [118] D. S. Petrov, G. V. Shlyapnikov, and J. T. M. Walraven. Phase-fluctuating 3d bose-einstein condensates in elongated traps. *Phys. Rev. Lett.*, 87:050404, 2001.
- [119] S. Dettmer, D. Hellweg, P. Ryytty, J. J. Arlt, W. Ertmer, K. Sengstock, D. S. Petrov, G. V. Shlyapnikov, H. Kreutzmann, L. Santos, and M. Lewenstein. Observation of phase fluctuations in elongated bose-einstein condensates. *Phys. Rev. Lett.*, 87:160406, 2001.
- [120] D. Hellweg, S. Dettmer, P. Ryytty, J. J. Arlt, W. Ertmer, K. Sengstock, D. S. Petrov, G. V. Shlyapnikov, H. Kreutzmann, L. Santos, and M. Lewenstein. Phase fluctuations in bose-einstein condensates. *Appl. Phys. B*, 73:781, 2001.
- [121] YI. Shvarchuck, Ch. Buggle, D. S. Petrov, K. Dieckmann, M. Zielonkowski, M. Kemmann, T. G. Tiecke, W. von Klitzing, G. V. Shlyapnikov, and J. T. M. Walraven. Bose-Einstein condensation into nonequilibrium states studied by condensate focusing. *Phys. Rev. Lett.*, 89:270404, 2002.
- [122] H. Kreutzmann, A. Sanpera, L. Santos, M. Lewenstein, D. Hellweg, L. Cacciapuoti, M. Kottke, T. Schulte, K. Sengstock, J. J. Arlt, and W. Ertmer. Characterization and control of phase fluctuations in elongated Bose-Einstein condensates. *Appl. Phys. B*, 76:165, 2003.
- [123] D. Hellweg, L. Cacciapuoti, M. Kottke, T. Schulte, K. Sengstock, W. Ertmer, and J. J. Arlt. Measurement of the spatial correlation function of phase fluctuating Bose-Einstein condensates. *Phys. Rev. Lett.*, 91:010406, 2003.
- [124] F. Gerbier, J. H. Thywissen, S. Richard, M. Hugbart, P. Bouyer, and A. Aspect. Momentum distribution and correlation function of quasicondensates in elongated traps. *Phys. Rev. A*, 67:051602, 2003.
- [125] C. Mora and Y. Castin. Extension of bogoliubov theory to quasicondensates. *Phys. Rev. A*, 67:053615, 2003.
- [126] L. Cacciapuoti, D. Hellweg, M. Kottke, T. Schulte, W. Ertmer, J. J. Arlt, K. Sengstock, L. Santos, and M. Lewenstein. Second-order correlation function of a phase fluctuating Bose-Einstein condensate. *Phys. Rev. A*, 68:053612, 2003.
- [127] S. Richard, F. Gerbier, J. H. Thywissen, M. Hugbart, P. Bouyer, and A. Aspect. Momentum spectroscopy of 1d phase fluctuations in Bose-Einstein condensates. *Phys. Rev. Lett.*, 91:010405, 2003.
- [128] U. Al Khawaja, N. P. Proukakis, J. O. Andersen, M. W. J. Romans, and H. T. C. Stoof. Dimensional and temperature crossover in trapped Bose gases. *Phys. Rev. A*, 68:043603, 2003.
- [129] N. Schlosser, G. Reymond, I. Protsenko, and P. Grangier. Sub-poissonian loading of single atoms in a microscopic dipole trap. *Nature*, 411:1024, 2001.
- [130] R. Folman, P. Krüger, J. Schmiedmayer, J. Denschlag, and C. Henkel. *Adv. At. Mol. Opt. Phys.*, 48:263.
- [131] R. Dumke, M. Volk, T. Mütther, F. B. J. Buchkremer, G. Birkl, and W. Ertmer. Micro-optical realization of arrays of selectively addressable dipole traps: A scalable configuration for quantum computation with atomic qubits. *Phys. Rev. Lett.*, 89:097903, 2002.
- [132] W. Ketterle and H.-J. Miesner. Coherence properties of Bose-Einstein condensates and atom lasers. *Phys. Rev. A*, 56(4):3291, 1997.
- [133] P. Engels, I. Coddington, P. C. Haljan, V. Schweikhard, and E. A. Cornell. Observation of long-lived vortex aggregates in rapidly rotating Bose-Einstein condensates. *Phys. Rev. Lett.*, 90(17):170405, 2003.
- [134] L. Dobrek, M. Gajda, Maciej Lewenstein, K. Sengstock, G. Birkl, and W. Ertmer. Optical generation of vortices in trapped Bose-Einstein condensates. *Phys. Rev. A*, 60(5):R3381, 1999.
- [135] O. Morsch, J. H. Müller, M. Cristiani, D. Ciampini, and E. Arimondo. Bloch oscillations and mean-field effects of Bose-Einstein condensates in 1d optical lattices. *Phys. Rev. Lett.*, 87:140402, 2001.
- [136] M. R. Matthews, B. P. Anderson, P. C. Haljan, D. S. Hall, C. E. Wieman, and E. A. Cornell. Vortices in a Bose-Einstein condensate. *Phys. Rev. Lett.*, 83(13):2498, 1999.
- [137] J. Denschlag, J. E. Simsarian, D. L. Feder, Charles W. Clark, L. A. Collins, J. Cubizolles, L. Deng, E. W. Hagley, K. Helmerson, W. P. Reinhardt, S. L. Rolston, B. I. Schneider, and W. D. Phillips. Generating solitons by phase engineering of a Bose-Einstein condensate. *Science*, 287:97, 2000.
- [138] S. Burger, K. Bongs, S. Dettmer, W. Ertmer, K. Sengstock, A. Sanpera, G. V. Shlyapnikov, and M. Lewenstein. Dark solitons in Bose-Einstein condensates. *Phys. Rev. Lett.*, 83(25):5198, 1999.

- [139] W. Ketterle. Atom laser. In *McGraw-Hill 1999 Yearbook of Science & Technology*, page 43. McGraw-Hill, 1998.
- [140] M. Köhl, M. J. Davis, C. W. Gardiner, T. W. Hänsch, and T. Esslinger. Growth of Bose-Einstein condensates from thermal vapor. *Phys. Rev. Lett.*, 88:080402, 2002.
- [141] M. Olshani, Y. Castin, and J. Dalibard. A model for an atom laser. In Massimo Inguscio, Maria Allegrini, and Antonio Sasso, editors, *Laser Spectroscopy, XII International Conference*, page 7. World Scientific, 1995.
- [142] M. Holland, K. Burnett, C. Gardiner, J. I. Cirac, and P. Zoller. Theory of an atom laser. *Phys. Rev. A*, 54(3):R1757, 1996.
- [143] H. Wiseman, A. Martins, and D. Walls. An atom laser based on evaporative cooling. *Journal of the European Optical Society: Part B, Quantum and Semiclassic Optics*, 8:737, 1996.
- [144] H. M. Wiseman. Defining the (atom) laser. *Phys. Rev. A*, 56(3):2068, 1997.
- [145] R. J. Dodd, Charles W. Clark, Mark Edwards, and K. Burnett. Characterizing the coherence of Bose-Einstein condensates and atom lasers. *Opt. Exp.*, 1(10):284, 1997.
- [146] G. M. Moy and C. M. Savage. Output coupling for an atom laser by state change. *Phys. Rev. A*, 56(2):R1087, 1997.
- [147] G. M. Moy, J. J. Hope, and C. M. Savage. Atom laser based on Raman transitions. *Phys. Rev. A*, 55(5):3631, 1997.
- [148] M. G. Moore and P. Meystre. Dipole-dipole selection rules for an atom laser cavity. *Phys. Rev. A*, 56(4):2989, 1997.
- [149] H. Steck, M. Naraschewski, and H. Wallis. Output of a pulsed atom laser. *Phys. Rev. Lett.*, 80(1):1, 1998.
- [150] B. Kneer, T. Wong, K. Vogel, W. P. Schleich, and D. F. Walls. Generic model of an atom laser. *Phys. Rev. A*, 58(6):4841, 1998.
- [151] Y. B. Band, P. S. Julienne, and M. Trippenbach. Radio-frequency output coupling of the Bose-Einstein condensate for atom lasers. *Phys. Rev. A*, 59(5):3823, 1999.
- [152] H. P. Breuer, D. Faller, B. Kappler, and F. Petruccione. Non-Markovian dynamics in pulsed and continuous-wave atom lasers. *Phys. Rev. A*, 60(4):3188, 1999.
- [153] M. Trippenbach, Y. B. Band, M. Edwards, M. Doery, P. S. Julienne, E. W. Hagley, L. Deng, M. Kozuma, K. Helmerson, S. L. Rolston, and W. D. Phillips. Coherence properties of an atom laser. *J. Phys. B*, 33:47, 2000.
- [154] S. Bhongale and M. Holland. Loading a continuous-wave atom laser by optical pumping techniques. *Phys. Rev. A*, 62:043604, 2000.
- [155] J. Jeffers, P. Horak, S. M. Barnett, and P. M. Radmore. Bound mode of an atom laser. *Phys. Rev. A*, 62:043602, 2000.
- [156] Y. Wu and X. Yang. Output rate of atom lasers in a Raman-type output-coupling scheme. *Phys. Rev. A*, 62:013603, 2000.
- [157] P. D. Drummond, A. Eleftheriou, K. Huang, and K. V. Kheruntsyan. Theory of a mode-locked atom laser with toroidal geometry. *Phys. Rev. A*, 63:053602, 2001.
- [158] H. M. Wiseman and John A. Vaccaro. Atom lasers, coherent states, and coherence II. Maximally robust ensembles of pure states. *Phys. Rev. A*, 65:043606, 2002.
- [159] F. Gerbier, P. Bouyer, and A. Aspect. Quasicontinuous atom laser in the presence of gravity. *Phys. Rev. Lett.*, 86:4729, 2001.
- [160] B. Borca, J. W. Dunn, V. Kokoouline, and C. H. Greene. Atom-molecule laser fed by stimulated three-body recombination. *Phys. Rev. Lett.*, 91:070404, 2003.
- [161] A. S. Bradley, J. J. Hope, and M. J. Collett. Steady-state quantum statistics of a non-markovian atom laser. ii. *Phys. Rev. A*, 68:063611, 2003.
- [162] J. Ruostekoski, T. Gasenzer, and D. A. W. Hutchinson. Pulsed raman output coupler for an atom laser. *Phys. Rev. A*, 68:011604, 2003.
- [163] Y. Castin, J. I. Cirac, and M. Lewenstein. Reabsorption of light by trapped atoms. *Phys. Rev. Lett.*, 80(24):5305, 1998.
- [164] L. Santos and M. Lewenstein. Condensation of laser cooled gases. *Euro. Phys. J. D*, 7:379, 1999.
- [165] L. Santos and M. Lewenstein. Dynamical cooling of trapped gases. ii: Many-atom problem. *Phys. Rev. A*, 60:3851, 1999.
- [166] L. Santos, Z. Idziaszek, J. I. Cirac, and M. Lewenstein. Laser-induced condensation of trapped bosonic gases. *J. Phys. B*, 33:4131, 2000.
- [167] M. Lewenstein, J. I. Cirac, and L. Santos. Cooling of a small sample of Bose atoms with accidental degeneracy. *J. Phys. B*, 33:4107, 2000.
- [168] F. Floegel, L. Santos, and M. Lewenstein. Loading of a Bose-Einstein condensate in the boson accumulation regime. *Europhys. Lett.*, 54(3):279, 2001.

- [169] L. Santos, F. Floegel, T. Pfau, and M. Lewenstein. Continuous optical loading of a Bose-Einstein condensate. *Phys. Rev. A*, 63:063408, 2001.
- [170] M. Olshanii and D. Weiss. Producing Bose-Einstein condensates using optical lattices. *Phys. Rev. Lett.*, 89(9):090404, 2002.
- [171] V. Vuletic, C. Chin, A. J. Kerman, , and S. Chu. Degenerate raman sideband cooling of trapped cesium atoms at very high atomic densities. *Phys. Rev. Lett.*, 81:5768, 1998.
- [172] A. J. Kerman, V. Vuletic, C. Chin, and S. Chu. Beyond optical molasses: 3d raman sideband cooling of atomic cesium to high phase-space density. *Phys. Rev. Lett.*, 84:439, 2000.
- [173] D.-J. Han, S. Wolf, S. Oliver, C. McCormick, M. T. DePue, and D. S. Weiss. 3d raman sideband cooling of cesium atoms at high density. *Phys. Rev. Lett.*, 85:724, 2000.
- [174] S. Wolf, S. J. Oliver, and D. S. Weiss. Suppression of recoil heating by an optical lattice. *Phys. Rev. Lett.*, 85:4249, 2000.
- [175] P. Treutlein, K. Y. Chung, and S. Chu. High-brightness atom source for atomic fountains. *Phys. Rev. A*, 63:051401, 2001.
- [176] E. Mandonnet, A. Minguzzi, R. Dum, I. Carusotto, Y. Castin, and J. Dalibard. Evaporative cooling of an atomic beam. *Eur. Phys. J. D*, 10:9, 2000.
- [177] P. Cren, C. F. Roos, D. Guéry-Odelin, and J. Dalibard. Loading of a cold atomic beam into a magnetic guide. *Eur. Phys. Jour. D*, 20:107, 2002.
- [178] A. P. Chikkatur, Y. Shin, A. E. Leanhardt, D. Kielpinski, E. Tsikata, T. L. Gustavson, D. E. Pritchard, and W. Ketterle. A continuous source of Bose-Einstein condensed atoms. *Science*, 296:2193, 2002.
- [179] T. L. Gustavson, A. P. Chikkatur, A. E. Leanhardt, A. Görlitz, A. Gupta, D. E. Pritchard, and W. Ketterle. Transport of Bose-Einstein condensates with optical tweezers. *Phys. Rev. Lett.*, 88(2):020401, 2001.
- [180] Dale G. Fried, Thomas C. Killian, Lorenz Willmann, David Landhuis, Stephen C. Moss, Daniel Kleppner, and Thomas J. Greytak. Bose-Einstein condensation of atomic hydrogen. *Phys. Rev. Lett.*, 81(18):3811, 1998.
- [181] M.-O. Mewes, M. R. Andrews, D. M. Kurn, D. S. Durfee, C. G. Townsend, and W. Ketterle. Output coupler for Bose-Einstein condensed atoms. *Phys. Rev. Lett.*, 78(4):582, 1997.
- [182] I. Bloch, T. W. Hänsch, and T. Esslinger. Atom laser with a cw output coupler. *Phys. Rev. Lett.*, 82(15):3008, 1999.
- [183] I. Bloch, T. W. Hänsch, and T. Esslinger. Measurement of the spatial coherence of a trapped Bose gas at the phase transition. *Nature*, 403(6766):166, 2000.
- [184] M. Köhl, T. W. Hänsch, and T. Esslinger. Measuring the temporal coherence of an atom laser beam. *Phys. Rev. Lett.*, 87:160404, 2001.
- [185] B. P. Anderson and M. A. Kasevich. Macroscopic quantum interference from atomic tunnel arrays. *Science*, 282:1686, 1998.
- [186] G. Cennini, G. Ritt, C. Geckeler, and M. Weitz. All-optical realization of an atom laser. *Phys. Rev. Lett.*, 91:240408, 2003.
- [187] M. J. Bijlsma, E. Zaremba, and H. T. C. Stoof. Condensate growth in trapped Bose gases. *Phys. Rev. A*, 62:063609, 2000.
- [188] M. J. Davis, C. W. Gardiner, and R. J. Ballagh. Quantum kinetic theory: VII. The influence of vapor dynamics on condensate growth. *Phys. Rev. A*, 62:063608, 2000.
- [189] M. D. Lee and C. W. Gardiner. Quantum kinetic theory. vi. the growth of a Bose-Einstein condensate. *Phys. Rev. A*, 62:033606, 2000.
- [190] S. Inouye, A. P. Chikkatur, D. M. Stamper-Kurn, J. Stenger, D. E. Pritchard, and W. Ketterle. Superradiant Rayleigh scattering from a Bose-Einstein condensate. *Science*, 285:571, 1999.
- [191] S. Inouye, R. F. Löw, S. Gupta, T. Pfau, A. Görlitz, T. L. Gustavson, D. E. Pritchard, and W. Ketterle. Amplification of light and atoms in a Bose-Einstein condensate. *Phys. Rev. Lett.*, 85:4225, 2000.
- [192] D. Schneble, G. K. Campbell, E. W. Streed, M. Boyd, D. E. Pritchard, and W. Ketterle. Raman amplification of matter waves. *cond-mat/*, 0311138, 2003.
- [193] M. Kozuma, Y. Suzuki, Y. Torii, T. Sugiura, T. Kuga, E. W. Hagley, and L. Deng. Phase-coherent amplification of matter waves. *Science*, 286:2309, 1999.
- [194] S. Pötting C. Henkel and M. Wilkens. Loss and heating of particles in small and noisy traps. *Appl. Phys. B*, 69:379, 1999.
- [195] S. Pötting C. Henkel. Coherent transport of matter waves. *Appl. Phys. B*, 72:73, 2001.
- [196] S. Kraft, A. Günther, H. Ott, D. Wharam, C. Zimmermann, and J. Fortágh. Anomalous longitudinal magnetic field near the surface of copper conductors. *J. Phys. B: At. Mol. Opt. Phys.*, 35:L469, 2002.
- [197] J. Fortágh, H. Ott, S. Kraft, A. Günther, and C. Zimmermann. Surface effects in magnetic

- microtraps. *Phys. Rev. A*, 66:041604(R), 2002.
- [198] W. Belzig, C. Schroll, and C. Bruder. Decoherence of cold atomic gases in magnetic microtraps. *Phys. Rev. A*, 68:043618, 2003.
- [199] M. P. A. Jones, C. J. Vale, D. Sahagun, B. V. Hall, and E. A. Hinds. Spin coupling between cold atoms and the thermal fluctuations of a metal surface. *Phys. Rev. Lett.*, 91:080401, 2003.
- [200] D. M. Harber, J. M. McGuirk, J. M. Obrecht, and E. A. Cornell. Thermally induced losses in ultra-cold atoms magnetically trapped near room-temperature surfaces. *J. Low Temp. Phys.*, 133(3):229, 2003.
- [201] Y. j. Lin, I. Teper, C. Chin, and V. Vuletic. Impact of the casimir-polder potential and johnson noise on Bose-Einstein condensate stability near surfaces. *Phys. Rev. Lett.*, 92:050404, 2004.
- [202] D.-W. Wang, M. D. Lukin, and E. Demler. Disordered Bose-Einstein condensates in quasi-one-dimensional magnetic microtraps. *Phys. Rev. Lett.*, 92:076802, 2004.
- [203] L. Deng, E. W. Hagley, J. Wen, M. Trippenbach, Y. Band, P. S. Julienne, J. E. Simsarian, K. Helmerson, S. L. Rolston, and W. D. Phillips. Four-wave mixing with matter waves. *Nature*, 398(6724):218, 1999.
- [204] J. M. Vogels, K. Xu, and W. Ketterle. Generation of macroscopic pair-correlated atomic beams by four-wave mixing in Bose-Einstein condensates. *Phys. Rev. Lett.*, 89(2):020401, 2002.
- [205] P. Bouyer and M. A. Kasevich. Heisenberg-limited spectroscopy with degenerate Bose-Einstein gases. *Phys. Rev. A*, 56(2):R1083, 1997.
- [206] L. Khaykovich, F. Schreck, G. Ferrari, T. Bourdel, J. Cubizolles, L. D. Carr, Y. Castin, and C. Salomon. Formation of a matter-wave bright soliton. *Science*, 296(5571):1290, 2002.
- [207] K. E. Strecker, G. B. Partridge, A. G. Truscott, and R. G. Hulet. Formation and propagation of matter-wave soliton trains. *Nature*, 417:150, 2002.
- [208] B. P. Anderson, P. C. Haljan, C. A. Regal, D. L. Feder, L. A. Collins, C. W. Clark, and E. A. Cornell. Watching dark solitons decay into vortex rings in a Bose-Einstein condensate. *Phys. Rev. Lett.*, 86(14):2926, 2001.
- [209] V. E. Zakharov and A. B. Shabat. *Sov. Phys. JETP*, 34:62, 1999.
- [210] P. O. Fedichev, A. E. Muryshev, and G. V. Shlyapnikov. Dissipative dynamics of a kink state in a Bose-condensed gas. *Phys. Rev. A*, 60(4):3220, 1999.
- [211] A. E. Muryshev, H. B. van Linden van den Heuvell, and G. V. Shlyapnikov. Stability of standing matter waves in a trap. *Phys. Rev. A*, 60(4):R2665, 1999.
- [212] B. Eiermann, P. Treutlein, Th. Anker, M. Albiez, M. Taglieber, K.-P. Marzlin, and M. K. Oberthaler. Dispersion management for atomic matter waves. *Phys. Rev. Lett.*, 91:060402, 2003.
- [213] A. Trombettoni and A. Smerzi. Discrete solitons and breathers with dilute Bose-Einstein condensates. *Phys. Rev. Lett.*, 86:2353, 2001.
- [214] F. Kh. Abdullaev, E. N. Tsoy, B. A. Malomed, and R. A. Kraenkel. Array of Bose-Einstein condensates under time-periodic feshbach-resonance management. *Phys. Rev. A*, 68:053606, 2003.
- [215] P. J. Y. Louis, E. A. Ostrovskaya, C. M. Savage, and Yu. S. Kivshar. Bose-Einstein condensates in optical lattices: Band-gap structure and solitons. *Phys. Rev. A*, 67:013602, 2003.
- [216] E. A. Ostrovskaya and Yu. S. Kivshar. Matter-wave gap solitons in atomic band-gap structures. *Phys. Rev. Lett.*, 90:160407, 2003.
- [217] V. Ahufinger, A. Sanpera, P. Pedri, L. Santos, and M. Lewenstein. Creation of discrete solitons and observation of the peierls-nabarro barrier in Bose-Einstein condensates. *cond-mat/*, 0310042, 2003.
- [218] M. R. Matthews, D. S. Hall, D. S. Jin, J. R. Ensher, C. E. Wieman, E. A. Cornell, F. Dalfovo, C. Minniti, and S. Stringari. Dynamical response of a Bose-Einstein condensate to a discontinuous change in internal state. *Phys. Rev. Lett.*, 81(2):243, 1998.
- [219] D. M. Stamper-Kurn, M. R. Andrews, A. P. Chikkatur, S. Inouye, H.-J. Miesner, J. Stenger, and W. Ketterle. Optical confinement of a Bose-Einstein condensate. *Phys. Rev. Lett.*, 80(10):2027, 1998.
- [220] H.-J. Miesner, D. M. Stamper-Kurn, J. Stenger, S. Inouye, A. P. Chikkatur, and W. Ketterle. Observation of metastable states in spinor Bose-Einstein condensates. *Phys. Rev. Lett.*, 82(11):2228, 1999.
- [221] A. E. Leanhardt, Y. Shin, D. Kielpinski, D. E. Pritchard, and W. Ketterle. Coreless vortex formation in a spinor Bose-Einstein condensate. *Phys. Rev. Lett.*, 90(14):140403, 2003.
- [222] D. S. Hall, M. R. Matthews, J. R. Ensher, C. E. Wieman, and E. A. Cornell. Dynamics of component separation in a binary mixture of Bose-Einstein condensates. *Phys. Rev. Lett.*, 81(8):1539, 1998.

- [223] M. R. Matthews, B. P. Anderson, P. C. Haljan, D. S. Hall, M. J. Holland, J. E. Williams, C. E. Wieman, and E. A. Cornell. Watching a superfluid untwist itself: Recurrence of Rabi oscillations in a Bose-Einstein condensate. *Phys. Rev. Lett.*, 83(17):3358, 1999.
- [224] J. M. McGuirk, H. J. Lewandowski, D. M. Harber, T. Nikuni, J. E. Williams, and E. A. Cornell. Spatial resolution of spin waves in an ultracold gas. *Phys. Rev. Lett.*, 89(9):090402, 2002.
- [225] D. M. Harber, H. J. Lewandowski, J. M. McGuirk, and E. A. Cornell. Effect of cold collisions on spin coherence and resonance shifts in a magnetically trapped ultracold gas. *Phys. Rev. A*, 66:053616, 2002.
- [226] J. M. McGuirk, D. M. Harber, H. J. Lewandowski, and E. A. Cornell. Normal-superfluid interaction dynamics in a spinor Bose gas. *Phys. Rev. Lett.*, 91:150402, 2003.
- [227] H. J. Lewandowski, J. M. McGuirk, D. M. Harber, and E. A. Cornell. Decoherence-driven cooling of a degenerate spinor Bose gas. *Phys. Rev. Lett.*, 91:240404, 2003.
- [228] H. Schmaljohann, M. Erhard, and J. Kronj. Dynamics of $f = 2$ spinor Bose-Einstein condensates.
- [229] K. Góral, K. Rzazewski, and T. Pfau. Bose-Einstein condensation with magnetic dipole-dipole forces. *Phys. Rev. A*, 61:051601(R), 2000.
- [230] L. Santos, G. V. Shlyapnikov, P. Zoller, and M. Lewenstein. Bose-Einstein condensation in trapped dipolar gases. *Phys. Rev. Lett.*, 85(9):1791, 2000.
- [231] S. Giovanazzi and A. G. Tuning the dipolar interaction in quantum gases.
- [232] B. Damski, L. Santos, E. Tiemann, M. Lewenstein, S. Kotochigova, P. Julienne, and P. Zoller. Creation of a dipolar superfluid in optical lattices. *Phys. Rev. Lett.*, 90:110401, 2003.
- [233] S. Yi and L. You. Expansion of a dipolar condensate. *Phys. Rev. A*, 67:045601, 2003.
- [234] T.-L. Ho. Spinor Bose condensates in optical traps. *Phys. Rev. Lett.*, 81(4):742, 1998.
- [235] M. Koashi and M. Ueda. Exact eigenstates and magnetic response of spin-1 and spin-2 Bose-Einstein condensates. *Phys. Rev. Lett.*, 84:1066, 2000.
- [236] M. Ueda and M. Koashi. Theory of spin-2 Bose-Einstein condensates: Spin correlations, magnetic response, and excitation spectra. *Phys. Rev. A*, 65:063602, 2002.
- [237] J. Stenger, S. Inouye, D. M. Stamper-Kurn, H.-J. Miesner, A. P. Chikkatur, and W. Ketterle. Spin domains in ground-state Bose-Einstein condensates. *Nature*, 396:345, 1999.
- [238] D. M. Stamper-Kurn, H.-J. Miesner, A. P. Chikkatur, S. Inouye, J. Stenger, and W. Ketterle. Quantum tunneling across spin domains in a Bose-Einstein condensate. *Phys. Rev. Lett.*, 83(4):661, 1999.
- [239] A. Görlitz, T. L. Gustavson, A. E. Leanhardt, R. Löw, A. P. Chikkatur, S. Gupta, S. Inouye, D. E. Pritchard, and W. Ketterle. Sodium Bose-Einstein condensates in the $F = 2$ state in a large-volume optical trap. *Phys. Rev. Lett.*, 90(9):090401, 2003.
- [240] M.-S. Chang, C. D. Hamley, M. D. Barrett, J. A. Sauer, K. M. Fortier, W. Zhang, L. You, and M. S. Chapman. Observation of spinor dynamics in optically trapped 87Rb Bose-Einstein condensates. *cond-mat/*, 0309164, 2003.
- [241] M. Erhard, H. Schmaljohann, J. Kronjäger, K. Bongs, and K. Sengstock. Measurement of a mixed spin channel feshbach resonance in rubidium 87. *cond-mat/*, 0309318, 2003.
- [242] M. Key, I. G. Hughes, W. Rooijackers, B. E. Sauer, E. A. Hinds, D. J. Richardson, and P. G. Kazansky. Propagation of cold atoms along a miniature magnetic guide. *Phys. Rev. Lett.*, 84:1371, 2000.
- [243] J. Schmiedmayer. Guiding and trapping a neutral atom on a wire. *Phys. Rev. A*, 52:R13, 1995.
- [244] J. Fortagh, A. Grossmann, C. Zimmermann, and T. W. Hänsch. Miniaturized wire trap for neutral atoms. *Phys. Rev. Lett.*, 81(24):5310, 1998.
- [245] J. Denschlag, D. Cassettari, and J. Schmiedmayer. Guiding neutral atoms with a wire. *Phys. Rev. Lett.*, 82:2014, 1999.
- [246] J. D. Weinstein and K. G. Libbrecht. Microscopic magnetic traps for neutral atoms. *Phys. Rev. A*, 52:4004, 1995.
- [247] W. Hänsel, J. Reichel, and T. W. Hänsch. Atomic micromanipulation with magnetic surface traps. *Phys. Rev. Lett.*, 83:3398, 1999.
- [248] D. Müller, D. Z. Anderson, R. J. Grow, P. D. D. Schwindt, and E. A. Cornell. Guiding neutral atoms around curves with lithographically patterned current-carrying wires. *Phys. Rev. Lett.*, 83:5194, 1999.
- [249] N. H. Dekker, C. S. Lee, V. Lorent, J. H. Thywissen, S. P. Smith, M. Drndic, R. M. Westervelt, and M. Prentiss. Guiding neutral atoms on a chip. *Phys. Rev. Lett.*, 84:1124, 2000.
- [250] R. Folman, P. Krüger, D. Cassettari, B. Hessmo, T. Maier, and J. Schmiedmayer. Controlling cold atoms using nanofabricated surfaces: Atom chips. *Phys. Rev. Lett.*, 84:4749.
- [251] M. Drndic, C. S. Lee, and R. M. Westervelt. Three-dimensional microelectromagnet traps for neutral and charged particles. *Phys. Rev. B*, 63:085321, 2001.

- [252] H. Ott, J. Fortagh, G. Schlotterbeck, A. Grossmann, and C. Zimmermann. Bose-Einstein condensation in a surface microtrap. *Phys. Rev. Lett.*, 87:230401, 2001.
- [253] W. Hänsel, P. Hommelhoff, T.W. Hänsch, and J. Reichel. Bose-Einstein condensation on a microelectronic chip. *Nature*, 413:498, 2001.
- [254] A. E. Leanhardt, A. P. Chikkatur, D. Kielpinski, Y. Shin, T. L. Gustavson, W. Ketterle, and D. E. Pritchard. Propagation of Bose-Einstein condensates in a magnetic waveguide. *Phys. Rev. Lett.*, 89(4):040401, 2002.
- [255] S. Schneider, A. Kasper, C. vom Hagen, M. Bartenstein, B. Engeser, T. Schumm, I. Bar-Joseph, R. Folman, L. Feenstra, and J. Schmiedmayer. Bose-Einstein condensation in a simple microtrap. *Phys. Rev. A*, 67:023612, 2003.
- [256] J. Reichel and J. H. Thywissen. Using magnetic chip traps to study tonks-girardeau quantum gases. *cond-mat/*, 0310330, 2003.
- [257] R. Grimm, M. Weidemüller, and Y. B. Ovchinnikov. Optical dipole traps for neutral atoms. *Adv. At. Mol. Opt. Phys.*, 42:95, 2000.
- [258] G. A. Askar'yan. *Sov. Phys. JETP*, 15:1088, 1962.
- [259] V. S. Letokhov. *JETP Lett.*, 7:272, 1968.
- [260] S. Chu, J. E. Bjorkholm, A. Ashkin, and A. Cable. Experimental observation of optically trapped atoms. *Phys. Rev. Lett.*, 57(3):314, 1986.
- [261] H.-R. Noh, X. Xu, and W. Jhe. Manipulation of cold atoms in hollow laser beams. *Adv. At. Mol. Opt. Phys.*, 48:153, 2002.
- [262] H.-R. Noh and W. Jhe. Atom optics with hollow optical systems. *Physics Report*, 372:269, 2002.
- [263] G. M. Gallatin and P. L. Gould. *J. Opt. Soc. Am. B*, 8:502, 1991.
- [264] J. J. McClelland and M. R. Scheinfein. *J. Opt. Soc. Am. B*, 8:1974, 1991.
- [265] S. Kuppens, M. Rauner, M. Schiffer, G. Wokurka, T. Slawinski, M. Zinner, K. Sengstock, and W. Ertmer. In K. Burnett, editor, *Ultracold Atoms and Bose-Einstein Condensation - Vol. 7 of OSA Trends in Optics and Photonics Series*, page 102. Optical Society of America, 1996.
- [266] T. Kuga, Y. Torii, N. Shiokawa, T. Hirano, Y. Shimizu, and H. Sasada. Novel optical trap of atoms with a doughnut beam. *Phys. Rev. Lett.*, 78:4713, 1997.
- [267] S. Kuppens, M. Rauner, M. Schiffer, K. Sengstock, and W. Ertmer. Polarization-gradient cooling in a strong doughnut-mode dipole potential. *Phys. Rev. A*, 58:3068, 1998.
- [268] X. Xu, V. G. Minogin, K. Lee, Y. Z. Wang, and W. Jhe. Guiding cold atoms in a hollow laser beam. *Phys. Rev. A*, 60:4796, 1999.
- [269] Y. Song, D. Milam, and W. T. Hill III. Long, narrow all-light atom guide. *Optics Lett.*, 24:1805, 1999.
- [270] X. Xu, K. Kim, W. Jhe, and N. Kwon. Efficient optical guiding of trapped cold atoms by a hollow laser beam. *Phys. Rev. A*, 63:063401, 2001.
- [271] M. J. Renn, D. Montgomery, O. Vdovin, D. Z. Anderson, C. E. Wieman, and E. A. Cornell. Laser-guided atoms in hollow-core optical fibers. *Phys. Rev. Lett.*, 75:3253, 1995.
- [272] M. J. Renn, E. A. Donley, E. A. Cornell, C. E. Wieman, and D. Z. Anderson. Evanescent-wave guiding of atoms in hollow optical fibers. *Phys. Rev. A*, 53:R648, 1996.
- [273] H. Ito, T. Nakata, K. Sakaki, and M. Ohtsu. Laser spectroscopy of atoms guided by evanescent waves in micron-sized hollow optical fibers. *Phys. Rev. Lett.*, 76:4500, 1996.
- [274] M. J. Renn, A. A. Zozulya, E. A. Donley, E. A. Cornell, and D. Z. Anderson. Optical-dipole-force fiber guiding and heating of atoms. *Phys. Rev. A*, 55:3684, 1997.
- [275] H. Ito, T. Nakata, K. Sakaki, and M. Ohtsu. Evanescent-light guiding of atoms through hollow optical fiber for optically controlled atomic deposition. *Appl. Phys. Lett.*, 70:2496, 1997.
- [276] J. Yin, Y. Zhu, and Y. Wang. Evanescent light-wave atomic funnel: A tandem hollow-fiber, hollow-beam approach. *Phys. Rev. A*, 57:1957, 1998.
- [277] D. Müller, E. A. Cornell, D. Z. Anderson, and E. R. I. Abraham. Guiding laser-cooled atoms in hollow-core fibers. *Phys. Rev. A*, 61:033411, 2000.
- [278] S. Hayashi, A. Ishimizu, T. Tohei, and M. Tachikawa. Parametric excitation of laser-guided cs atoms in a hollow-core optical fiber. *Phys. Rev. A*, 68:053408, 2003.
- [279] G. Birkl, F. B. J. Buchkremer, R. Dumke, and W. Ertmer. Atom optics with microfabricated optical elements. *Opt. Commun.*, 191:67, 2001.
- [280] R. Dumke, T. Mütther, M. Volk, W. Ertmer, and G. Birkl. Interferometer-type structures for guided atoms. *Phys. Rev. Lett.*, 89:220402, 2002.
- [281] C. S. Adams, M. Sigel, and J. Mlynek. Atom optics. *Phys. Rep.*, 240:143, 1994.
- [282] V. I. Balykin, V. S. Letokhov, Yu. B. Ovchinnikov, and A. I. Sidorov. Quantum-state-selective mirror reflection of atoms by laser light. *Phys. Rev. Lett.*, 60:2137, 1988.

- [283] M. A. Kasevich, D. S. Weiss, and S. Chu. Normal-incidence reflection of slow atoms from an optical evanescent wave. *Opt. Lett.*, 15:607, 1990.
- [284] C. G. Aminoff, A. M. Steane, P. Bouyer, P. Desbiolles, J. Dalibard, and C. CohenTannoudji. Cesium atoms bouncing in a stable gravitational cavity. *Phys. Rev. Lett.*, volume =.
- [285] P. Szriftgiser, D. Guéry-Odelin, M. Arndt, and J. Dalibard. Atomic wave diffraction and interference using temporal slits. *Phys. Rev. Lett.*, 77:4, 1996.
- [286] A. Landragin, J.-Y. Courtois, G. Labeyrie, N. Vansteenkiste, C. I. Westbrook, and A. Aspect. Measurement of the van der waals force in an atomic mirror. *Phys. Rev. Lett.*, 77:1464, 1996.
- [287] V. Savalli, D. Stevens, J. Estève, P. D. Featonby, V. Josse, N. Westbrook, C. I. Westbrook, and A. Aspect. Specular reflection of matter waves from a rough mirror. *Phys. Rev. Lett.*, 88:250404, 2002.
- [288] T. M. Roach, H. Abele, M. G. Boshier, H. L. Grossman, K. P. Zetie, and E. A. Hinds. Realization of a magnetic mirror for cold atoms. *Phys. Rev. Lett.*, 75:629, 1995.
- [289] A. Sidorov, R. J. McLean, W. J. Rowlands, D. C. Lau, J. E. Murphy, M. Walciewicz, G. I. Opat, and P. Hannaford. Specular reflection of cold caesium atoms from a magnetostatic mirror. *Quant. Semiclass. Opt.*, 8:713, 1996.
- [290] K. S. Johnson, M. Drndic, J. H. Thywissen, G. Zabow, R. M. Westervelt, and M. Prentiss. Atomic deflection using an adaptive microelectromagnet mirror. *Phys. Rev. Lett.*, 81:1137, 1998.
- [291] D. C. Lau, A. I. Sidorov, G. I. Opat, R. J. McLean, W. J. Rowlands, and P. Hannaford. Reflection of cold atoms from an array of current-carrying wires. *Eur. Phys. J. D*, 5:193, 1999.
- [292] M. Drndic, G. Zabow, C. S. Lee, J. H. Thywissen, K. S. Johnson, M. Prentiss, R. M. Westervelt, P. D. Featonby, V. Savalli, L. Cagnet, K. Helmerson, N. Westbrook, C. I. Westbrook, W. D. Phillips, and A. Aspect. Properties of microelectromagnet mirrors as reflectors of cold rb atoms. *Phys. Rev. A*, 60:4012, 1999.
- [293] F. Lison, D. Haubrich, P. Schuh, and D. Meschede. Reflection of a slow cesium atomic beam from a naturally magnetized nd-fe-b surface. *Appl. Phys. B*, 69:501, 1999.
- [294] C. V. Saba, P. A. Barton, M. G. Boshier, I. G. Hughes, P. Rosenbusch, B. E. Sauer, and E. A. Hinds. Reconstruction of a cold atom cloud by magnetic focusing. *Phys. Rev. Lett.*, 82:468, 1999.
- [295] E. A. Hinds and I. G. Hughes. Magnetic atom optics: mirrors, guides, traps, and chips for atoms. *J. Phys. D: Appl. Phys.*, 32:R119, 1999.
- [296] P. Rosenbusch, B. V. Hall, I. G. Hughes, C. V. Saba, and E. A. Hinds. Manipulation of cold atoms using a corrugated magnetic reflector. *Phys. Rev. A*, 61:031404, 2000.
- [297] R. P. Bertram, H. Merimeche, and M. M. Magnetic whispering-gallery mirror for atoms.
- [298] A. S. Arnold, C. MacCormick, and M. G. Boshier. Adaptive inelastic magnetic mirror for Bose-Einstein condensates. *Phys. Rev. A*, 65:031601, 2002.
- [299] I. Bloch, M. Köhl, M. Greiner, T. W. Hänsch, and T. Esslinger. Optics with an atom laser beam. *Phys. Rev. Lett.*, 87:030401, 2001.
- [300] D. Cassettari, B. Hessmo, R. Folman, T. Maier, and J. Schmiedmayer. Beam splitter for guided atoms. *Phys. Rev. Lett.*, 85:5483, 2000.
- [301] R. Folman M. Andersson B. Hessmo E. Andersson, T. Calarco and J. Schmiedmayer. Multimode interferometer for guided matter waves. *Phys. Rev. Lett.*, 88:100401, 2002.
- [302] H. Kreutzmann, U. V. Poulsen, M. Lewenstein, R. Dumke, W. Ertmer, and G. Birkl and A. Sanpera. Coherence properties of guided-atom interferometers. *cond-mat/*, 0309227, 2003.
- [303] F. Ruschewitz, J. L. Peng, H. Hinderthür, N. Schaffrath, K. Sengstock, and W. Ertmer. Sub-kilohertz optical spectroscopy with a time domain atom interferometer. *Phys. Rev. Lett.*, 80:3173, 1998.
- [304] A. Peters, K. Y. Chung, and S. Chu. High-precision gravity measurements using atom interferometry. *Metrologia*, 38:25, 2001.
- [305] Th. Becker, J. v. Zanthier, A. Yu. Nevsky, Ch. Schwedes, M. N. Skvortsov, H. Walther, and E. Peik. High-resolution spectroscopy of a single in+ ion: Progress towards an optical frequency standard. *Phys. Rev. A*, 63:051802, 2001.
- [306] Th. Udem, S. A. Diddams, K. R. Vogel, C. W. Oates, E. A. Curtis, W. D. Lee, W. M. Itano, R. E. Drullinger, J. C. Bergquist, and L. Hollberg. Absolute frequency measurements of the hg+ and ca optical clock transitions with a femtosecond laser. *Phys. Rev. Lett.*, 86:4996, 2001.
- [307] C. Degenhardt U. Sterr J. Helmcke G. Wilpers, T. Binnewies and F. Riehle. Optical clock

- with ultracold neutral atoms. *Phys. Rev. Lett.*, 89:230801, 2002.
- [308] J. M. McGuirk, G. T. Foster, J. B. Fixler, M. J. Snadden, and M. A. Kasevich. Sensitive absolute-gravity gradiometry using atom interferometry. *Phys. Rev. A*, 65:033608, 2002.
- [309] M. Takamoto and H. Katori. Spectroscopy of the $1s03p0$ clock transition of 87Sr in an optical lattice. *Phys. Rev. Lett.*, 91:223001.
- [310] N. Kolachevsky, M. Fischer, S. G. Karshenboim, and T. W. H. High-precision optical measurement of the $2s$ hyperfine interval in atomic hydrogen.
- [311] M. V. Tiberg T. D. Roberts, A. D. Cronin and D. E. Pritchard. Dispersion compensation for atom interferometry. *Phys. Rev. Lett.*, 92:060405, 2004.
- [312] H. Pu and P. Meystre. Creating macroscopic atomic Einstein-Podolsky-Rosen states from Bose-Einstein condensates. *Phys. Rev. Lett.*, 85:3987, 2000.
- [313] K. Helmerson and L. You. Creating massive entanglement of Bose-Einstein condensed atoms. *Phys. Rev. Lett.*, 87(17):170402, 2001.
- [314] A. Sørensen, L.-M. Duan, J. I. Cirac, and P. Zoller. Many-particle entanglement with Bose-Einstein condensates. *Nature*, 409:63, 2001.
- [315] U. V. Poulsen and K. Mølmer. Positive-p simulations of spin squeezing in a two-component Bose condensate. *Phys. Rev. A*, 64:013616, 2001.
- [316] L.-M. Duan, J. I. Cirac, and P. Zoller. Quantum entanglement in spinor Bose-Einstein condensates. *Phys. Rev. A*, 65:033619, 2002.
- [317] A. Micheli, D. Jaksch, J. I. Cirac, and P. Zoller. Many-particle entanglement in two-component Bose-Einstein condensates. *Phys. Rev. A*, 67:013607, 2003.
- [318] M. Zhang, K. Helmerson, and L. You. Entanglement and spin squeezing of Bose-Einstein-condensed atoms. *Phys. Rev. A*, 68:043622, 2003.
- [319] M. Zhang and L. You. Quantum zero subspace and entangled Bose-Einstein condensates. *Phys. Rev. Lett.*, 91:230404, 2003.
- [320] Z. Hadzibabic S. Gupta, K. Dieckmann and D. E. Pritchard. Contrast interferometry using Bose-Einstein condensates to measure h/m and α . *Phys. Rev. Lett.*, 89:140401, 2002.
- [321] P. L. Gould, G. A. Ruff, and D. E. Pritchard. Diffraction of atoms by light: The near-resonant Kapitza-Dirac effect. *Phys. Rev. Lett.*, 56:827, 1986.
- [322] O. Mandel, M. Greiner, A. Widera, T. Rom, T. W. Hänsch, and I. Bloch. Controlled collisions for multi-particle entanglement of optically trapped atoms. *Nature*, 425:937, 2003.
- [323] J. A. Dunningham, K. Burnett, and Stephen M. Barnett. Interferometry below the standard quantum limit with Bose-Einstein condensates. *Phys. Rev. Lett.*, 89(15):150401, 2002.
- [324] K. I. Petsas, A. B. Coates, and G. Grynberg. Crystallography of optical lattices. *Phys. Rev. A*, 50:5173, 1994.
- [325] M. Greiner, I. Bloch, O. Mandel, T.W. Hänsch, and T. Esslinger. Bose-Einstein condensates in 1d- and 2d optical lattices. *Appl. Phys. B*, 73:769, 2001.
- [326] M. Greiner, I. Bloch, O. Mandel, T. W. Hänsch, and T. Esslinger. Exploring phase coherence in a 2d lattice of Bose-Einstein condensates. *Phys. Rev. Lett.*, 87:160405, 2001.
- [327] J. Reichel Y. Castin M. Ben Dahan, E. Peik and C. Salomon. Bloch oscillations of atoms in an optical potential. *Phys. Rev. Lett.*, 76:4508, 1996.
- [328] F. S. Cataliotti, S. Burger, C. Fort, P. Maddaloni, F. Minardi, A. Trombettoni, A. Smerzi, and M. Inguscio. Josephson junction arrays with Bose-Einstein condensates. *Science*, 293:843, 2001.
- [329] B. D. Josephson. Possible new effects in superconductive tunnelling. *Phys. Lett.*, 1(7):251, 1962.
- [330] S. Sachdev. *Quantum Phase Transitions*. Cambridge Univ. Press., 2001.
- [331] M. P. A. Fischer, P. B. Weichman, G. Grinstein, and D. S. Fischer. Boson localization and the superfluid-insulator transition. *Phys. Rev. B*, 40:546, 1989.
- [332] M. Greiner, O. Mandel, T. W. Hänsch, and I. Bloch. Collapse and revival of the matter wave field of a Bose-Einstein condensate. *Nature*, 419:51, 2002.
- [333] O. Mandel, M. Greiner, A. Widera, T. Rom, T. W. Hänsch, and I. Bloch. Coherent transport of neutral atoms in spin-dependent optical lattice potentials. *Phys. Rev. Lett.*, 91:010407, 2003.